ASSESSMENT OF NATURAL RADIOACTIVITY IN THE SOILS OF THE OHORONGO CEMENT PLANT AND THE TOWN OF OTAVI, NAMIBIA

A MINI THESIS SUBMITTED IN PARTIAL FULFILMENT OF THE REQUIREMENTS FOR THE DEGREE OF MASTER OF SCIENCE IN NUCLEAR SCIENCE

OF

THE UNIVESITY OF NAMIBIA

BY

MONICA MWADINOMO NAMBINGA

200970941

APRIL, 2020

Main- Supervisor: PROF JAMES A. OYEDELE (University of Namibia)

Co-Supervisor: MR. SIMON A. SHIMBOYO (University of Namibia)

ABSTRACT

The activity concentrations of the naturally occurring radionuclides ^{238}U, ^{232}Th, and ^{40}K in soil samples collected from the Ohorongo Cement plant and the town of Otavi, Namibia have been determined using a High-Purity Germanium (HPGe) detector. In addition, an assessment of the radiological hazards due to these natural radionuclides in the soils of the plant and town was carried out. The plant was divided into three geographical areas, and fifty soil samples were collected across the areas. Also, the town of Otavi was divided into ten geographical areas, and fifty soil samples were collected across the areas. These soil samples were processed and 500 g of each sample was placed in a well-labelled 500 ml polythene bottle and analyzed using an HPGe detector.

The average activity concentrations of the radionuclides ^{238}U, ^{232}Th, and ^{40}K in the soil samples from the Ohorongo Cement plant were 15.0 ± 4.7 Bq/kg, 25.1 ± 9.9 Bq/kg, and 310.7 ± 97.2 Bq/kg respectively. Similarly, the average activity concentrations of the radionuclides in the soil samples from Otavi were 21.6 ± 7.2 Bq/kg for ^{238}U, 20.3 ± 8.5 Bq/kg for ^{232}Th, and 256.4 ± 113.7 Bq/kg for ^{40}K. The average activity concentrations of ^{232}Th and ^{40}K were found to be higher in the Ohorongo Cement plant than in Otavi. In contrast, the average activity concentration of ^{238}U was higher in Otavi than in the Cement plant. These concentrations were used to calculate the absorbed dose rates and the effective dose rates in air across the different geographical areas in the plant and town. The values of $(4.3 \pm 1.5) \times 10^{-2}$ mSv/y and $(4.0 \pm 1.5) \times 10^{-2}$ mSv/y obtained respectively for the mean effective dose rates in the Cement plant and town are both less than the maximum permissible effective dose rate of 1.0 mSv/y recommended for the public by the International Commission on Radiological Protection. In order to evaluate the associated health hazard, the concentrations were also used to calculate the mean Radium equivalent activity (Ra_{eq}) and the mean external hazard index (H_{ex}) for the plant and for the town. The values obtained for Ra_{eq} in the Cement plant and town were 74.9 ± 25.6 Bq/kg and 70.4 ± 26.7 Bq/kg, respectively. These values are below the maximum permissible limit of 370 Bq/kg. Furthermore, the values of 0.20 and 0.19 obtained respectively for H_{ex} in the Cement plant and town are again below the maximum permissible limit of 1.0. It

is therefore concluded that radiation hazards are negligible in the plant and town and hence the plant and town have normal background radiation. The data generated in this study will contribute to the baseline data on radiological hazards in Namibia.

Table of Contents

LIST OF TABLES

LIST OF FIGURES

LIST OF ABBREVIATIONS

IAEA	International Atomic Energy Agency
ICRP	International Commission on Radiation Protection
HPGe	High Purity Germanium
MPL	Maximum permissible limit
UNAM	University of Namibia
UNSCEAR	United Nations Scientific Commission on the Effects of Atomic radiation

ACKNOWLEDGEMENTS

I would like to thank God for granting me good health throughout this project. This would remain a nightmare without him. In addition, I would like to thank my beloved husband, Mr. Josef Natangwe Nambinga, for his understanding and words of encouragements.

This thesis would not be possible without the support of my supervisors. Firstly, I would like to express my gratitude to the main supervisor, Prof. J.A Oyedele, for his encouragement, guidance and support from the start to the end of this study. Thanks also for his kindness, patience and good motivation for me to complete writing this thesis. Special thanks to Mr. S.A Shimboyo, the co-supervisor, for his advice, supervision and support. I would also like to express my appreciation to my colleagues in the Department of Physics for their support during this study.

Special thanks go to the University of Namibia for providing financial support for this project and the managers and staff of the Ohorongo Cement plant and the municipality of Otavi for their support during the collection of soil samples and granting me permission to do this research in their premises.

DEDICATION

I dedicate this thesis to the almighty God for his blessings and guidance, especially during this project. To my husband, **Mr. Josef N Nambinga**, and my beloved child, **Mr. Matheus T Nambinga,** for their encouragement, patience and support during my studies.

DECLARATION

I, Monica Mwadinomo Nambinga, hereby declare that this study is my own work and is a true reflection of my research, and that this work, or any part thereof has not been submitted for a degree at any other institution.

No part of this thesis/dissertation may be reproduced, stored in any retrieval system, or transmitted in any form, or by means (e.g. electronic, mechanical, photocopying, recording or otherwise) without the prior permission of the author, or The University of Namibia in that behalf.

I, Monica Mwadinomo Nambinga, grant The University of Namibia the right to reproduce this thesis in whole or in part, in any manner or format, which The University of Namibia may deem fit.

…….. …… …..

Name of Student **Signature** **Date**

CHAPTER 1: INTRODUCTION

1.1 Background of the study

There is increasing interest in the study of natural radioactivity in the soils of different countries [1-5]. Radioactivity is defined as the process of spontaneous decay and transformation of unstable atomic nuclei to stable nuclei [6, 7] . In this process, ionising radiation such as gamma ray is emitted. The radioactivity of naturally occurring unstable radionuclides are called "natural radioactivity". The radiation emitted by these naturally occurring unstable atoms is known as natural background radiation. Human beings are exposed daily to natural background radiation arising from cosmic rays, natural radionuclides in air, food and water, and the use of nuclear related equipment (x-ray, CT scan) [7, 8]. However, the most significant sources of background radiation are naturally occurring radioactive radionuclides (^{40}K, ^{238}U and ^{232}Th and their decay products) in soils [8].

When the concentrations of the primordial radionuclides in the soil are elevated, the background radiation will be high which could pose a health problem to the inhabitants of these areas. Therefore, the assessment of gamma radiation dose from natural sources is of particular importance as natural background radiation is the largest contributor to the external dose received by world population [9]. Natural radioactivity and the associated external exposure due to gamma radiation are widely spread in the earth's environment and depend primarily on geological and geographical conditions and appear at different levels in the soils of each region in the world. It is for this reason that natural radioactivity in the soils have been studied in many countries with the view to identify high background radiation areas.

In Namibia, there are many mineral resources including Uranium-238 and therefore the concentrations of primordial radionuclides in the soils may be high in certain regions or places such as the Ohorongo Cement plant and the town of Otavi. Therefore, it is of interest to study the natural radioactivity in the soils of these places in Namibia.

The aim of this study was to determine the levels of natural radioactivity in the soil samples collected from the Ohorongo Cement plant and the town of Otavi. The results of this study will provide information about the levels of background radiation in the Cement plant and town. In addition, the study will provide a baseline data of activity concentrations in the soils of the Ohorongo Cement plant and the town of Otavi. Also, the results will be useful for future monitoring of the area and for decision making.

1.2. Statement of the problem

Scientists have studied the natural radioactivity in the soils of some towns in Namibia [2, 3] .These studies have provided information on the level of background radiation in each of the towns. The level of radiation will determine whether or not a town has normal background radiation. Although, radionuclide concentrations in the soils of several places in Namibia have been studied, there is little or no information in the natural radioactivity levels in the soils of the Ohorongo Cement plant and the neighbouring town of Otavi. Also, the soils of the Cement plant and the town of Otavi may contain unstable nuclei that contribute significantly to background radiation. Furthermore, the many tourists passing through Otavi and workers of the Ohorongo Cement plant that are living in Otavi could be interested in knowing the levels of radiation in the pant and the town. Therefore, it is of interest to study the radioactivity in the soils of the Ohorongo Cement plant and the town of Otavi, and ascertain whether

or not the background radiation levels in these areas are below the maximum permissible limit of 1.0 mSv/y [10].

1.3. Objectives of the study

The objectives of this study were to:

a) Investigate the concentrations and the distributions of the primordial radionuclides, ^{232}Th, ^{238}U, and ^{40}K in the soils of the Ohorongo Cement plant and the town of Otavi;
b) calculate the radiological parameters needed to assess the radiological hazards in the study areas;
c) determine the levels of background radiation in the plant and town, and ascertain whether the levels are within the maximum acceptable limit; and
d) establish a baseline data of activity concentrations for further environmental assessment

1.4. Significance of the study

Ohorongo Cement plant is a Cement-producing company in Namibia. This plant is located on the farm Sargberg at about 25 km north-east of Otavi in the Otjozondjupa region at a latitude 19˚31' south and longitude 17˚27' east. The plant employs about 312 workers [11]. Also, the plant attracts many visitors from different parts of the world. There are large deposits of limestone, shale and some raw materials near the plant .Some of these raw materials in the soil may contain primordial radionuclides. Thus, this study will provide information on the level of background radiation at the plant to which the workers and visitors to the plant are exposed.

Otavi is a town on the main road between Otjiwarongo and Tsumeb, some 365 km away from the capital city, Windhoek. Otavi is an important centre for farming and has a large cereal milling plant in the town. Its name is derived from the Herero word 'Ondavi' meaning 'branch of a tree'. Most people, both tourists and locals travelling from Windhoek to the northern part of the country and vice versa, like to stop in this town for refreshments. Also, most of the Ohorongo Cement plant employees reside in this town. The population of the town is about 5242 in 2011 [12] .The world largest Meteorite is located 25km north-east of Otavi. This meteorite is one of the popular tourist attractions in the area. The town also has farming activities. Furthermore, the town has two primary schools and one secondary school that provide education to learners from surrounding farms and areas. It is therefore of interest to determine the background radiation level to which the inhabitants and visitors are exposed.

The study will provide information on the background radiation levels to which the inhabitants and visitors to the plant and town are exposed. The results will be used to establish baseline data of background radiation levels in the region under study for further environmental assessment.

CHAPTER 2: LITERATURE REVIEW

2.1. Discovery and history of radioactivity

On the 8th of November 1895 in Wuerzburg Germany, Roentgen was conducting an experiment with Crooke's tube when he observed that certain rays were emitted from the screen nearby [13, 14]. Upon further observation, he found out that it was originating from a partially evacuated Crooke's tube covered with a black paper and in a darkened room which he was using to study Cathode rays. He concluded that the fluorescence that penetrated the opaque black paper must have been caused by the rays [14, 15]. This phenomenon was later named x-rays.

In 1896, Henri Becquerel accidentally discovered radioactivity. Upon learning about the discovery of Roentgens [13], he (Becquerel) began looking for a connection between the phosphorescence he had already been investigating and the newly discovered x-rays of Roentgen. He thought of placing concealed phosphorescence uranium salt in direct sunlight and observing if it might emit penetrating x-rays when illuminated by sunlight, but his hypothesis failed. After performing other experiments involving non-phosphorescent Uranium salt, he found out that a penetrating radiation was given off. The source of the radiation was the Uranium itself [14]. The radiation was emitted spontaneously in apparently undiminishing intensity and, like x-rays, could also discharge an electroscope. What Becquerel discovered was radioactivity.

The discovery of Becquerel was further investigated in 1897 by the couples Pierre and Marie Curie [16], who suspected that a Uranium ore, known as Pitchblende, contained other radioactive elements. After one year of investigation, they discovered other elements -Polonium and Radium- in 1898 [17]. Both Polonium and Radium were more

radioactive than Uranium. Since these discoveries, many other radioactive elements have been discovered. Even though the discovery of radioactivity was made by Becquerel, Marie was the one who named the process of spontaneous emission of ionizing radiation rays as Radioactivity. Radioactivity is defined as the process by which an unstable atomic nucleus loses energy by emitting radiation [14, 17].

In 1899, an experiment conducted by British physicist Ernest Rutherford showed that radioactive elements emit different kinds of radiation, and he named them alpha, beta, and gamma rays. The radiations were classified by their ability to penetrate matters.

2.2. Radioactive decay

2.2.1. The decay law

There are about 2500 known nuclides but less than 300 of them are stable. The others are unstable nuclides that decay to form other nuclides by emitting alpha particles, beta particles and gamma radiation [18] . A chain of decays takes place until a stable nucleus is reached as shown in Figure 2.1. Radioactive decay is a random process at the level of a single atom, according to quantum theory. Therefore, it is impossible to predict when a particular atom will decay [18].

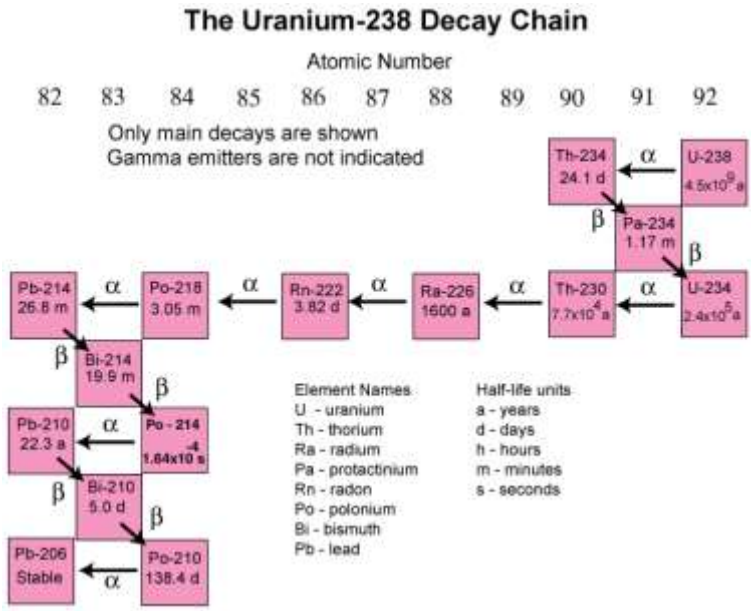

Figure 2.1: The decay chain of Uranium-238 [38]

Although, it is not possible to predict when the radioactive atom or nuclei in a sample will decay, the number of nuclei in a sample that will decay in a given time interval can be predicted by using radioactive decay law. The rate of transformation of radionuclide is called activity and is defined as the number of atoms that decay per unit time [14]. It was noted that the activity of the pure radionuclide decreases with time according to an exponential law [14, 15]. Experimentally, it was found out that the decay rate at any time t is directly proportional to the number of nuclei (atoms) present at that time and is expressed as [7, 14];

$$dN = -\lambda N dt \quad \text{---------- 2.1}$$

where λ is a constant of proportionality and it is called a decay constant. The negative sign indicates that N decreases as time t increases. The decay rate or activity is given by [14]

$$A = -\frac{dN}{dt} = \lambda N \quad \text{---------- 2.2}$$

Equation 2.1 can be re-written as

$$\frac{dN}{N} = -\lambda dt \quad \text{---------- 2.3}$$

Integrating both sides of equation 2.3 from $t = 0$ to $t = t$ gives

$$N = N_0 e^{-\lambda t} \quad \text{---------- 2.4}$$

where N_0 is the number of nuclei (atoms) present at $t = 0$.

Equation 2.4 is called the radioactive decay law. Figure 2.2 illustrates that the number of nuclei decreases exponentially with time.

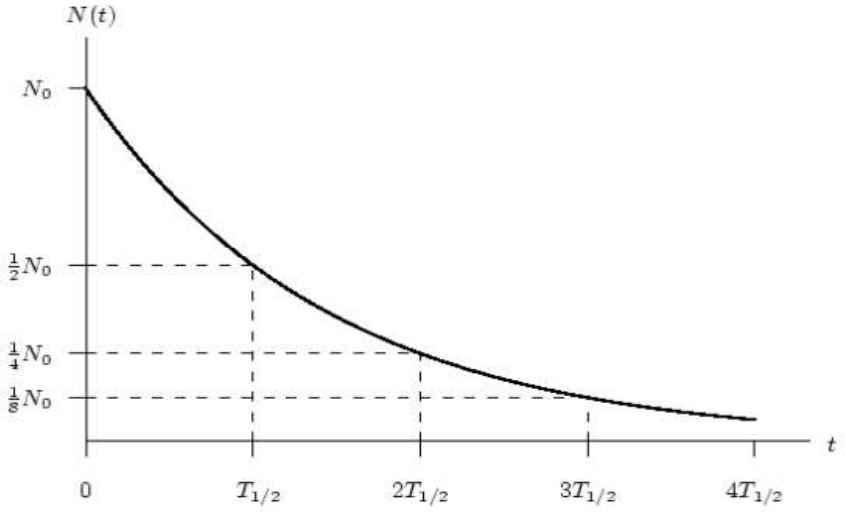

Figure 2.2: Exponential decay law for radioactive nuclei [19]

The decay rate can be described in terms of half-life and mean life [20]. Half-life is defined as the time required for one half of the original nuclei to disintegrate [18]. Putting $N = \frac{N_0}{2}$ into equation 2.4 at $t = T$ gives

$$\frac{1}{2} = e^{-\lambda T} \quad \text{---------- 2.5}$$

Taking the natural logarithms of equation 2.5 and solving for T gives [14]

$$T = \frac{ln2}{\lambda} = \frac{0.693}{\lambda} \quad \text{----------2.6}$$

If the decay constant is known or calculated, then the half-life can be obtained and compared with the measured values.

Mean-life time, is defined as the average time that a nucleus is likely to survive before it decays [14]. It is equal to the mean value of t under the exponential curve. Thus, the mean-life in terms of the half-life is given by

$$\tau = \frac{1}{\lambda} = \frac{T}{0.693} \quad \text{---------- 2.7}$$

showing that $\tau > T$.

2.2.2. Radioactive equilibrium

Radioactive equilibrium is when the decay rate of a radioactive isotope equals to the production rate of that isotope by another source [21]. Actually, there are three states of equilibrium, as explained below.

2.2.2.1. Secular equilibrium

Secular equilibrium is a condition when the half-life of the parent is very long compared to that of the daughter, so that $\lambda_p \ll \lambda_d$ [21] where λ_p is the decay constant of the parent nucleus and λ_d is the decay constant of daughter nucleus.

Consider a case in which a radioactive nuclide A decay into nuclide B which is also radioactive and therefore decays to another nuclide C which is stable. The first radionuclide A is referred to as the parent, while the radionuclide B is referred to as the daughter.

$$A \overset{\lambda_A}{\rightarrow} B \overset{\lambda_B}{\rightarrow} C(Stable)$$

Assuming that there are N_0 parent atoms at time $t = 0$ with no other decay products present at that time, then [22]

$$N_A(t = 0) = N_0 \quad -------------------------- 2.8$$

To consider the number of nuclei of A, B and C at time t, their rate of change is given by the following three equations [23]

$$\frac{dN_A}{dt} = -\lambda_A N_A \quad -------------------------- 2.9$$

$$\frac{dN_B}{dt} = \lambda_A N_A - \lambda_B N_B \quad -------------------------- 2.10$$

$$\frac{dN_C}{dt} = -\lambda_B N_B \quad -------------------------- 2.11$$

From the above three equations, the activity A_A of parent can be treated as constant [21]. The rate of change $\frac{dN_B}{dt}$ in the number of daughter nuclei N_B per unit time is equal to the rate at which they are produced, A_A, minus their rate of decay, $\lambda_B N_B$ [7, 14, 21].

According to equation 2.5, the number of parent nuclei can be written as [6, 24]

$$N_A = N_0 e^{-\lambda_A t} \quad \text{---------- 2.12}$$

Substituting equation 2.12 into eq.2.10 gives

$$\frac{dN_B}{dt} = \lambda_A N_0 e^{-\lambda_A t} - \lambda_B N_B \quad \text{----------2.13}$$

Multiplying equation 2.13 with $e^{-\lambda_B t} dt$ and integrating, gives the solution

$$N_B = \frac{N_0 \lambda_A}{\lambda_B - \lambda_A}\left(e^{-\lambda_A t} - e^{-\lambda_B t}\right) \quad \text{----------2.14}$$

Equation 2.14 gives the number of daughter nuclei present at time t [14, 22].

Since in secular equilibrium, the half-life of the daughter is far shorter than that of the parent, $T_B \ll T_A$ so that $\lambda_A \ll \lambda_B$. Since $\lambda_A \ll \lambda_B$, and $\lambda_A \cong 0$, then $e^{-\lambda_A t} \approx 1$. Hence, equation 2.13 reduces to [7, 14, 20, 21] [14,21].

$$N_B = \frac{N_0 \lambda_A}{\lambda_B}\left(1 - e^{-\lambda_B t}\right) \quad \text{---------- 2.15}$$

When time t is large, then $e^{-\lambda_B t}$ is negligible. Thus equation 2.15 reduces to

$$N_B \lambda_B = N_A \lambda_A \quad \text{---------- 2.16}$$

Equation 2.16 shows that the parent and daughter activities are equal. That is, parent and daughter are in a secular equilibrium state [14]. Secular equilibrium is established when the activity of the daughter builds up to that of the parent and it takes about seven half-lives of the daughter to reach this equilibrium [14, 21]. Figure 2.3 shows the build-up and establishment of daughter and parent activities.

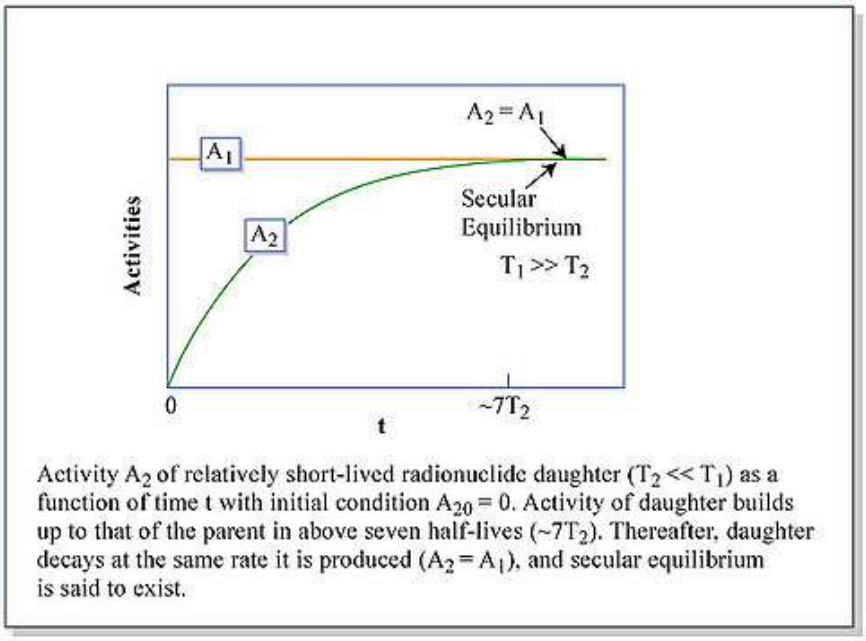

Activity A_2 of relatively short-lived radionuclide daughter ($T_2 << T_1$) as a function of time t with initial condition $A_{20} = 0$. Activity of daughter builds up to that of the parent in above seven half-lives ($\sim 7T_2$). Thereafter, daughter decays at the same rate it is produced ($A_2 = A_1$), and secular equilibrium is said to exist.

Figure 2.3: Illustration of secular equilibrium [25]

2.2.2.2. Transient equilibrium

This equilibrium occurs if the daughter has a shorter half-life than the parent $(i.e.\ T_{(1/2)A} > T_{(1/2)B})$ [14].

As time increases, the term $e^{-\lambda_B t}$ in equation 2.14 becomes negligible compared to $e^{-\lambda_A t}$, since, $\lambda_B > \lambda_A$ [7, 22]. Therefore, Eq. 2.14 reduces to

$$N_B = \frac{N_0 \lambda_A}{\lambda_B - \lambda_A}\left(e^{-\lambda_A t}\right) \quad ---------- 2.17$$

Using Eq. 2.12 then Eq. 2.17 can be written as

$$\frac{N_B}{N_A} = \frac{\lambda_A}{\lambda_B - \lambda_A} \quad \text{---------- 2.18}$$

Equation 2.18 shows that the ratio of parent and daughter activities is a constant [22]. Under this condition (equation 2.18), transient equilibrium is said to exist as illustrated in Figure 2.4.

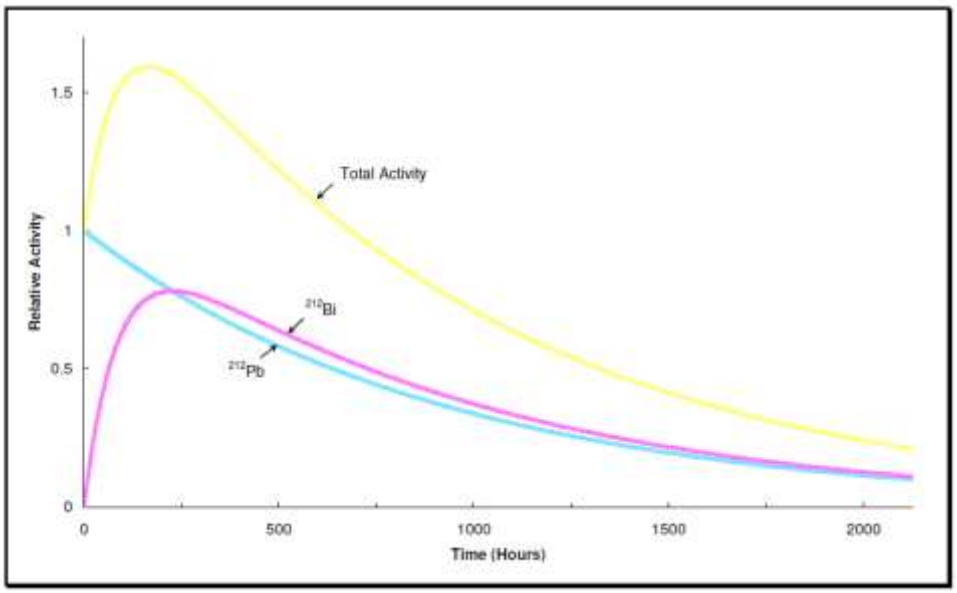

Figure 2.4: Illustration of transient equilibrium between ^{212}Pb and daughter ^{212}Bi [23]

The time at which transient equilibrium is established depends on the magnitude of the half-lives of the daughter and parent [7].

2.2.2.3. No equilibrium

In this case the daughter has a longer half-life than the parent ($T_{(1/2)A} < T_{(1/2)B}$), therefore its activity builds up to a maximum and then declines [14]. The parent will decay eventually because of its shorter half-life and only the

daughter is left, therefore, no equilibrium state will occur [21]. Figure 2.5 illustrates the condition of no equilibrium.

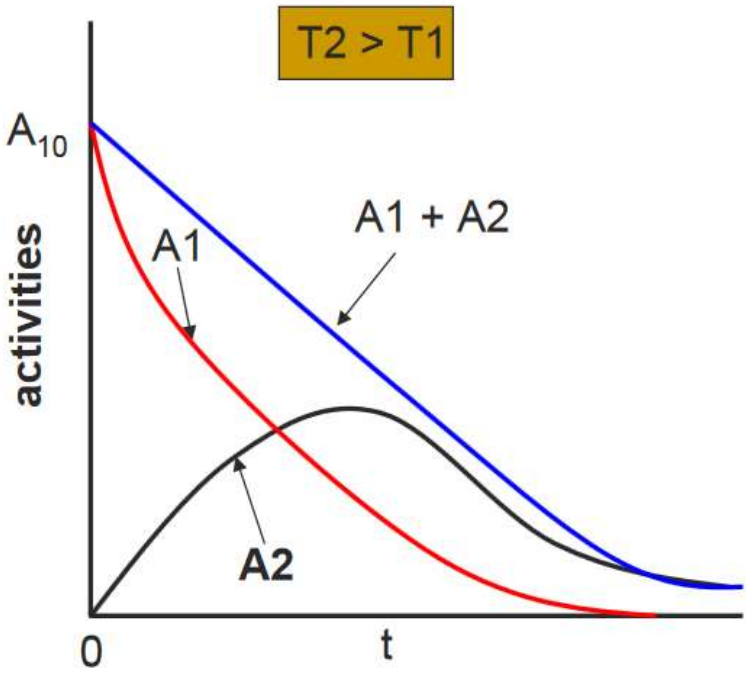

Figure 2.5: Schematic diagram of no equilibrium in radioactive decay [26]

2.2.3. Types of decays

As discussed in section 2.2.1, there exist unstable nuclei in nature. These nuclei decay in order to become stable or more stable. In this section, various kinds of radioactive decay will be discussed.

2.2.3.1. Alpha decay

In alpha decay, the nucleus emits a Helium nucleus known as an alpha particle, symbolized as α [21, 27]. An alpha particle consists of two protons and two neutrons, which is identical to a Helium nucleus. Alpha decay is commonly observed in all the naturally occurring heavy radionuclides with an atomic number greater than 82 ($Z > 82$) [14, 20]. Alpha decay can be written as follows [27]:

$$^{A}_{Z}X \longrightarrow ^{A-4}_{Z-2}Y + ^{4}_{2}He\ (\alpha)$$

where X and Y represent the parent and daughter nuclei respectively, while A and Z represent the mass and proton numbers.

An example of alpha decay is

$$^{238}_{92}U \longrightarrow ^{234}_{90}Th + ^{4}_{2}He$$

Alpha particles cause intense ionisation in air, but they can be stopped by a thin sheet of paper.

Figure 2.6 illustrate the process of alpha decay of a $^{238}_{92}U$ nucleus

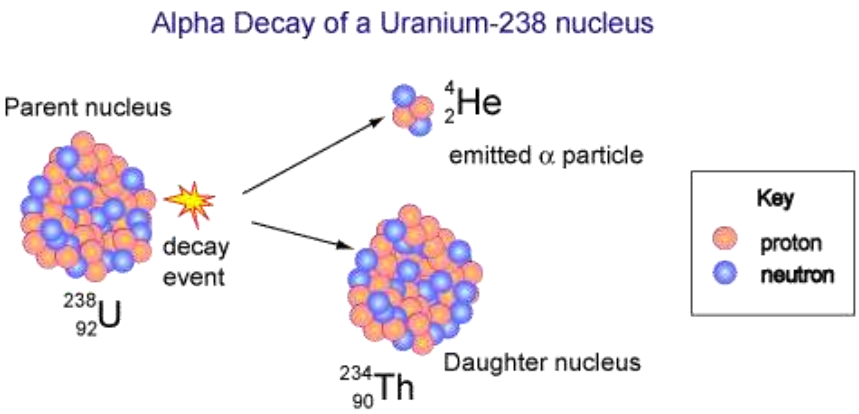

Figure 2.6: Alpha decay process [28]

2.2.3.2. Beta decay

In beta decay, a nucleus emits an electron or a positron and an antineutrino [6]. This decay is mediated by weak nuclear forces. There are two types of beta decay- beta minus (β^-) and beta plus (β^+) [27]. In both decays, a nucleon in the nucleus is transformed to a different nucleon, releasing particles in the process [6, 22]. Both beta decays are moderately penetrating.

In β^- process, a neutron in the nucleus changes into a proton, while a negative electron and an antineutrino are simultaneously created and emitted [21, 29].

This process can be written as

$$n \longrightarrow p + e^- + \bar{\upsilon}$$

where p and n denote neutrons and protons respectively while e^- and $\bar{\upsilon}$ denote electrons and antineutrino. In terms of nuclei, we can write β^- process as [22]

$${}^{A}_{Z}X \rightarrow {}_{Z+1}{}^{A}Y + e^- + \bar{\upsilon}$$

where X and Y are the parent and daughter nuclei.

A typical example of β^- process is

$${}^{14}_{6}C \rightarrow {}^{114}_{7}N + e^- + \bar{\upsilon}$$

In β^+ process, a proton in the nucleus changes to a neutron while positron and neutrino are simultaneously created and emitted. The positron is a particle of the same mass and spin as an electron but with a positive charge [21]. Bryan also define the neutrino and antineutrino as the particles with zero rest mass and spin $\frac{1}{2}$ [21] .This β^+ process can be represented as [14]

$$p \longrightarrow n + e^+ + \nu$$

Generic representation of a β^+ process in terms of the parent and daughter nuclei is

$${}^{A}_{Z}X \rightarrow {}_{Z-1}{}^{A}Y + e^+ + \upsilon$$

An example of this process is

$$^{10}_{6}C \rightarrow ^{10}_{5}B + e^{+} + \upsilon$$

Figure 2.7 is an illustration of the beta decay process.

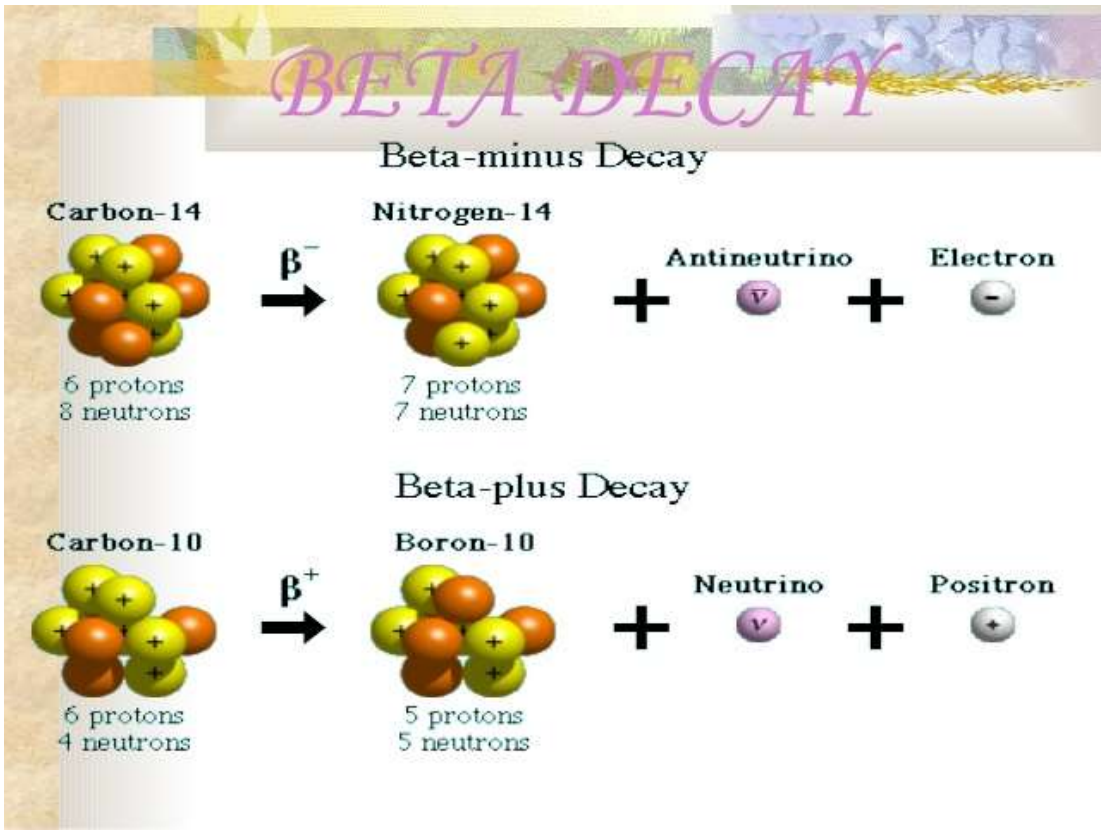

Figure 2.7: An illustration of the beta decay process [30]

2.2.3.3. Gamma decay

Gamma radiation is electromagnetic radiation emitted by an unstable nucleus of an atom during radioactive decay and it has no electric charge [21, 31]. It is similar to visible light and *X*-rays in its nature [7]. Gamma radiation is different from other electromagnetic radiation in terms of its wavelength, frequency, and origin [24, 32]. Unlike α-decay or β-decay, neither the mass number A nor the atomic number Z changes during γ decay [29]. γ-decay follows either α- decay or β-decay. For example,

if a radioactive parent nucleus decays by β-decay to an excited state of the daughter nucleus, the daughter nucleus then decays to its ground state by γ emission [14, 29]. Assuming that the nucleus is at rest while in an initial excited state E_i which decays to a final state E_f , conservation of total mass-energy can be used to calculated the energy of the emitted gamma-ray transition, given by [21, 24]

$$E_i = E_f + E_R + E_\gamma \quad \text{---------- 2.19}$$

which can be rearranged as

$$\Delta E = E_i - E_f = E_R + E_\gamma \quad \text{----------2.20}$$

In most cases, the recoil energy,E_R, of the final product can be considered to be negligible [23, 24] . Thus, the gamma-ray energy, E_γ, is almost equal to the energy of de-excitation (ΔE), which is the energy difference between the initial and final states. Thus,

$$\Delta E = E_i - E_f = E_\gamma \quad \text{----------2.21}$$

Typically, the energies of gamma rays cover a range from 0.1 to 10 MeV [24, 32].

If the excited state and the ground state of a nucleus are denoted by $({}^{A}_{Z}X)^*$and ${}^{A}_{Z}X$ respectively, then one can write the gamma decay process as [29]

$$({}^{A}_{Z}X)^* \longrightarrow {}^{A}_{Z}X + \gamma$$

An example of this decay is

$$({}^{12}_{6}C)^* \longrightarrow {}^{12}_{6}C + \gamma$$

Figure 2.8 illustrates the process of gamma decay

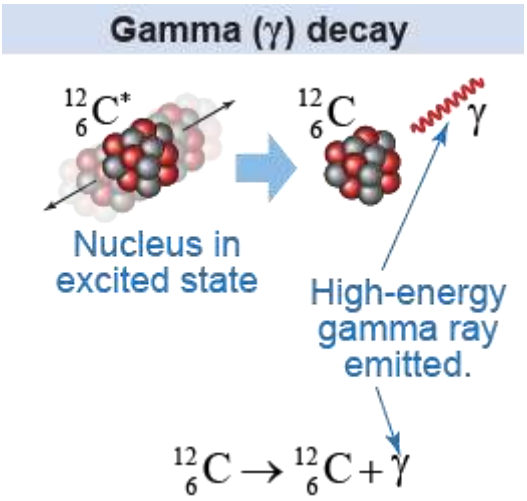

Figure 2.8: Illustration of the gamma decay process [33]

2.3. Environmental sources of radioactivity

Humans are exposed to radiation from various sources in the environment. There are two main sources of radioactivity in the environment: (i) natural sources and (ii) artificial sources [34]. The naturally occurring background radiation arises mainly from terrestrial radionuclides in the soil, food and water and from cosmic ray from space [34]. Artificial sources arise from the use of radiation and radioactive materials by human beings [35].

2.3.1. Natural sources

Human beings are exposed to radiation that is caused by the natural radioactive materials present in the surrounding. These radionuclides are categorized into two types: primordial and cosmogenic radionuclides.

2.3.1.1. Primordial radionuclides

Terrestrial radionuclides are common in rocks, soil, water and oceans and also in building materials used for homes [6].These radionuclides have been present since the creation of the planet. They have very long half-lives (in the order of hundreds of millions of years or more) [23]. Some main primordial radionuclides and their half-lives are listed Table 2.1

Table 2.1: Some primordial radionuclides and their half-lives [7]

Radionuclide	Half-life (Years)
^{40}K	1.38×10^{9}
^{87}Rb	4.8×10^{10}
^{138}La	1.1×10^{11}
^{147}Sm	1.1×10^{11}
^{187}Re	4.0×10^{10}
^{232}Th	1.4×10^{10}
^{235}U	7.8×10^{8}
^{238}U	4.5×10^{9}

In nature, there are three main decay chains. The naturally occurring radioactive parents have atomic numbers mostly between Z = 81 and Z = 92 and are characterized by substantial neutron excess [15, 36]. Nevertheless, the presence of many protons in these nuclei leads to strong Coulomb repulsion and instability. Such nuclei can decay by successive emissions of α, β or γ, until they reach their stability [21, 29]

The three natural decay series are headed by Uranium-238, Thorium- 232, and Uranium-235 [22, 27], the decay chains are known as (4n+2), (4n) and (4n+3) for ^{238}U, ^{232}Th and ^{235}U respectively, where n is an integer [22, 37] .

The radionuclides of the uranium-238, thorium-232, and uranium- 235 decay series are shown in Figures 2.9, 2.10, and 2.11, along with the major mode of radioactive decay for each series [37].

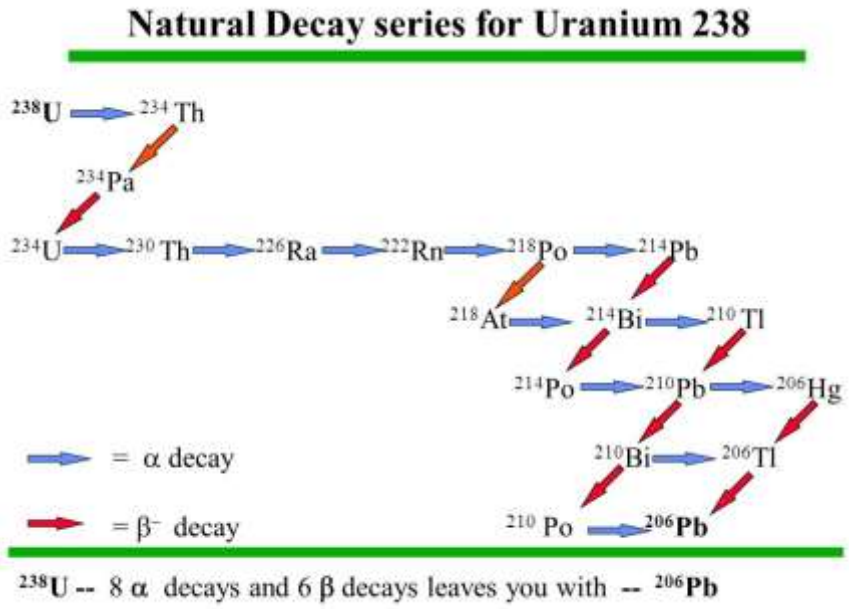

Figure 2.9: The radioactive decay chain of Uranium-238. [38]

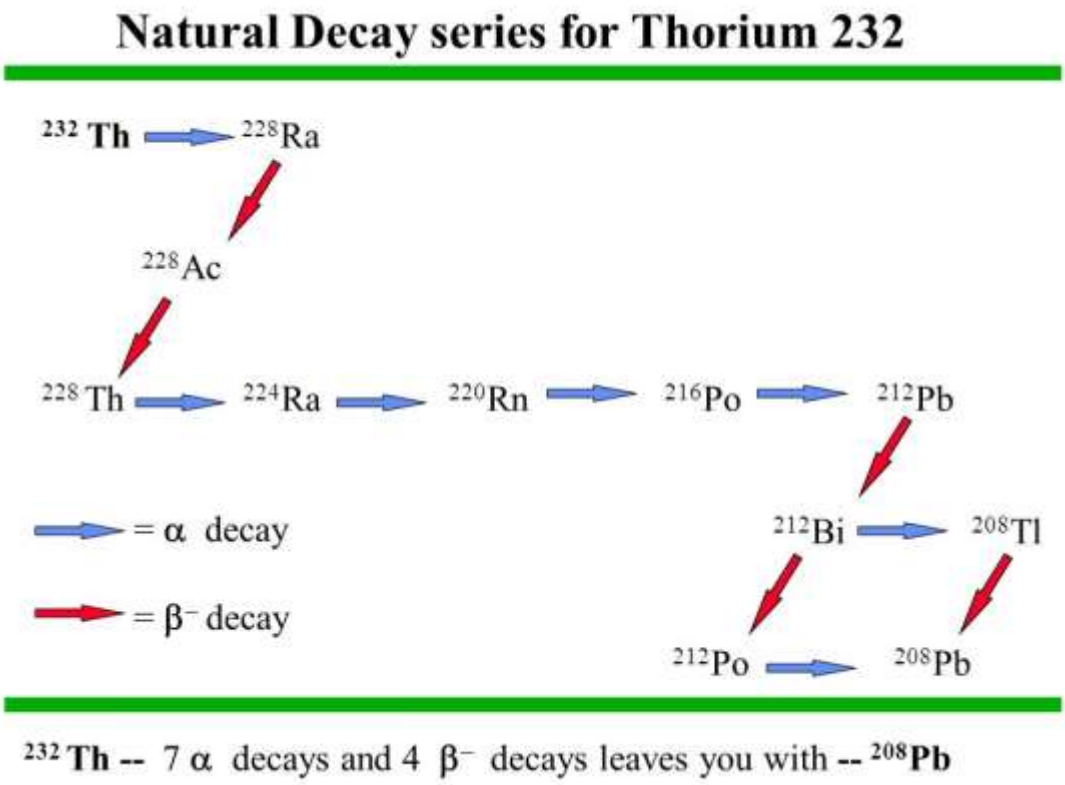

Figure 2.10: The decay series of Thorium-232 [38]

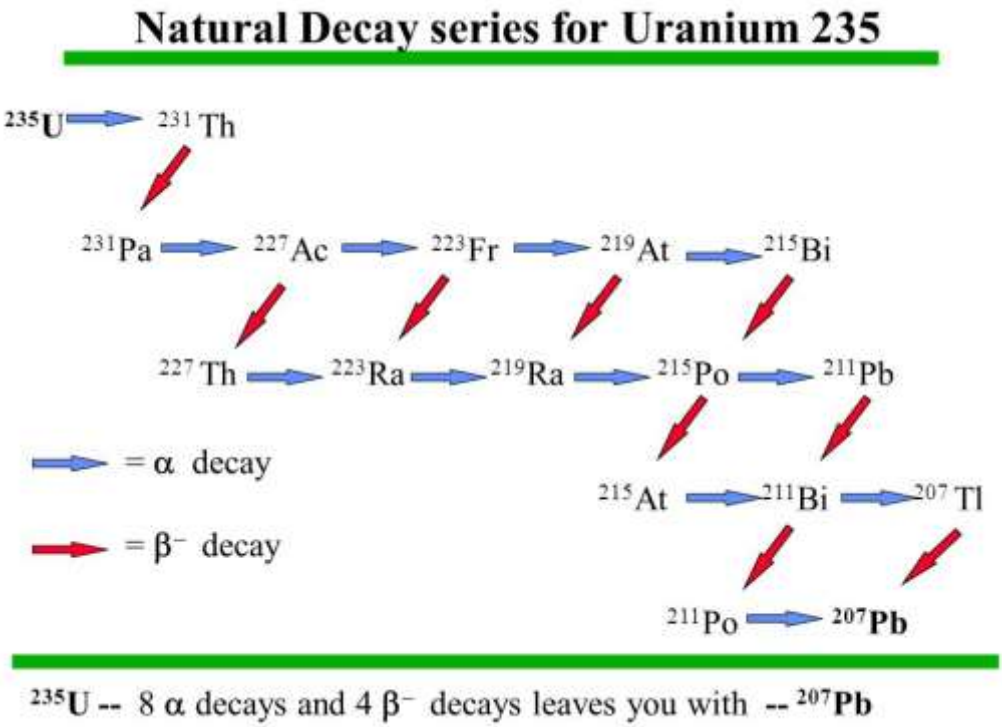

Figure 2.11: The decay chain of Uranium-235 [38]

2.3.1.2. Cosmogenic radionuclides

These radionuclides are produced continuously by the interaction of nucleons released from cosmic radiation with target nuclei in the earth atmosphere, mostly upper atmosphere [39]. When cosmic rays strike the atmosphere, they produce a nuclear cascade or the shower of secondary particles. Most of these are eventually stopped before they reach the surface of the earth except for the muons (μ) and neutrons (n).The majority of the target atom in the earth's atmosphere are from argon, oxygen and nitrogen gas. There are several cosmogenic radionuclides with a range of half-lives from minutes to millions of years. However, only four of them contribute a significant measurable dose of radioactivity to humans [24].

From radiation health aspect, the main cosmogenic radionuclides are Tritium (^{3}H), Berryllium-7 (^{7}Be), Carbon-14 (^{14}C), and Sodium-22 (^{22}Na) [24]. The most significant cosmogenic radionuclide is ^{14}C which can be taken up by plants and enter the food chain [7, 37].

2.3.2. Artificial sources

Some radionuclides have been released into the environment through the use of man-made radiation sources for various purposes. For example, testing of nuclear weapons, nuclear reactors accidents (e.g. Chernobyl), radioisotope manufacturing industry (^{137}Cs, ^{90}Sr and ^{131}I) and medicine (going for x-rays) [40] .

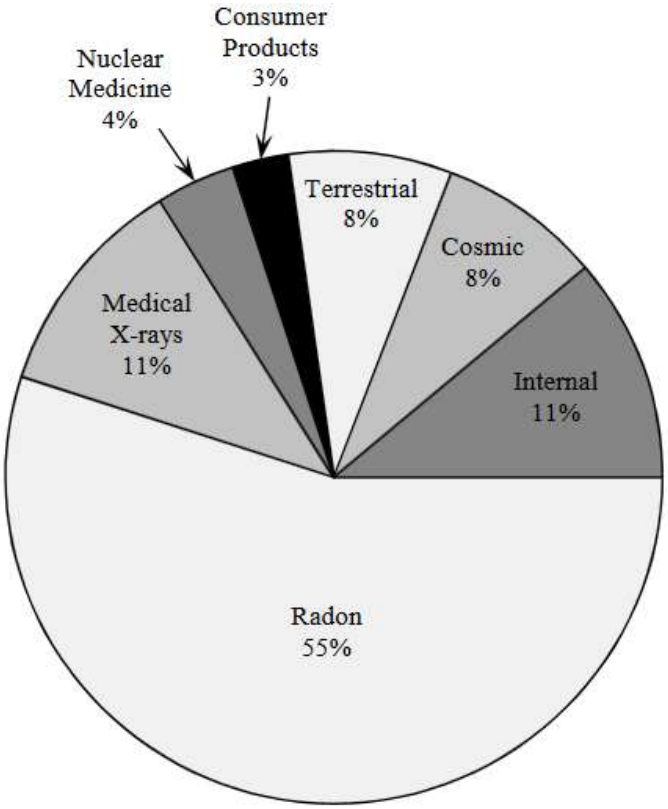

Figure 2.12: Exposure of the public to ionizing radiation [41]

Figure 2.12 shows that the radiation exposure from natural sources accounts for about 82% of the total exposure, while the remaining 18% is from artificial or man-made sources.

2.4. Interaction of gamma rays with matter

Understanding the interactions of gamma rays with matter is important for radiation measurements. There are nine possible interaction processes for γ-rays with matter, but this study will only consider three mechanisms that play significant roles in radiation measurements [14, 27, 29]. The three processes are photoelectric absorption, Compton scattering, and pair production [14].

2.4.1. Photoelectric absorption

In the process of photoelectric absorption, a photon undergoes an interaction with an electron which is bound in an atom [21, 27]. In this interaction, the incident photon disappears, and an electron called photoelectron is ejected from one of the electron shells. The kinetic energy,E_e, transmitted to the photoelectron is equal to the incident photon energy,E_γ, minus the binding energy of the electron in its original shell,E_b, [21]. For gamma rays of enough energy, the emission of the photoelectron is most likely originating from its tightly bound or K shell of the atoms [14]. Figure 2.13 illustrates the process of photoelectric absorption.

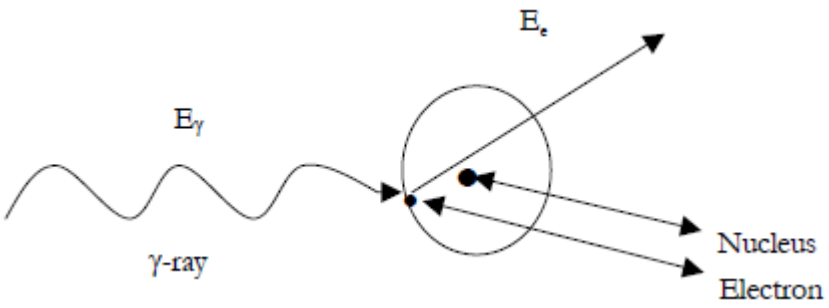

Figure 2.13: Schematic diagram of the photoelectric absorption process [42]

The energy of the ejected photoelectron can be expressed as

$$E_e = E_\gamma - E_b$$

The probability for photoelectric absorption is most significant for gamma rays with energies of about one hundred keV [22, 27] .

Accordingly, this interaction creates an ionized absorber atom with a vacancy in one of the bound electron shells. A free electron can then be captured from the medium or

a rearrangement of electrons from outer shell orbits of the atom, then fills this vacancy. Therefore, characteristic X-ray photons are also produced. These may be reabsorbed through photoelectric absorption involving electrons from the less tightly bound shells. Auger electrons may also be generated following this type of interaction [7].

The interaction cross section ($\boldsymbol{\tau}$) of the photoelectric process varies hastily with E_γ and with the value of Z of the absorber. A single analytic expression cannot describe the probability of this process, but an approximation is given by [27, 32, 34]

$$\tau \cong constant \times \frac{Z^n}{{E_\gamma}^m} \quad -----------2.22$$

where the power indices n and m are numbers ranging from 3 to 5 over the gamma-ray energy region of interest. The photoelectric absorption probability strongly depends on photon energy and the atomic number of an absorber material [14]. The strong Z dependence shows that a high-Z material is very effective in the absorption of photons. The strong dependence on photon energy is the reason the photoelectric process is significant at the low energy of photons, but becomes less dominant at higher energies [14, 29].

2.4.2. Compton scattering

An incident photon interacts with an atomic electron (which can be regarded as free) in such a way that the photon or gamma ray is not completely absorbed but merely scattered out of the beam with reduced energy. In this process, the incoming gamma-ray photon is deflected through an angle θ with respect to its original direction. A portion of the photon energy is transferred to the valence electron known as a recoil

electron [27]. This energy may vary from zero to a significant or large fraction of the gamma-ray energy depending on the angle of scattering.

The expression that relates the energy transfer and the scattering angle for any interaction can simply be derived by writing simultaneous equations for the conservation of energy and momentum [27]. The solution for the scattered energy, can be written as follows [14, 22]

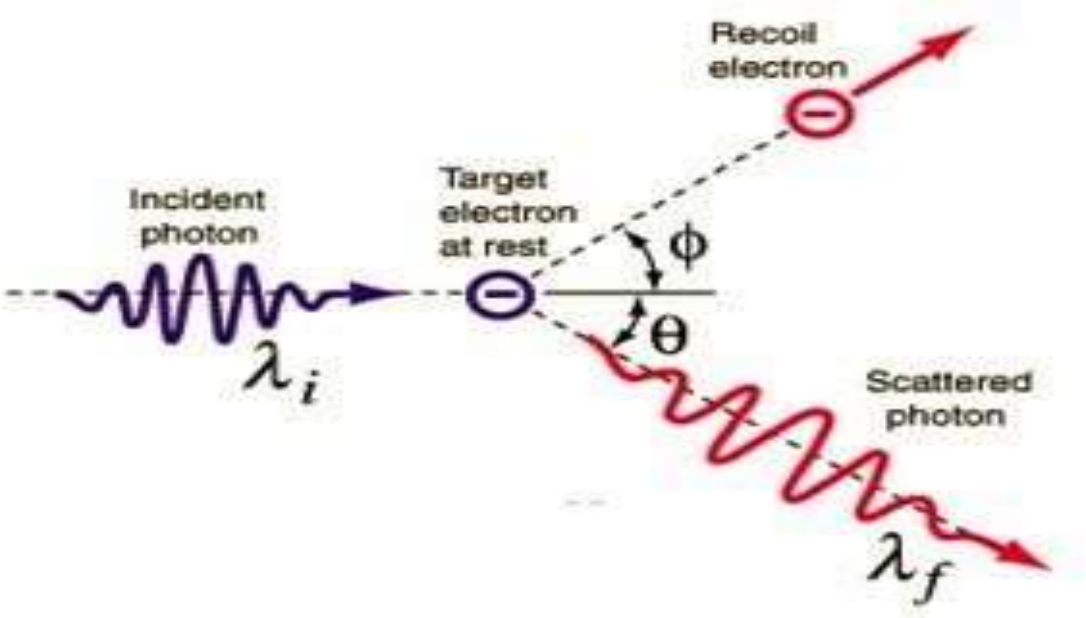

Figure 2.14: Schematic diagram of the Compton scattering process [43]

$$h\nu' = \frac{h\nu}{1 + \frac{h\nu}{(m_o c^2)}(1 - cos\ \theta)} \quad \text{----------2.23}$$

where $m_o c^2$ is the rest-mass energy of the ejected electron (0.511 MeV). It then follows that the kinetic energy of the recoil electron is given by [14, 42] .

$$E_{e^-} = hv - hv' = hv\left(\frac{(\frac{hv}{m_o c^2})(1-cos\theta)}{1+(\frac{hv}{m_o c^2})(1-cos\theta}\right) - - - - - - - - - - - - - - - 2.24$$

When angle $\theta \approx 0$, the recoil electron carries away minimum energy and the scattered gamma ray has almost the same energy as the incident gamma ray. However, when $\theta \approx 180°$, the recoiling electron carries the maximum energy. This maximum amount of energy absorbed during Compton scattering is called the "Compton edge". Therefore, the energy of the recoil electron can vary from zero (when $\theta \approx 0$) to a maximum (when $\theta \approx 180°$) depending on the scattering angle.

The maximum energy of the recoil electron is given by [14, 22]

$$E_{e^-} = \frac{2hv}{2+\frac{m_o c^2}{hv}} - 2.25$$

The probability of Compton scattering depends strongly on the number of electrons per unit mass of the interacting material. It also depends on the incoming gamma-ray energy as a function of $1/E_\gamma$ [6, 29].

2.4.3. Pair production

When the energy of the photon or gamma ray is very large ($E > 2m_oc^2 = 1.02$ MeV) its absorption can result in creating a positron and an electron (both having a rest mass energy equivalent of 0.511 MeV) with a total energy equal to that of the photon. The probability of this interaction remains low until the gamma ray energy approaches several MeV and therefore, pair production is predominantly confined to high energy gamma rays [27, 37]. In the interaction (which takes place in the coulomb field of a

nucleus), the gamma ray or photon disappears and is replaced by an electron-positron pair. All the excess energy carried in by the photon above the 1.02 MeV required to create the pair goes into the kinetic energy shared by the positron and the electron [27, 29]. When a positron comes to rest, it interacts with another electron, resulting in the annihilation of both particles and the complete conversion of their rest mass back to pure energy (according to the $E = mc^2$ formula) in the form of two oppositely directed 0.511 MeV gamma rays (photons) [14]. Pair production cannot take place in a free space because conservation of energy and conservation of momentum cannot be simultaneously observed. This process requires the presence of a massive atom for momentum conservation [37]. Figure 2.15 illustrates the process of the pair production interaction.

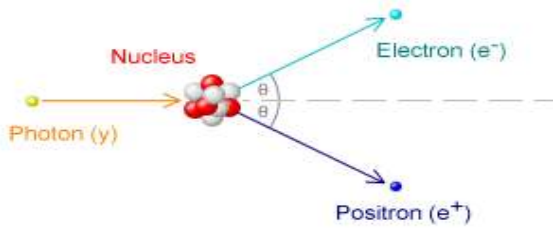

Figure 2.15: Schematic diagram of the pair production process [44]

Figure 2.16 shows the importance of the three principal gamma-ray interaction processes as a function of energy and atomic number Z of the material.

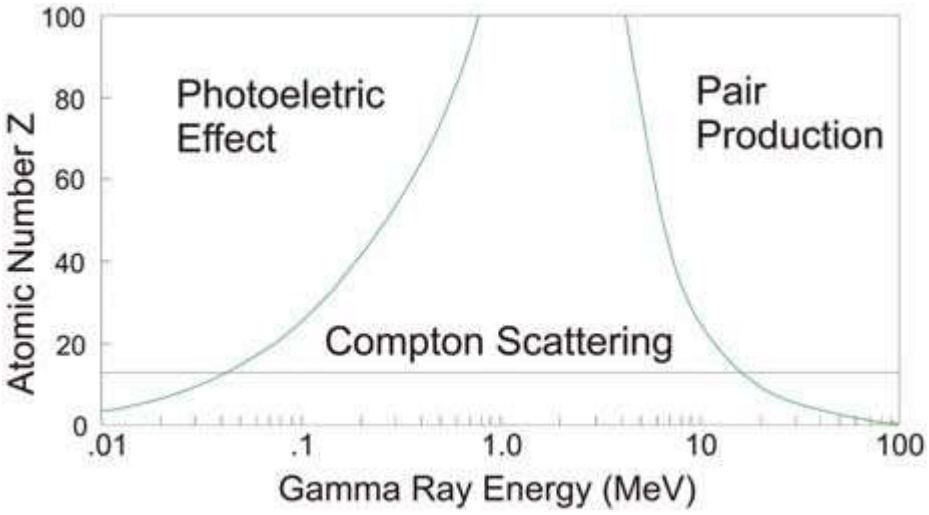

Figure 2.16: Energy dependence of the three gamma ray interaction processes [45]

2.5. Radiation detectors

Since ionizing radiation cannot be seen with the naked eyes, or be smelled or tasted even though they can pass through a human body, then one depends on instruments to detect this radiation. Some detectors used in detecting radiation will be discussed in this section.

In nuclear physics, radiation detector is defined as an instrument used to detect, track, and/or identify ionizing particles, such as those produced by nuclear decay, cosmic radiation, or reactions in a particle accelerator [29]. These detectors are used widely in research and teaching laboratories, industries and in the health or medical field.

2.5.1. Gas-filled counters

This instrument works on the principle that when ionizing radiation passes through air or a specific gas, ionization of the molecules in the air or gas occur and ion pair will be produced depending on the type and pressure of the gas [21, 46]. When a voltage is applied between electrodes in a gas-filled space, the positive ions will be attracted to

the negative side of the detector (the cathode) and the free electrons will travel to the positive side (the anode) [21, 29]. When these ions hit the surface, they produce a current or electrical signal that can be measured by the detector [46]. The strength of the electric field between the electrodes and the type and pressure of the gas determine the detector's response to ionizing radiation. Gas-filled detectors include ionization chambers, proportional counters, and Geiger-Muller (GM) counters [47]. Figure 2.17 illustrates the operations of the gas-filled counters.

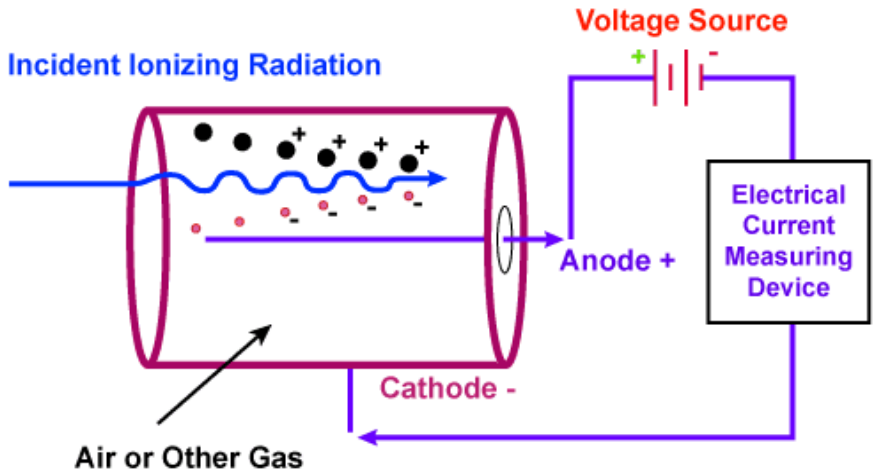

Figure 2.17: Schematic diagram of the gas-filled counter [48]

Figure 2.18 shows the variation of the generation of ion pairs with applied voltage. The ion pairs collected in the detector chamber are influenced by the applied voltage, which also determines operations for alpha and beta particles. When there is a low voltage in the chamber, there would be no charge passing to the external circuit for alpha or beta radiation and the ion pairs would recombine [21]. The response is minimal and not valid for radiation detection. This region is called a region of recombination [46]. As the voltage increases gradually, the recombination decreases

and the response increases and the region of ion saturation is created. As the voltage increases further, the system brings the output into the proportional region. Ionized electrons cause additional ionization of the gas [47]. However, this is proportional to the amount of the original ion pairs produced. This is termed a gas amplification. In the proportional region, the increased voltage causes the ions to move with increased kinetic energy toward the electrodes [21, 29, 46]. These energized electrons collide with other gas atoms and create additional ion pairs. The increased voltage affects these ion pairs also, and the effect is amplified [49]. If the applied voltage is increased further, there is a point where a single electron-ion pair generated is enough to initiate an avalanche of electron-ion pairs, and it is called the limited proportional region [29]. In this region, the new ions produced are no longer proportional to those produced by the primary radiation [22]. With further increase in the applied voltage, the new ion pairs produced are so many that even a low energy ionization particle incident on the counter will produce a very large pulse. This region is called the Geiger-Mueller region (GM-region). A Geiger-Mueller counter (GM survey meter) operates in this region and is a useful tool for detecting and searching for often unknown sources of radiation [27, 49]. If the applied voltage is increased further (beyond the voltage in the GM region), then a single ionization will result in the continuous discharge of the gas. No gas-filled detectors operate in this region.

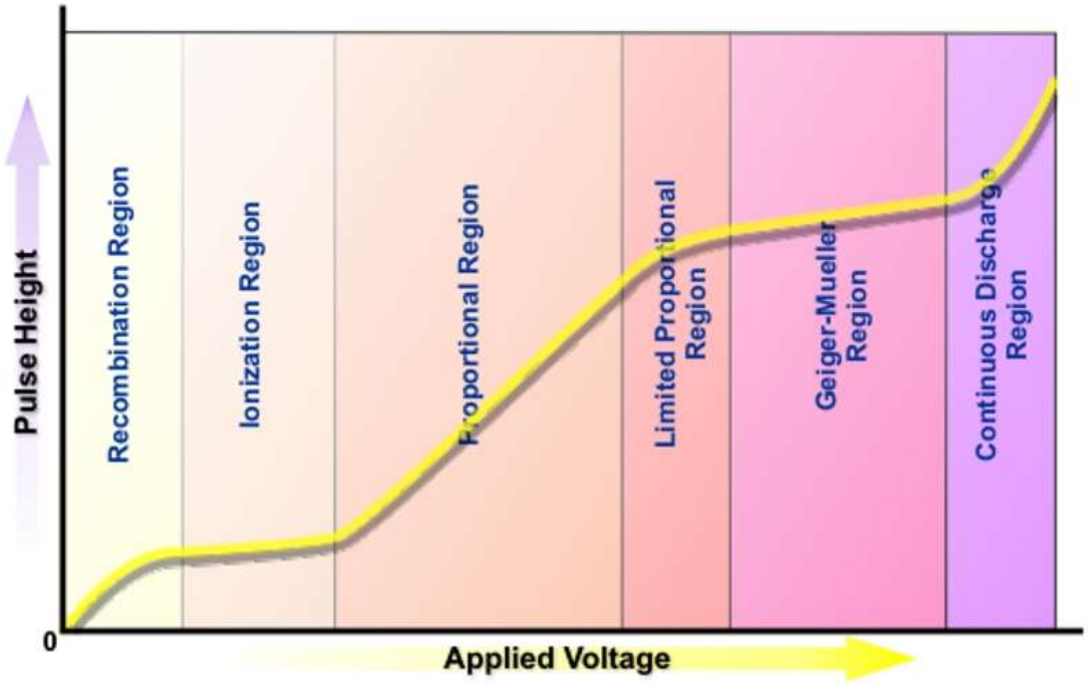

Figure 2.18: Variation of pulse height with applied voltage in a gas-filled counter [50]

2.5.2. Scintillation detector

The basic principle behind this instrument is the use of a special material that glows or "scintillates" when radiation interacts with it. The most common type of material is a salt called sodium-iodide [29]. The light produced from the scintillation crystal hits the photomultiplier tube, as shown in Figure 2.19. The photomultiplier tube is made of the special material called a photocathode [21]. The photocathode produces electrons when light strikes its surface [14, 21]. These electrons are then pulled towards a series of plates called dynodes through the application of a positive high voltage. When electrons from the photocathode hit the first dynode, several electrons are produced for each initial electron hitting its surface [47]. This "bunch" of electrons is then pulled towards the next dynode where more electron "multiplication" occurs. The sequence continues until the last dynode is reached, and finally a shower of electrons is collected at the anode at the end of the tube, forming an electronic pulse

[21, 29]. The pulse is then detected and displayed by the instrument. Figure 2.19 shows the operations of scintillation detectors.

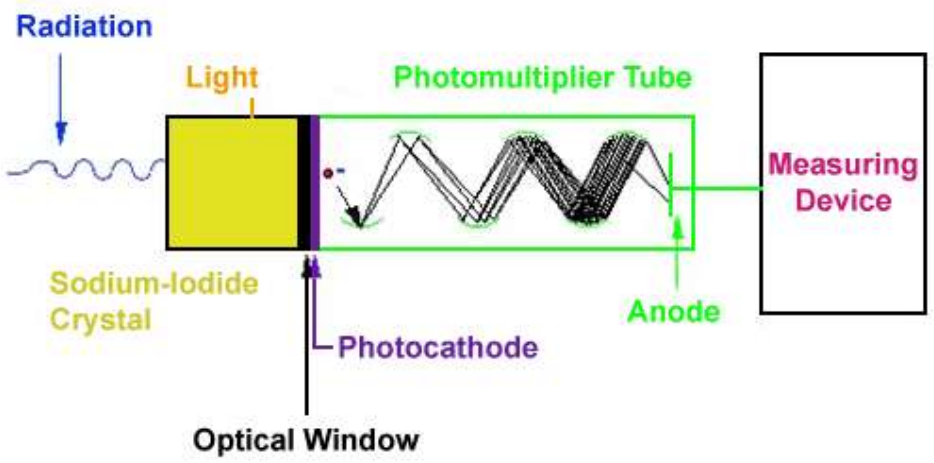

Figure 2.19: Schematic diagram of the operation of a scintillation detector [48]

2.5.3. High-Purity Germanium (HPGe) detector

High-Purity Germanium (HPGe) detectors are semiconductor diodes having a p-i-n structure in which the intrinsic region is sensitive to ionizing radiation, particularly x-rays and gamma rays [29]. Under reverse bias, an electric field extends across the intrinsic or depleted region [21]. When photons interact with the material within the depleted volume of a detector, charge carriers (holes and electrons) are produced and are swept by the electric field to the P and N electrodes. This charge, which is proportional to the energy deposited in the detector by the incoming photon, is converted into a voltage pulse by an integral charge sensitive preamplifier.

Germanium has a relatively low band gap. Therefore, these detectors must be cooled to reduce the thermal generation of charge carriers (thus reverse leakage current) to an acceptable level. Otherwise, leakage current induced noise destroys the energy resolution of the germanium detector. Liquid nitrogen, which has a temperature

of 77 K, is the common cooling medium for such detectors [27, 29]. The germanium detector is mounted in a vacuum chamber that is attached to or inserted into an LN2 Dewar. It thus protects the sensitive detector surfaces from moisture and condensable contaminants [29]. The energy resolution of these detectors is high, but because of their small volume, their efficiency is low and it may take several minutes to record a spectrum. Arrangement of p-type and n-type semiconductor detectors is shown in Figure 2.20

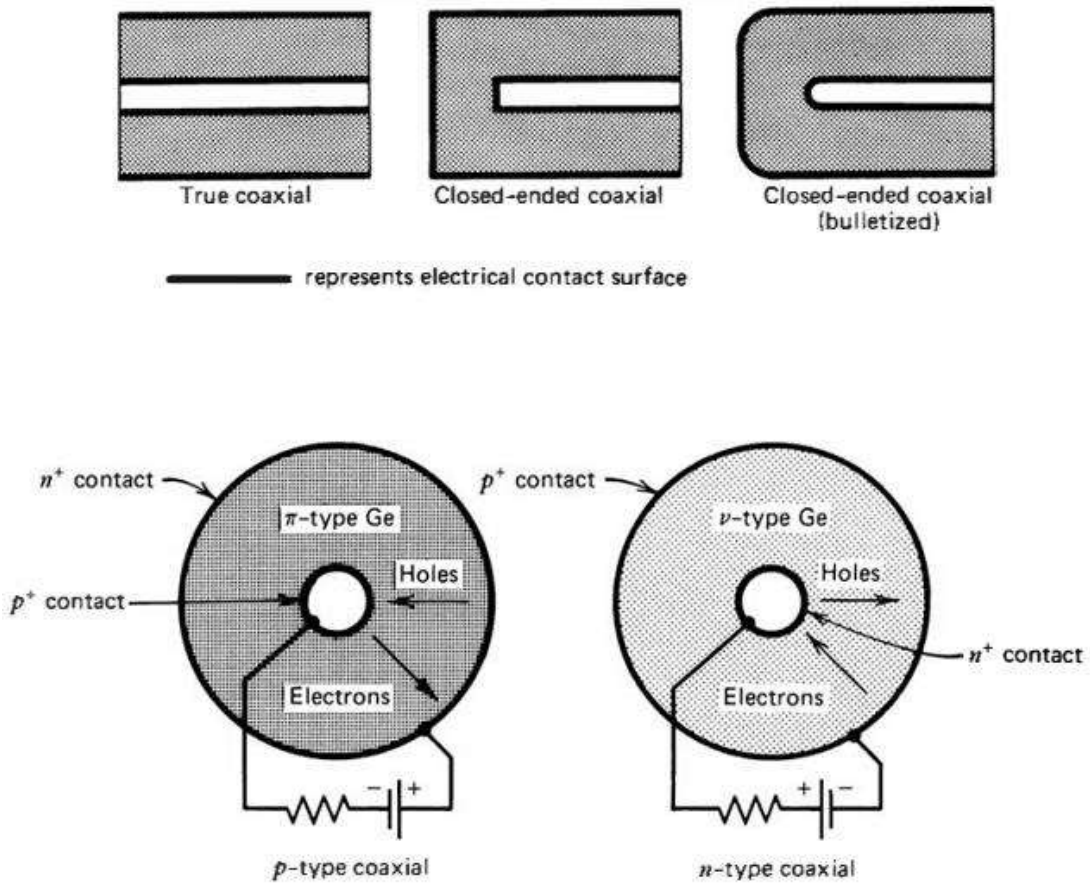

Figure 2.20: Configuration of closed end coaxial n-type and p-type semiconductor detectors and cross-sections perpendicular to the cylindrical axis of the high-purity Germanium p or n type crystal and corresponding electrode configuration for each type [51]

2.6. Biological effects of ionizing radiation

The interaction of ionizing radiation with the human body, arising either from external or internal sources, can affect the atoms inside the body, and it could pose a health risk. Consequently, the interaction of radiation with the human body could result in the damage and death of living cells and mutations of genetic materials [14, 21]. The amount of damage depends on the type, energy and amount of radiation absorbed [6, 34]. In general, the risks associated with ionizing radiation may be grouped into two groups, which are stochastic and deterministic risks [52].

2.6.1 Stochastic risks

Stochastic effects are typically associated with long term, low-level (chronic) exposure to radiation [14]. The word stochastic refers to the likelihood or probability that an effect will happen; thus, this occurs randomly. There is no threshold level, as shown in Figure 2.21(a). This means that for any amount of radiation dose received, there is a probability that it may cause an effect (some time later, probably years) [52]. However, the probability the effect will occur increases with the dose received. Threshold level is defined as the minimum dose of ionizing radiation that can produce a detectable degree of an effect. Hereditary effects and cancer incidence are examples of this risk.

2.6.2. Deterministic effects

Deterministic effects depend on time of exposure, doses and type of radiation. It has a threshold of dose below which effect does not occur. However, the severity of effects on human beings increases with increasing doses [7, 34, 53]. Examples of these are

erythema (skin reddening), cataracts to lens of the eye, sterility & epilation (loss of hairs).

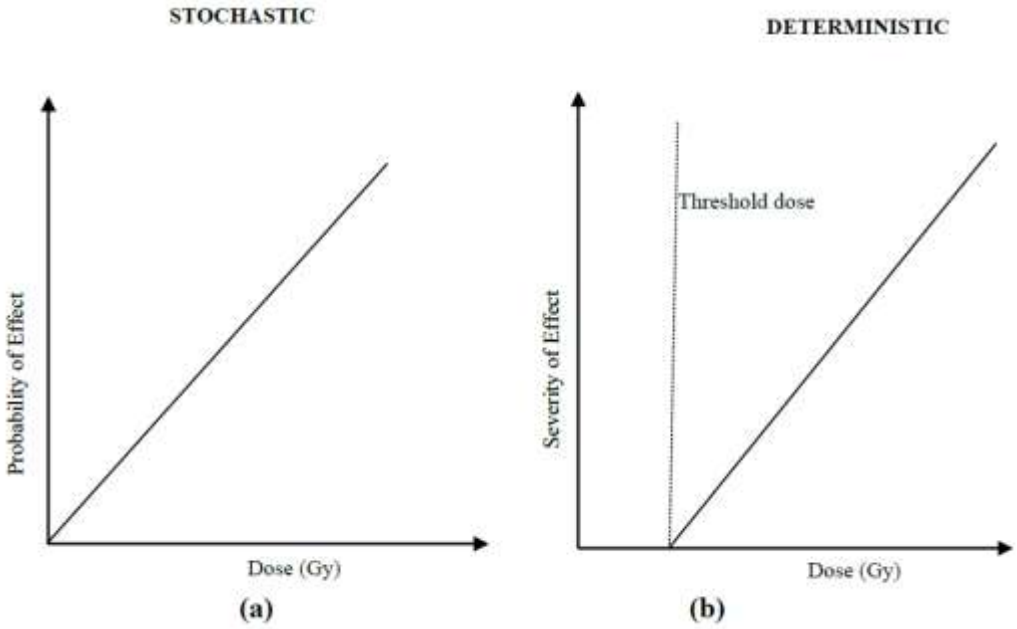

Figure 2.21: Differences between (a) stochastic and (b) deterministic effects of radiation [54]

2.7. Radiation quantities and units

Exposure

Exposure is defined as the amount of ionizations that gamma and X-rays produce in air. The first unit of exposure is called roentgen (R) which was introduced in 1928. This unit is based on the production of a 1esu of charge (of either sign) per 0.001293 g or 1 cm^3 of air at standard temperature and pressure [14, 29]. The unit of exposure is based on charge/mass of air (C/kg), so that $1R = 2.58 \times 10^{-4}\ {}^{\mathrm{C}}/_{\mathrm{kg}}$ [6, 14, 29] since $1\ esu = 3.34 \times 10^{-10} C$ [37]. Thus, the SI unit of exposure is given as C/kg. The exposure unit is only measured in air and only applies to electromagnetic radiation.

Absorbed Dose

The concept of exposure and its unit (roentgen) was only defined in terms of electromagnetic radiation in air and does not reflect the biological effect of the radiation. However, there was a need to introduce a unit that considers the quantity of energy absorbed by any kind of ionizing radiation in any kind of material. For this reason, the quantity called absorbed dose was introduced. Absorbed dose is defined as the amount of energy absorbed per unit weight of the organ or tissue and is expressed in the unit of Gray (Gy), where 1Gy is equivalent to one joule of radiation absorbed energy per kilogram of the material [7, 14]. The original unit of absorbed dose is rad, which is defined as 100 erg per gram and is related to SI unit Gy as [14, 29]

$$1Gy \equiv \frac{1\text{J}}{\text{kg}} = \frac{10^7\text{erg}}{10^3\text{g}} = 10^4\,\frac{\text{erg}}{\text{g}} = 100\text{ rad}$$

Equivalent Dose

The absorbed dose only tells us the amount of energy deposited, but it does not take into account the biological effects due to radiation. For this reason a new unit had to be introduced. Equal doses of all types of ionizing radiation do not produce equal biological effects [52]. For a given absorbed dose, an alpha particle produces more harm than beta particles and gamma rays. The concept of equivalent dose (H_T) was introduced, which is defined as a measure of the radiation dose to tissue where an attempt has been made to allow for the different relative biological effects of different ionizing radiation and expressed in the unit of Sievert (Sv) [14, 37]. H_T is obtained from the product of absorbed dose ($D_{T,R}$) deposited over the tissues or organ T, and

radiation weighting factor w_R [37, 52]. This factor is independent of the type and energy of the radiation.

The equivalent dose is calculated from the absorbed dose as follows [14, 29] ;

$$H_T = \sum w_R . D_{T,R} \quad \text{---------- 2.26}$$

where H_T is the equivalent dose in sieverts (Sv) absorbed by tissue T, $D_{T,R}$ is the absorbed dose in grays (Gy) in tissue T by radiation type R and w_R is the radiation weighting factor defined by regulation.

In 2007, the International Commission on Radiological Protection published a new set of radiation weighting factors, as presented in Table 2.2

Table 2.2: Recommended radiation weighting factors [52]

Type of radiation	**Energy range**	**Weighting factors (w_R)**
X-rays, gamma rays, beta particles, muons	All energies	1
Neutrons	< 1 MeV	$2.5 + 18.2e^{-\lvert\ln(E_n)\rvert^2/6}$
	1 MeV- 50 MeV	$5.0 + 17.0e^{-\lvert\ln(2E_n)\rvert^2/6}$
	> 50 MeV	$2.5 + 3.25e^{-\lvert\ln(0.04E_n)\rvert^2/6}$
Protons, charged pions		2
Alpha particles, fission fragments, heavy ions		20

Effective dose

The radiation dose to the body is not uniform. Because of this non-uniformity, the concept of effective dose was introduced. Effective dose is used to measure the

radiation risk to which the individual is exposed [52]. This also considers the sensitivity of the affected body parts. The probability of the effect from radiation exposure depends on the parts of the body exposed. Organs or tissues have different sensitivity to the radiation; some are more sensitive than the other. The SI unit of the effective dose is Sievert (Sv) [7, 29]. Effective dose (E) is the sum of the equivalent doses weighted by the tissue weighting factor for each tissue [7, 14, 52].

$$E = \sum_{T} H_T w_T \quad \text{---------- (2.27)}$$

where H_T is the equivalent dose weighted by the tissues T and w_T is the tissue weighting factor.

The tissue weighting factors for different organ or tissue according to report 103 of ICRP 2007 are shown in Table 2.3.

Table 2.3: Recommended tissue weighting factors [52]

Tissue or Organ	**Tissue weighting factors w_T**
Red bone-marrow, Colon, Stomach, Lung, Breast, Remainder tissues	0.12
Gonads	0.08
Bladder, Oesophagus, Liver, Thyroid	0.04
Bone surfaces, Brain, Salivary glands, Skin	0.01

Remainder tissues : Adrenals, Extrathoracic (ET) region, Gall bladder, Heart, Kidneys, Lymphatic nodes, Muscle, Oral mucosa, Pancreas, Prostate, Small intestine, Spleen, Thymus, Uterus/cervix .

2.8. Review of studies on natural radioactivity

There have been many studies on natural radioactivity in the soils of different towns and places in different countries. These studies provide information on the levels of background radiation in these towns and places.

2.8.1 International studies

An investigation of the activity concentrations and distributions of radioactive nuclides in river sediments and coastal soils of Chittagong, Bangladesh was done by Chowdhurry, Alam and Hazari in 1999. The results obtained for the activity concentrations of ^{238}U, ^{232}Th and ^{40}K were higher than the worldwide average values of 35, 30 and 400 Bq kg^{-1} respectively [55].

Similarly, in 2004 a study on the activity concentration levels arising from the radionuclides ^{238}U, ^{232}Th and ^{40}K in the surface soils of Cyprus was carried out by Tzortzis, Svoukis and Tsertos. The concentrations of ^{238}U, ^{232}Th and ^{40}K were found to range between 0.01 and 39.3, 0.01 and 39.8 and 0.04 and 565.8 Bq kg^{-1}, respectively [56] . Also, measurement of the activity concentrations of Radium-226 (^{226}Ra) in the soil samples collected from Karbala Governorate has been made using gamma ray spectroscopy with NaI (TL) scintillation detector. The activity concentration of ^{226}Ra was found to vary from 11.41 ± 3.37 to 99.6 ± 16.8 Bq kg^{-1} [57].

In addition, the Natural radioactive concentration analysis was carried out in the sand sediments that were collected from the shallow inner shelf region of an ecologically sensitive mangrove forest area at Krusadai Island in Gulf of Mannar near

Rameswaram, Tamil Nadu, India [58]. Gamma spectrometry was employed in the study and a NaI (Tl) detector was used to detect gamma rays. The mean activity concentration of ^{238}U was found to below the detectable limit (BDL) while ^{232}Th had the range between BDL to 27.81 ± 8.9 Bq/kg while ^{40}K had the range from BDL to 413.13 ± 49.6 Bq/kg. It was also reported that the other radiological parameters were all found to be below their prescribed limit.

A similar study of the activity concentrations of naturally occurring radionuclides in soils was carried out in the Punjab province of Pakistan, a neighbor of India. A p-type coaxial HPGe-based gamma ray spectrometer was used in the study. The mean concentrations of ^{232}Th, ^{238}U and ^{40}K were found to be 41 ± 8 Bq kg^{-1}, 35 ±7 Bq kg^{-1} and 615 ± 143 Bq kg^{-1} respectively [31].

In Ghana, the activity concentration of natural radionuclides ^{226}Ra, ^{232}Th and ^{40}K in soil, rock, waste and tailing samples were measured by gamma spectrometry using high-purity germanium detector. The average activity concentrations of ^{226}Ra, ^{232}Th and ^{40}K were 13.61 ± 5.39 Bq kg^{-1}, 24.22 ± 17.15 Bq kg^{-1} and 162.08 ± 63.69 Bq kg^{-1} and the average annual effective dose was 0.17 ± 0.09 mSv y^{-1} [59].

There are other studies carried out in different countries on determining the natural radioactivity due to ^{232}Th, ^{238}U and ^{40}K [60-62].

2.8.2. National studies

The natural radioactivity in the soil samples of the University Of Namibia, Windhoek have been studied. The concentrations were measured using a sensitive γ-ray spectroscopic system consisting of an HPGe detector and associated equipment. ^{40}K was found to have the highest specific concentration varying between 306.8 ± 15.2

Bq kg^{-1} and 720.8 ± 428.4 Bq kg^{-1} with a mean value of 444.7 ± 101.8 Bq kg^{-1} while the concentration of ^{232}Th varied between 17.5 ± 2.3 Bq kg^{-1} and 38.1 ± 3.3 Bq kg^{-1} with a mean value of 20.5 ± 4.7 Bq kg^{-1} and ^{238}U varied between 14.7 ± 1.5 Bq kg^{-1} and 29.7 ± 2.0 Bq kg^{-1} with a mean value of 20.4 ± 4.0 Bq kg^{-1}. The corresponding effective dose rate was 0.06 ± 0.01 mSv y^{-1}. This result shows that the University of Namibia is in an area of normal background radiation [2].

The natural radioactivity in the soils of Henties Bay has also been studied. The activity concentrations of radionuclides were measured using sensitive γ-ray spectroscopic system consisting of an HPGe detector and associated accessories. The corresponding annual effective dose obtained was 0.16 ± 0.04 mSv y^{-1}. Thus, the results reveal that Henties Bay has normal background radiation [63].

Other studies were carried out to determine the concentration of ^{232}Th, ^{238}U and ^{40}K in the soils of different parts of Namibia. Such studies are those on the soils of the *International High-energy stereoscopic system (HESS) project*, in the four major towns in northern Namibia [64, 65] and Windhoek city [66]

CHAPTER 3: RESEARCH METHODOLOGY

3.1. Description of the study areas

Ohorongo Cement plant is located 25 km from Otavi in the farm called Sargberg, in the Otjozondjupa region. It is 435 km north of the capital city, Windhoek, at coordinates 19˚30'68''S and 17˚27'23''E. The word Ohorongo means Kudu in the Otjiherero language. The Ohorongo Cement plant is owned by the German Schwenk Zement KG, and a group of development finance institutions - namely, the South African Industrial Development Corporation and the Development Banks of Namibia and South Africa and was opened in 2011 [11]. This Cement plant in Namibia, is a major source of employment for the people around the area. The environment of the plant has a large deposit of raw materials used for Cement production such as limestone, shale and marl, and they are estimated to be sufficient for another 300 years. The soil type appears to be sandy, ranging in colour from pale brown and grey with broken calcrete pieces in it, to a fine red sand – apparently of aeoloian origins.

Otavi is a town in the Otjozondjupa region and had a population of 5242 in 2011 [12]. Together with the towns of Grootfontein and Tsumeb they form the so-called Otavi-triangle, also known as the Copper or Maize triangle, which is referring to an area used for cultivation and mining activities. The town is covered by Arenosols soils. The Arenosols are low water holding soils with low nutrient levels. The river systems and marimbas contain the highly fertile Fluvisols, which is valuable for agriculture land. The rocks are dominated by limestone that dissolves easily in water, forming large underground caverns, lakes (such as Lake Otjikoto and Lake Guinas) and aquifers of underground water [67].

The town of Otavi is situated within the higher rainfall area of the country where annual rainfall is between 500-550 mm. Rainfall is between October and April, with the wettest months being January and February. The region is also prone to high levels of humidity, with the most humid month (March) recording between 80-90% humidity.

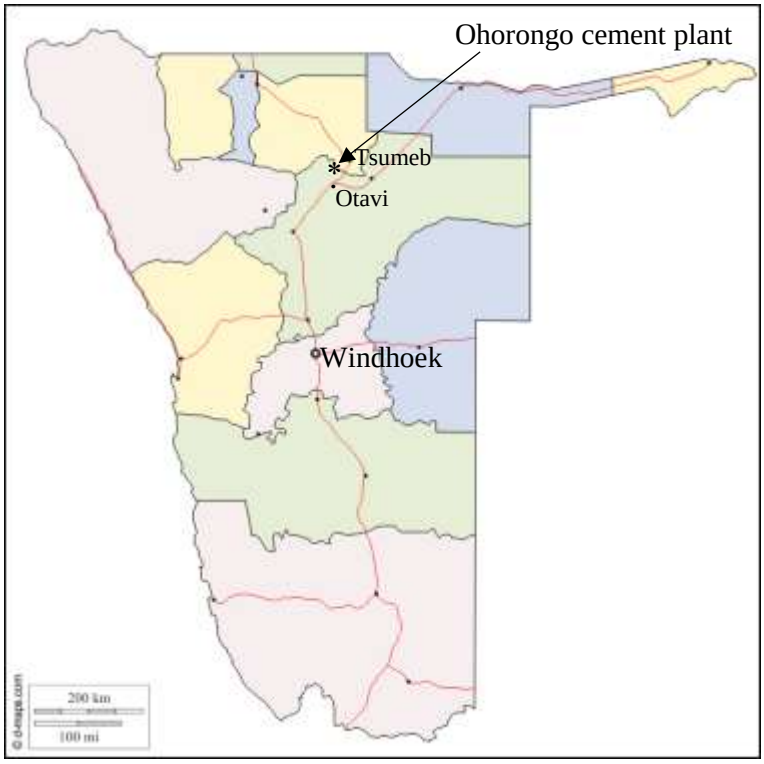

Figure 3.1: Map of Namibia showing the locations of the Ohorongo Cement plant and Otavi

3.2. Sample collection

Fifty soil samples were collected around and inside the Cement plant and another fifty samples were collected across ten different geographical areas of the town of Otavi using clean hand augers (Figure 3.2 (a)) at a depth of about 5 cm below the surface of the soil. The soil samples were collected randomly but away from disturbed areas,

roads, buildings, and rivers. Figure 3.2 (b) shows the photographs of the people that collected soil samples. A mass of about one kilogram of soil was collected from each point and was placed in a well-labeled plastic bag and tightened. The label on the plastic includes information such as sample ID. The soil samples were then transported to the nuclear laboratory at the University of Namibia in Windhoek. Figures 3.3 and 3.4 shows the different areas from which soil samples were collected.

Figure 3.2: (a) Photograph of shovels and spade used in sample collection and (b) Photograph of people who took part in sample collection- from left to far right are: (1) a local worker (2) Mr. S A Shimboyo (3) Prof J A Oyedele (4) another local worker and (5) Mrs. M M Nambinga (the researcher)

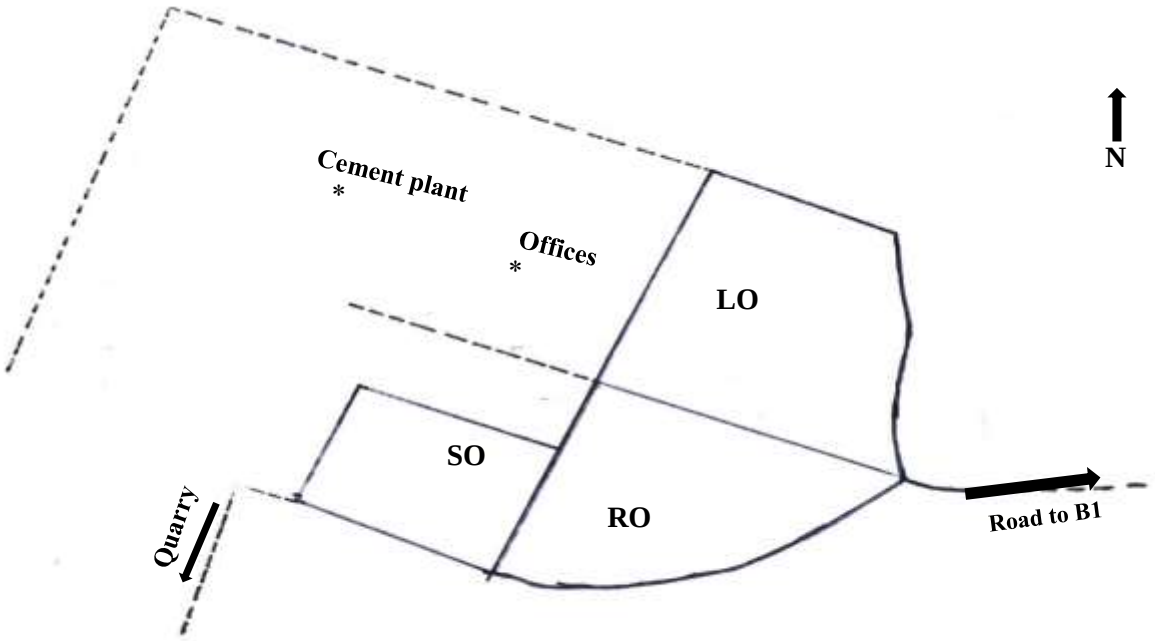

Key	
Location ID	**Location name**
RO	Right side (outside) the plant
LO	Left side (outside) the plant
SO	Inside the plant

Figure 3. 3: The areas from which soil samples were collected at Ohorongo Cement plant

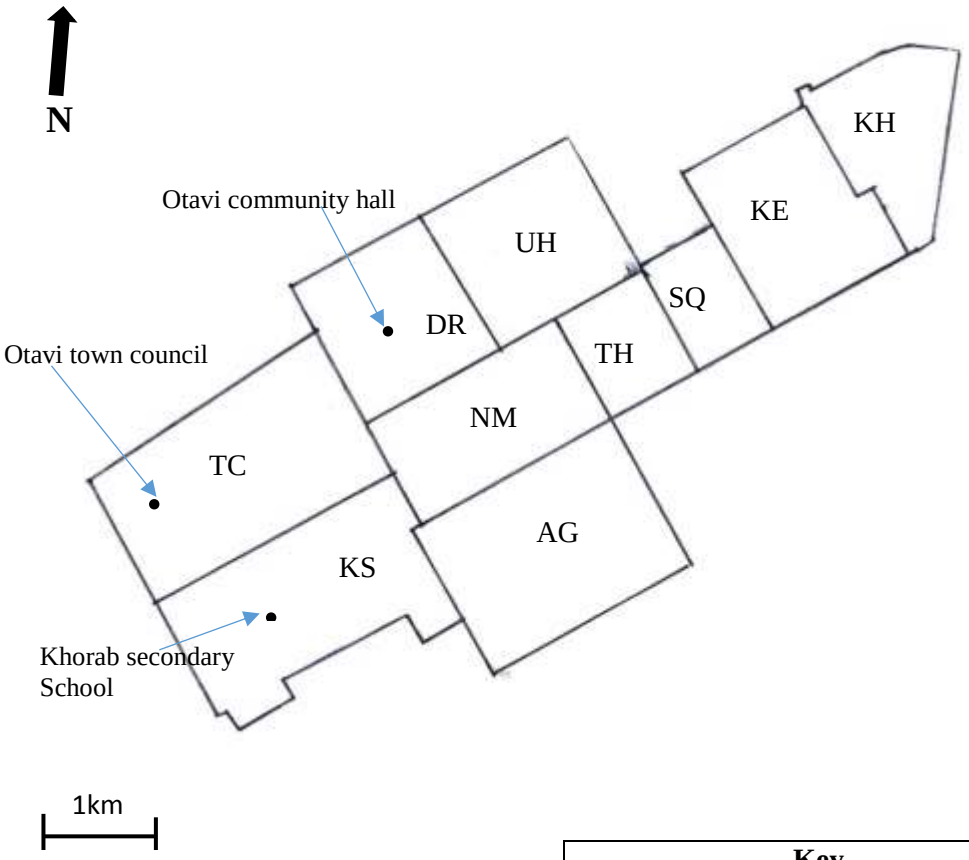

Key	
Location ID	**Location name**
TC	Town council area
KS	Khorab School area
DR	DRC location area
NM	Namib mill's area
AG	Agra Otavi extension 1
UH	Unita hostel area
TH	#Hoababere area
SQ	Ombili location area
KE	Khoaeb extension 2
KH	Khoaeb extension 1

Figure 3. 4: The areas from which soil samples were collected at Otavi

3.3 Sample Preparation

Samples were allowed to dry under laboratory temperature for about two weeks (Figure 3.5). The dried samples were crushed using a mortar and pestle (Figure 3.6 (a)) and sieved using a 2 mm mesh sieve (Figure 3.6 (b)). 500 g of each homogenized soil sample were placed in a well-labelled polythene bottle. All the samples were sealed and allowed to stand for about 31 days to achieve secular equilibrium between ^{238}U and ^{232}Th series and their progenies. Figures 3.5 -3.9 show the procedure for sample preparation.

Figure 3.5: Drying of soil samples at room temperature

Figure 3.6: Apparatus used for sample preparation. (a) A mortar and pestle for crushing and (b) 2 mm mesh sieve

Figure 3.7: Pulverizing and sieving of soil samples

Figure 3.8: Weighing of soil samples

Figure 3.9: Sealed soil samples left for 31 days

3.4. Experimental set-up and measurement techniques

3.4.1. Instrumentation

In this study, the activity concentrations of radionuclides in different soil samples were measured using a high-resolution, low background gamma ray spectrometry system. The gamma-ray spectrometry system consists of a coaxial high-purity germanium (HPGe) detector (Canberra model GC2519) (at the center of a lead shield as shown in figures 3.10. The detector was enclosed with a 10 cm thick cylindrical lead shield to reduce the contamination from background radiation from various radiation sources nearby. The lead shielding was graded with an inner layer of 0.1 cm thick copper to minimize the effect of X-ray from lead. A Model 7915-30 Cryostat (Base Model 7915-30) was used to supply liquid nitrogen (LN2) to the detector, with a Model 2002C Pre-amplifier as shown in Figure 3.11. The detector was cooled with liquid nitrogen to reduce the noise in the detector. Liquid nitrogen was provided regularly every week. The detector was connected to the preamplifier, amplifier, high voltage power supply and, multi-channel analyzer, as shown in Figure 3.12. A Genie® 2000 software version 3.2.1 was used to analyze the gamma-ray spectra acquired in the measurements.

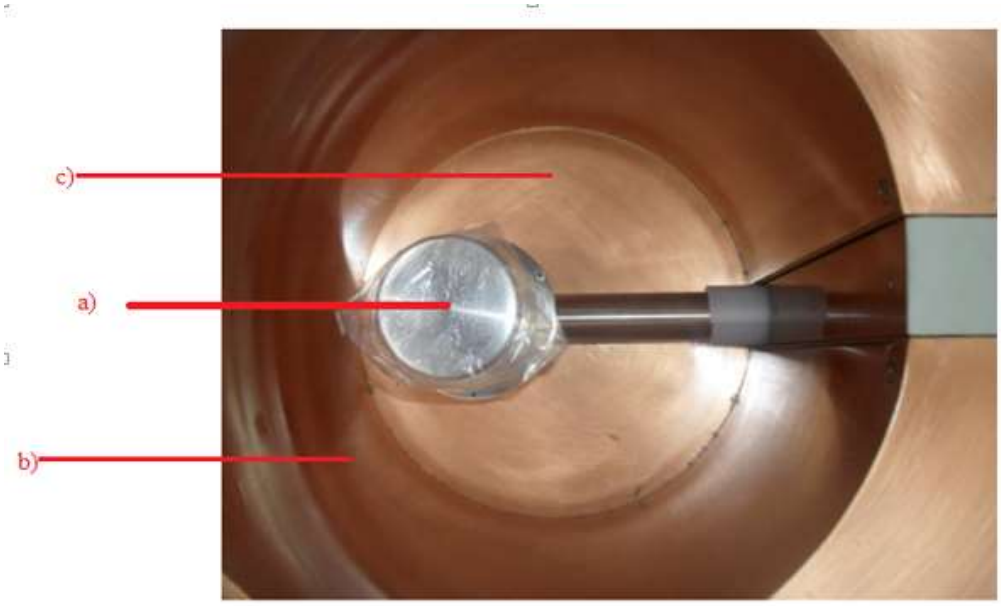

Figure 3.10: Configuration of the detector used in this study. (a) HPGe detector at the center of a lead shield (b) Cylindrical lead material (c) Inner layer of copper.

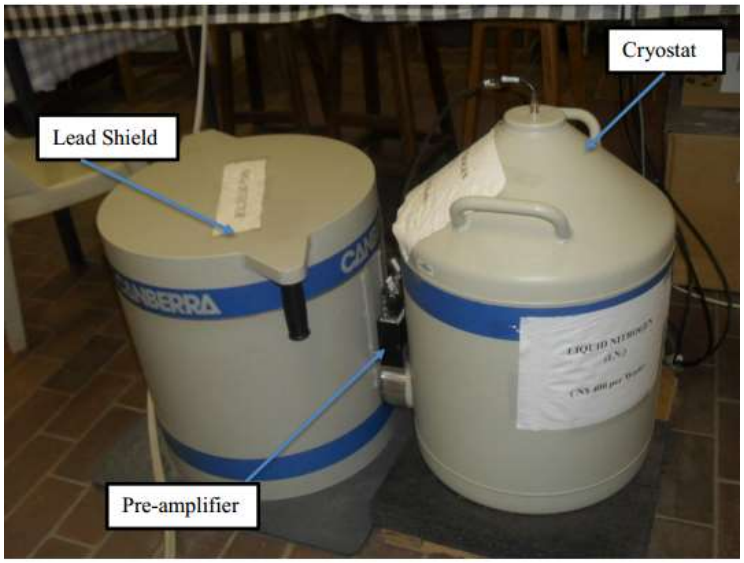

Figure 3.11: A coaxial HPGe detector and a cryostat

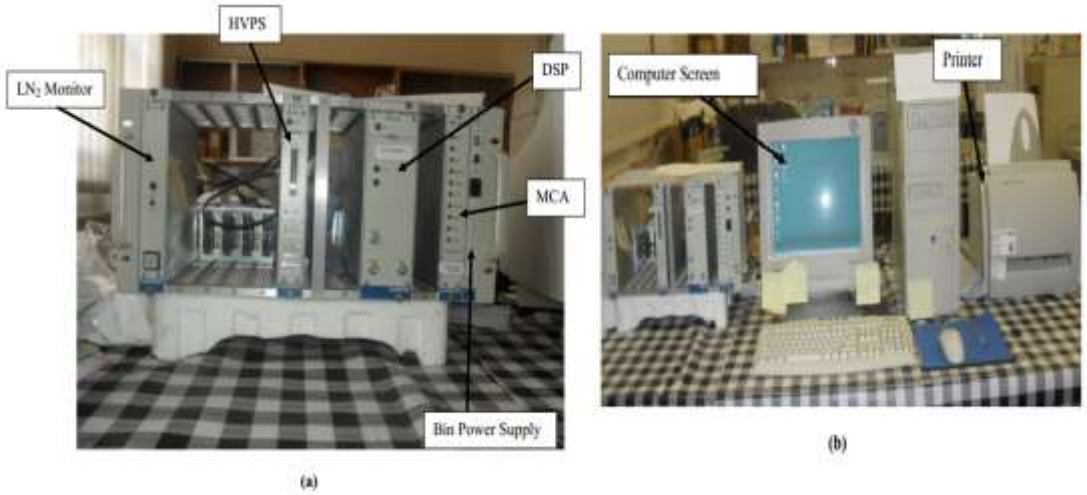

Figure 3.12: Electronic instrument used in the study. (a) Electronic system of an HPGe detector and (b) computer system with Genie 2000 software.

The electronic system consists of the detector, preamplifier, amplifier, Multi-channel analyzer (MCA) and a computer, as shown in figure 3.13. A bias voltage was been supplied and as photon interactions occurs within the depleted region, charging carriers are swept to their collecting electrodes by the electric field. The preamplifier then convert the charge into a voltage pulse proportional to the energy. The voltage pulse produced by the preamplifier travels a certain distance without much loss of energy to an amplifier that shapes and amplifies the signal. The signals then go to a digital signal processor (DSP) that quantifies the energy from the detector and sends it to a multi-channel analyzer (MCA). The MCA scan a whole range of energy and records the digital number of pulse according to their pulse height. After this was done the digital information was stored in the computer memory and γ-ray spectrum was generated.

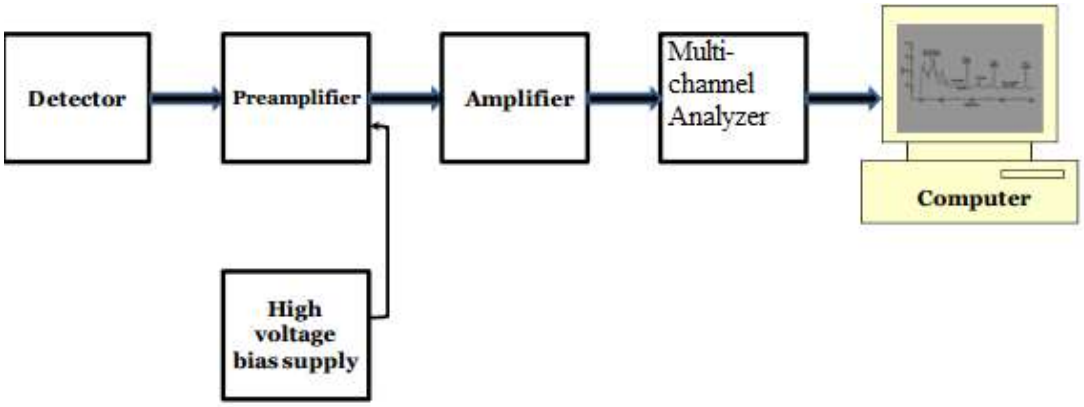

Figure 3. 13: Components of the radiation detection system

3.4.2. Calibration of detector

The relationship between channel numbers and gamma-ray energies was determined before taking any measurement. The establishment of this relationship is called energy calibration. This was done by using gamma lines of known energies.

In this study, ^{22}Na, ^{60}Co and ^{137}Cs point sources were used to calibrate the detector. The three point sources were placed on the detector and the radiation emitted was counted for the 1800s (30 min). The energy of each peak and the corresponding channel number were recorded as shown in Table 3.1. The energy calibration curve obtained using the point sources is shown in Figure 3.14.

Table 3.1: Energies and corresponding channel numbers of point sources

Point Source	**Energy (keV)**	**Channel number**
^{22}Na	1274.3	2154
^{60}Co	1172.5 1331.6	1982 2251
^{137}Cs	660.7	1117

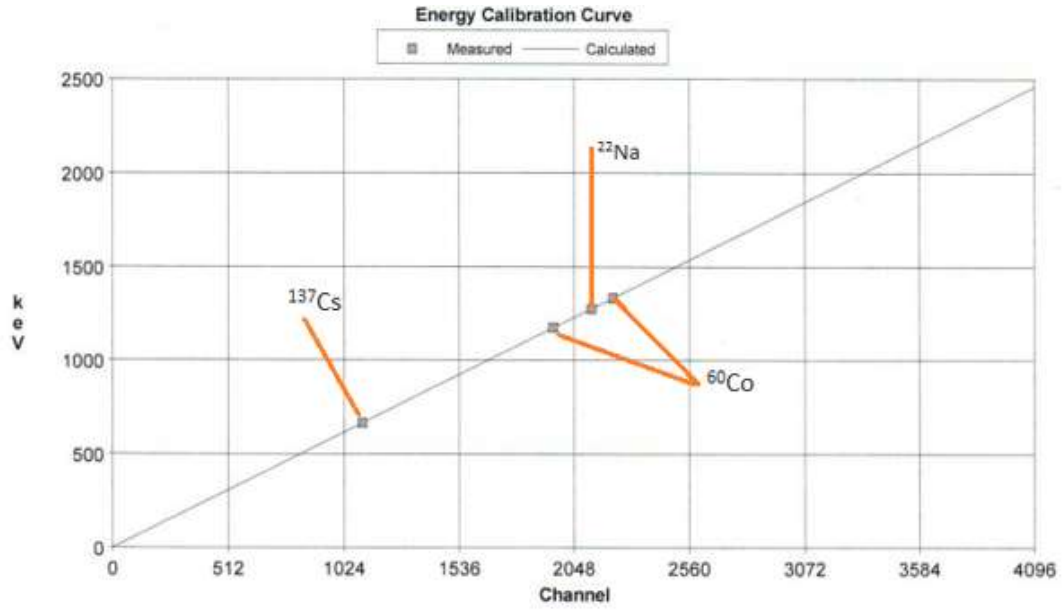

Figure 3.14: Energy calibration curve obtained using point sources

3.4.3. Measurement of background radiation

To determine the background radiation level due to naturally occurring radionuclides inside and outside the detector, the background radiation was counted for 10800s (or 3 hours) in the absence of a radiation source but with an empty 500ml polythene bottle on the detector. From the results obtained, there were no energy peaks corresponding to the energy peaks of interest (peaks of ^{238}U, ^{232}Th and ^{40}K) in this study.

3.4.4. Measurement of reference materials

The reference materials RGU-1, RGTh-1 and RGK-1(Figure 3.15), obtained from the International Atomic Energy Agency (IAEA), with the same geometry and mass as the soil sample, were analysed using an HPGe detector. One reference material at a time was placed on the detector and counted for 10800s (3 hours). The corresponding spectra obtained are shown in Figures 3.16 -3.18. A Genie 2000 version 3.2.1 software

was used to calculate the net peak areas in the spectra. The results obtained were used to identify radionuclides of interest in the soil samples.

Figure 3.15: Reference materials provided by the IAEA

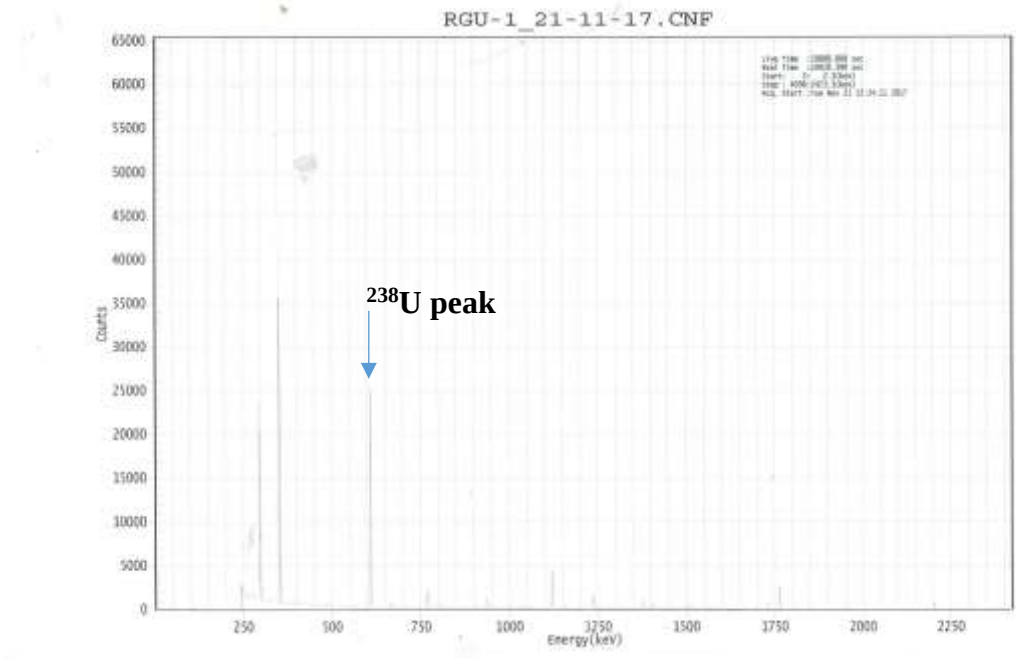

Figure 3.16: Spectrum of RGU-1

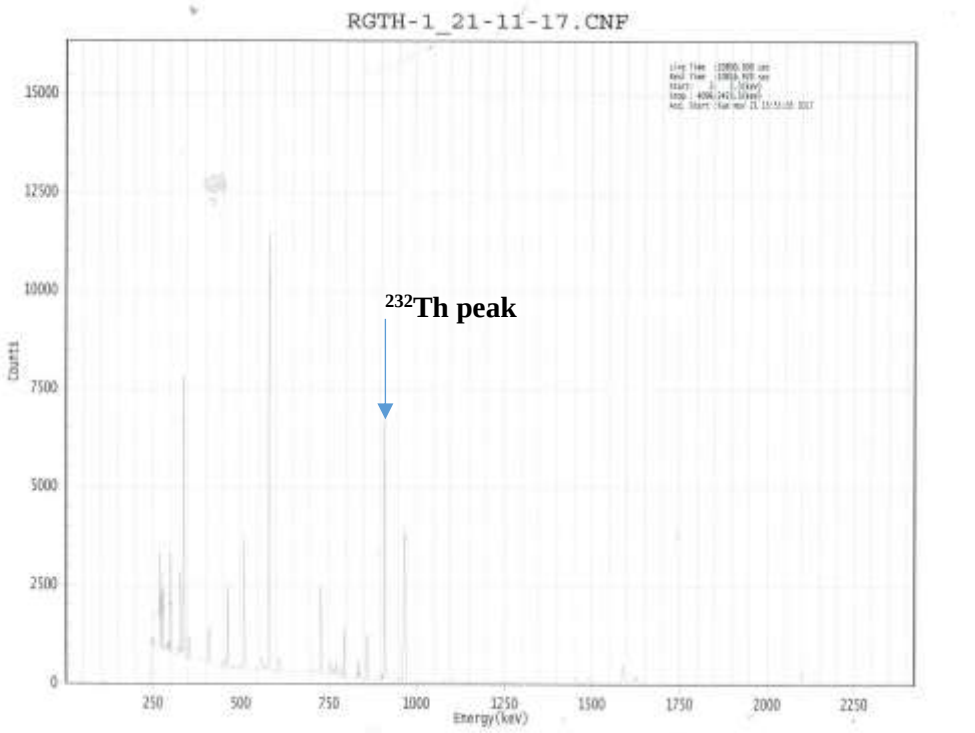

Figure 3.17: Spectrum of RGTh-1

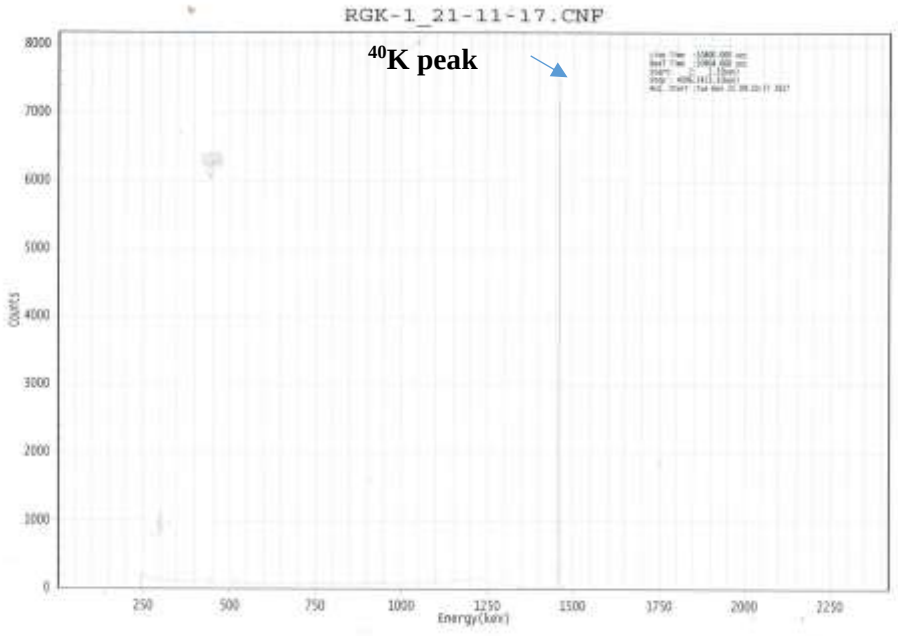

Figure 3.18: Spectrum of RGK-1

3.4.5. Measurement of soil sample

In order to identify and determine the activity concentrations of the radionuclides in different soil samples, each soil sample was placed at the center of the detector as shown in Figure 3.19 and the radiation emitted was measured for the 10800s (3 hours) using an HPGe detector. The data obtained was stored in a computer and the spectrum of each sample was analysed using the known energies of the reference materials. The net peak area of each peak in the spectra was calculated using a GENE 2000 computer software. The radionuclides were identified and the net peak areas under the peaks were used to calculate the activity concentrations of the radionuclides of interest in each sample.

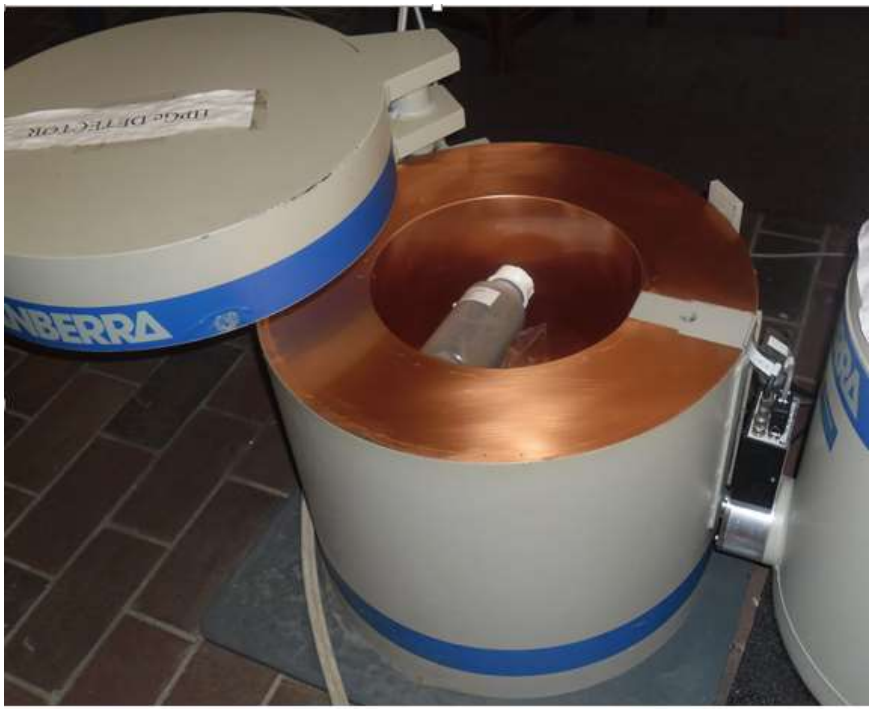

Figure 3. 19: A soil sample placed on a detector

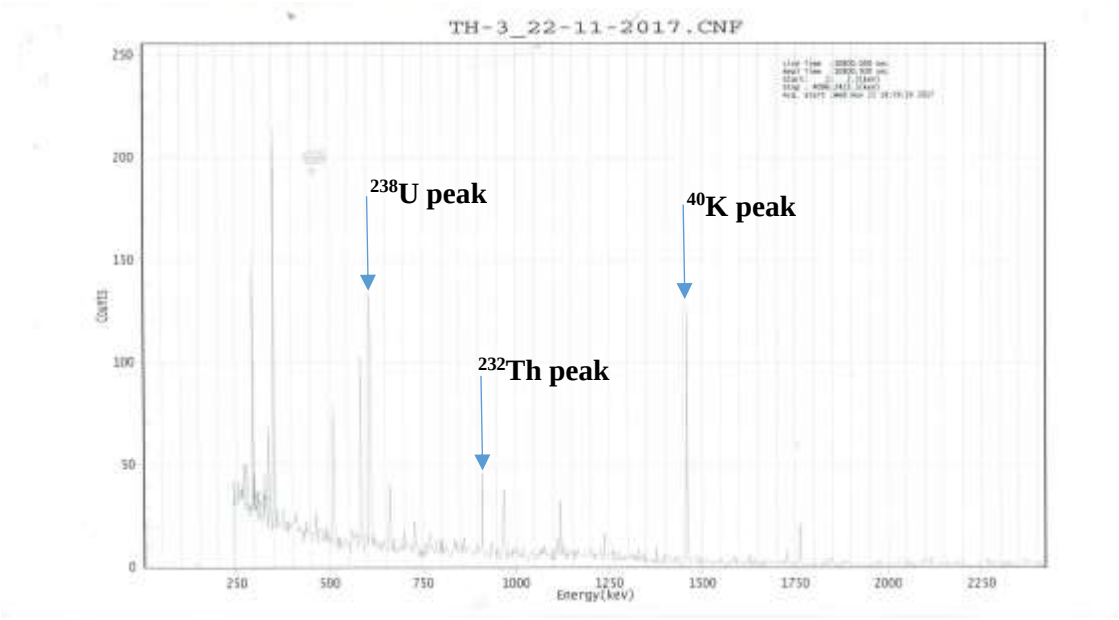

Figure 3.20: Spectrum of a sample

3.4.6. Determination of radionuclide activity concentrations

The net peak area corresponding to the energy of interest was used to calculate the activity concentration of a particular radionuclide in the sample. The activity concentrations of ^{238}U was determined from the gamma-ray transition line of 609 keV of ^{214}Bi, while ^{232}Th was determined from 911 keV of ^{228}Ac. Also, the gamma -ray transition line of 1460 keV was used to determine the activity of ^{40}K. In this study, the soil samples and the reference materials were counted under the same detector geometry and counting time. Since the detector geometry was fixed and the sensitivity of the detector was also kept constant, then the net peak area A is directly proportional to the corresponding activity concentration C of a radionuclide in a soil sample. That is,

$A \propto C$ Or $A = KC$

$$\therefore K = \frac{A}{C} \quad \text{---------- 3.1}$$

where K is a constant for the given radionuclide.

Therefore, for a given radionuclide X in a standard, constant K is given by

$$K^{X}{}_{standard} = \frac{A^{X}{}_{standard}}{C^{X}{}_{standard}} \quad \text{---------- } 3.2(a)$$

Also, for a given radionuclide X in a sample, constant K is given by

$$K^{X}{}_{sample} = \frac{A^{X}{}_{sample}}{C^{X}{}_{sample}} \quad \text{---------- } 3.2(b)$$

where $A^{X}{}_{standard}$ and $C^{X}{}_{standard}$ are the net peak area and activity concentration of the radionuclide X in reference material, while $A^{X}{}_{sample}$ and $C^{X}{}_{sample}$ are the net peak area and activity concentration of the radionuclide X in the soil sample.

Since $K^{X}{}_{standard} = K^{X}{}_{sample}$ for a given radionuclide X, then equating eq. 3.2(a) to eq .3.2(b) and rearranging gives

$$C^{X}{}_{sample} = \frac{A^{X}{}_{sample}}{K^{X}{}_{standard}} \quad \text{---------- } 3.3$$

Eq. 3.3 was used to calculate the activity concentration of the radionuclide X in the sample.

3.4.7. Equations for the assessment of radiation hazards

Absorbed dose rate

Human beings are always exposed to radiation when outdoors. The amount of radiation absorbed in the outdoor 1m above the ground due to natural radionuclides ^{238}U, ^{232}Th and ^{40}K can be calculated using the formula below [9]

$$D\left(^{\mathrm{nGy}}/_{\mathrm{h}}\right) = 0.0417A_k + 0.462A_U + 0.604A_{Th} - - - - - - - - - - - - - - - - 3.4$$

where A_k, A_U and A_{Th} are the activity concentrations of ^{238}U, ^{232}Th and ^{40}K of the sample.

Annual effective dose rate

The annual effective dose from external exposure to gamma rays from the soil can be calculated from the absorbed dose rate using the expression [9]

$$E\left(^{\mu\mathrm{Sv}}/_{\mathrm{y}}\right) = D\left(^{\mathrm{nGy}}/_{\mathrm{h}}\right) \times 8760h \times 0.7\,{}^{\mathrm{Sv}}/_{\mathrm{Gy}} \times 0.2 \times 10^{-3} \ldots\ldots\ldots\ldots 3.5$$

where $D\left(^{\mathrm{nGy}}/_{\mathrm{h}}\right)$ is the absorbed dose rate, 0.2 is the occupancy factor for outdoor, $0.7\,{}^{\mathrm{Sv}}/_{\mathrm{Gy}}$ is the conversion factor for external gamma radiation and 8760 h is the total time of the year in hours.

Radium equivalent activity($\mathbf{Ra_{eq}}$)

The distribution of ^{238}U, ^{232}Th and ^{40}K in the soil is not uniform. Radium equivalent activity($\mathrm{Ra_{eq}}$) is the radiological index used to represent the activity concentrations of materials containing ^{238}U, ^{232}Th and ^{40}K by a single quantity and it takes into

account the radiation hazards associated with them [68]. It was estimated based on the assumptions that 1 Bq/kg of ^{238}U , 0.7 Bq / kg of ^{232}Th and 13 Bq/kg of ^{40}K produces the same radiation dose. UNSCEAR 2000 recommended the upper limit value of 370Bq/kg. The $\mathrm{Ra_{eq}}$ is defined mathematically by [9, 37, 68]

$$\mathrm{Ra_{eq}(Bq/kg)} = A_U + 1.43A_{Th} + 0.077A_K \quad ----------3.6$$

where $A_U, A_{Th}, and\ A_K$ are the activity concentrations of ^{238}U, ^{232}Th and ^{40}K.

External hazard index (H_{ex})

This index is used to determine the exposure level of the individuals due to outdoor exposure of gamma radiation from the natural radionuclides in the soils. In order for the radiation hazard to be negligible this value should not exceed one [68] . The maximum value of H_{ex} of unity corresponds to the maximum limit of $\mathrm{Ra_{eq}}$ of 370 Bq/kg. The H_{ex} is calculated using the following relation

$$H_{ex} = \frac{A_u}{370} + \frac{A_{Th}}{259} + \frac{A_K}{4810} \quad ----------3.7$$

The MATLAB programme (Appendix 1) was written and used to calculate the radionuclide activity concentrations, absorbed dose rates, etc.

CHAPTER 4: RESULTS AND DISCUSSIONS

4.1. Natural radioactivity in the soil of the Ohorongo Cement plant

4.1.1. Activity concentrations of radionuclides in the soil of the Ohorongo Cement plant

The activity concentrations of the radionuclides ^{238}U, ^{232}Th, and ^{40}K measured in each of the 50 soil samples collected from the Ohorongo Cement plant are presented in Appendix 2. Also, the mean and range of activity concentrations of ^{238}U, ^{232}Th, and ^{40}K in each of the three geographical areas are summarized in Table 4.1 and shown in Figure 4.1. As could be observed in the Table, the activity concentrations vary between 7.3 ± 1.2 Bq/kg and 25.6 ± 1.8 Bq/kg (RO area), with a mean of 15.0 ± 4.7 Bq/kg for ^{238}U, between 12.7 ± 2.2 Bq/kg (LO area) and 43.1 ± 3.5 Bq/kg (RO area) ,with a mean of 25.1 ± 9.9 Bq/kg for ^{232}Th and between 132.2 ± 9.7 Bq/kg (SO area) and 507.8 ± 22.5 Bq/kg (RO area), with a mean of 310.7 ± 97.2 Bq/kg for ^{40}K. As could be observed in Table 4.1 and Figure 4.1, the average activity concentration of each of ^{238}U, ^{232}Th and ^{40}K is highest in the RO area and lowest in the SO area. Nevertheless, the average activity concentrations of ^{238}U and ^{40}K are lower than the worldwide average values of 35 and 400 Bq/kg, respectively for ^{238}U and ^{40}K. Conversely, the average activity concentration of ^{232}Th is slightly higher in the RO area than the worldwide average value of 30 Bq/kg. From the results in Figure 4.1 and Table 4.1, the activity concentrations of ^{40}K is the highest in all the areas while that of ^{238}U is the lowest. This high concentration of ^{40}K has also been observed in other towns in Namibia [3, 64].

The calculated overall average activity concentrations were also compared to the worldwide average values, as shown in Table 4.1 and Figure 4.2. Although, the activity concentration of ^{232}Th in RO is slightly higher than the worldwide average value, however the average concentrations of ^{238}U, ^{232}Th and ^{40}K calculated from all the soil samples are all below the corresponding worldwide average values.

Table 4.1: Average activity concentration of ^{238}U, ^{232}Th and ^{40}K in the three geographical areas of the Ohorongo Cement plant and the corresponding worldwide average values. The range of values is given in brackets.

Area	**Average activity concentration (Bq/kg)**		
	^{238}U	**^{232}Th**	**^{40}K**
LO	13.6 ± 3.6 (7.7 - 20.1)	21.2 ± 6.0 (12.7 – 33.1)	284.9 ± 51.5 (204.8 – 381.9)
SO	12.2 ± 3.4 (8.4 -18.6)	20.0 ± 7.0 (12.7 – 35.6)	248.9 ± 87.2 (132.2 – 390.2)
RO	17.9 ± 4.9 (7.3 - 25.6)	31.7 ± 10.8 (13.8 – 43.1)	367.4 ± 109.4 (137.9 – 507.8)
All three areas	**15.0 ± 4.7 (7.3 -25.6)**	**25.1 ± 9.9 (12.7 – 43.1)**	**310.7 ± 97.2 (132.2 – 507.8)**
Worldwide	35.0	30.0	400.0

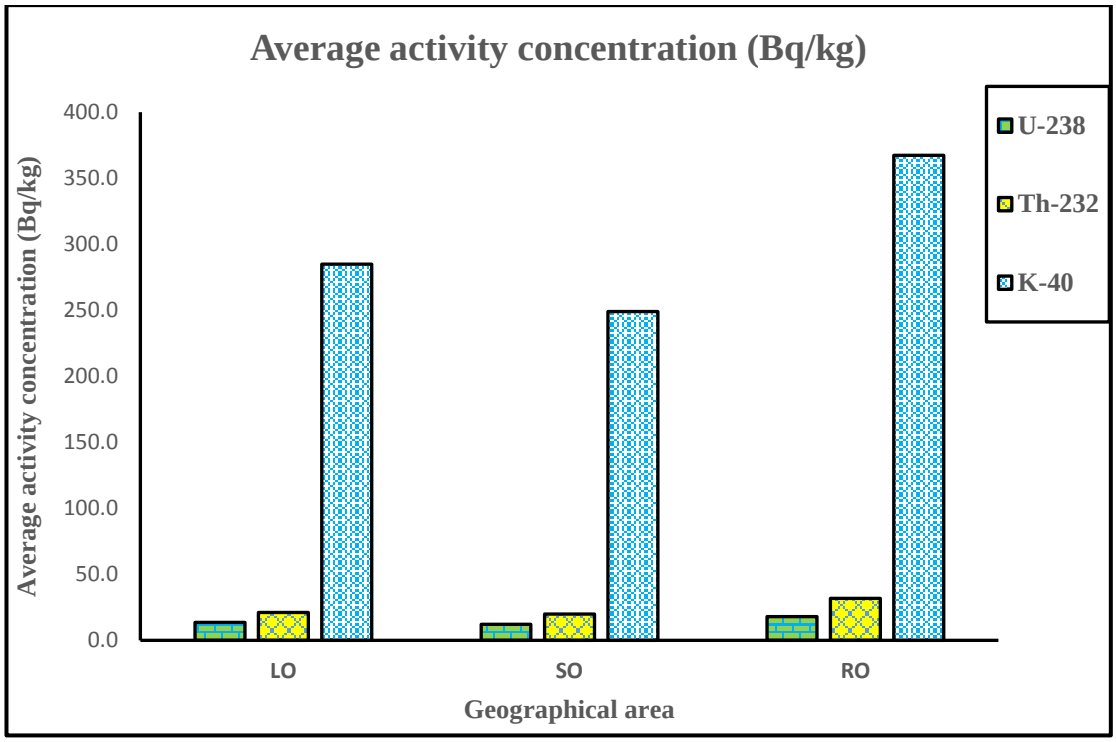

Figure 4.1: The average activity concentrations of ^{238}U, ^{232}Th and ^{40}K in the three geographical areas of the Ohorongo Cement plant

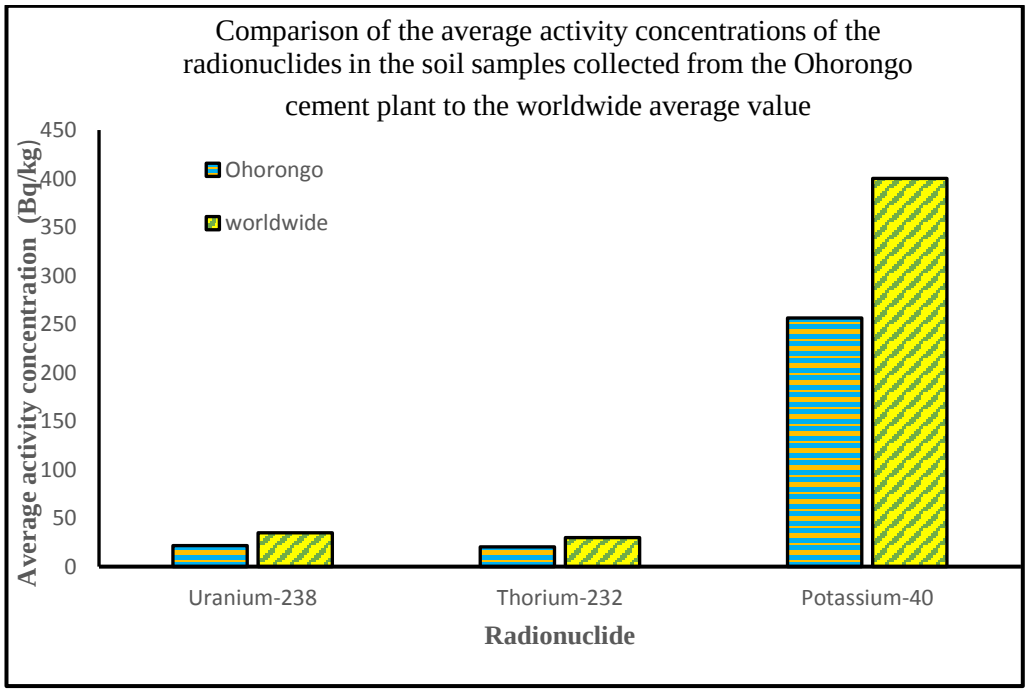

Figure 4.2: Comparison of the average activity concentrations of the radionuclides in the soil samples collected from the Ohorongo Cement plant to the corresponding worldwide average value.

4.1.2. Assessment of radiation hazards in the soil of the Ohorongo Cement plant

In order to assess the radiological hazards to humans due to the radionuclides in the soils of the Cement plant, the absorbed dose rate, annual effective dose, radium equivalent activity and external hazard index were calculated. These radiological parameters were calculated from the measured activity concentrations of the three main primordial radionuclides in the soil samples using the relations discussed in section 3.4.7. The average values of these radiological parameters are shown in Table 4.2.

Table 4.2: The mean absorbed dose rate *(D)*, effective dose rate, radium equivalent activity (Ra_{eq}) and external hazard index (H_{ex}) in the three geographical areas of the Ohorongo Cement plant. The range of values is given in brackets

Area	Absorbed dose rate (nGy/h)	Effective dose rate (µSv/y)	Radium equivalent activity, Ra_{eq} (Bq/kg)	External hazard index (H_{ex})
LO	31.0 ± 7.1 (20.9 - 45.2)	38.0 ± 8.7 (25.6 – 55.5)	65.8 ± 15.4 (44.1 - 65.8)	0.18 ± 0.04 (0.12 - 0.26)
SO	28.1 ± 9.2 (18.1 - 46.4)	34.4 ± 11.3 (22.2 - 56.8)	59.9± 19.6 (38.7 - 99.5)	0.16 ± 0.05 (0.10 - 0.27)
RO	42.7 ± 12.9 (18.8 - 58.0)	52.4 ± 15.8 (23.1 - 71.2)	91.5 ± 27.8 (40.3 - 124.2)	0.25± 0.07 (0.11 - 0.34
Average of all samples	**35.1 ± 11.8 (18.1 - 58.0)**	**43.0 ± 14.5 (22.2 -71.2)**	**74.9 ± 25.6 (38.7 - 124.2)**	**0.20 ± 0.07 (0.10 - 0.34)**

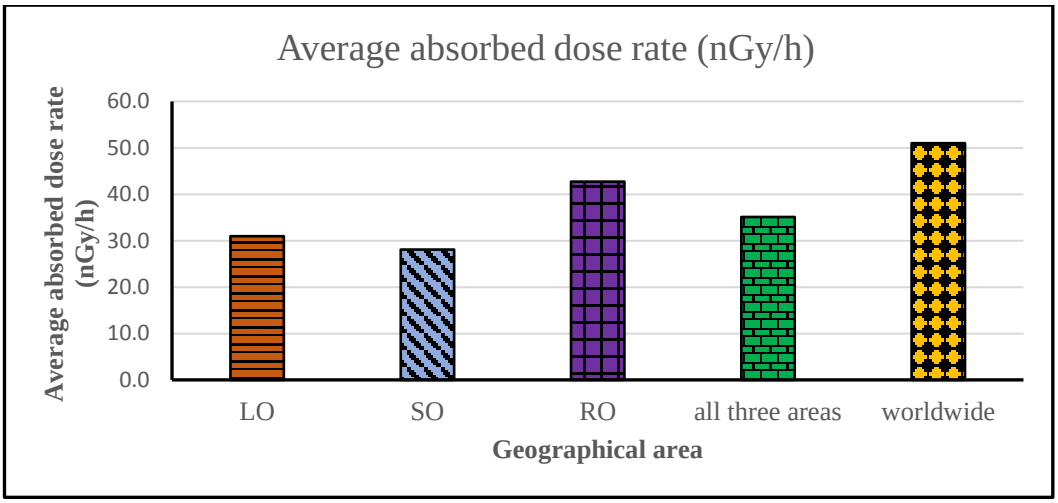

Figure 4.3: Average absorbed dose rates due to gamma radiation from ^{238}U, ^{232}Th and ^{40}K in the soil samples collected from the three different geographical areas (LO, SO and RO) of the Ohorongo Cement plant. The average dose rate over all the three areas and the corresponding worldwide average value are shown in the last two columns, respectively.

The average and range of absorbed dose rate in each geographical area are shown in Table 4.2 (column 2) and Figure 4.3. As observed in Table 4.2, the absorbed dose rate varies between 18.1 ± 1.4 nGy/h and 58.0 ± 2.5 nGy/h, with an overall average value of 35.1 ± 11.8 nGy/h. Also, as could be seen from Table 4.2 (column 2, row 3) and Figure 4.3, the average absorbed dose rate is highest in the RO area with an average value of 42.7 ± 12.9 nGy/h while it is lowest in the SO area with the average value of 28.1 ± 9.2 nGy/h. The relatively high value of the average absorbed dose rate in the RO area is not surprising because the same area has a relatively high average concentrations of ^{40}K. However, the calculated average absorbed dose rates are all below the worldwide average value of 51 nGy/h [9], as could be seen in Figure 4.3.

The range and average of the calculated effective dose rates in the three geographical areas are summarized in Table 4.2 (column 3) and shown in Figure 4.4. As shown in

the Table, the effective dose rate varies between 22.2 ± 1.7 μSv/y and 71.2 ± 3.0 μSv/y, with an average value of 43.0 ± 14.5 μSv/y. This average value (43.0 ± 14.5 μSv/y) is below the maximum permissible limit (MPL) of 1.0 mSv/y recommended by ICRP [52]. These results imply that the Ohorongo Cement plant has a normal background radiation.

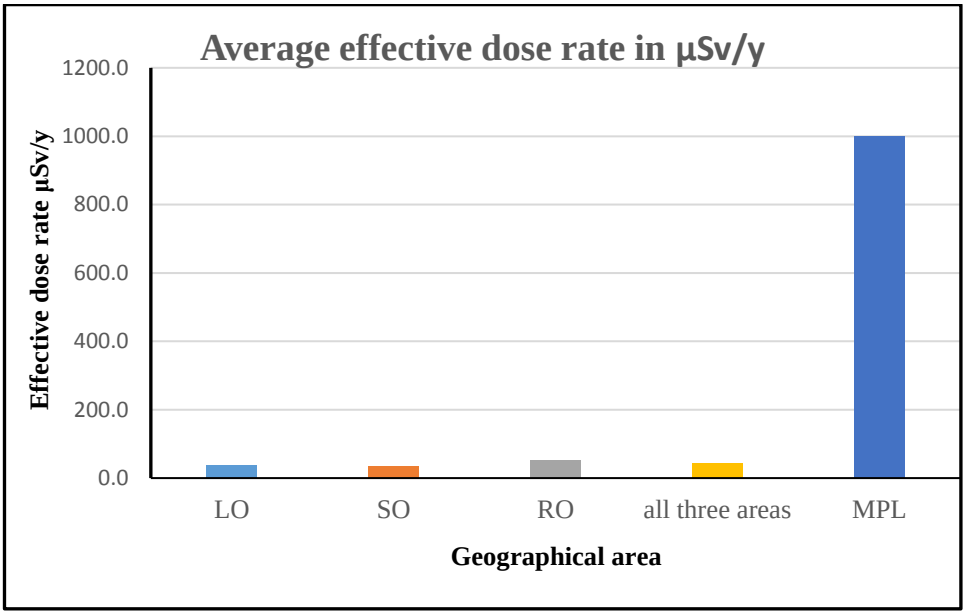

Figure 4.4: Average effective dose rate due to gamma radiation from ^{238}U, ^{232}Th and ^{40}K in the soil samples collected from the three different geographical areas of the Cement plant. The average effective dose rate over the three areas and the corresponding maximum permissible limit (MPL) are shown in the last two columns, respectively.

The radium equivalent activity (Ra_{eq}) and the external hazard index (H_{ex}) were also calculated for each area. The results obtained are summarized in Table 4.2 (columns 4 and 5) respectively. The values of Ra_{eq} range from 38.7 ± 3.2 Bq/kg to 124.2 ± 5.6 Bq/kg with an overall average value of 74.9 ± 25.6 Bq/kg as shown in Table 4.2 (column 4) and Figure 4.5. As could be observed in the Table, all the values of Ra_{eq} are below the maximum permissible limit of 370 Bq/kg [9]. Similarly, H_{ex} varies

between 0.10 ± 0.01 and 0.34 ± 0.02 with an overall average of 0.20 ± 0.07, as shown in Table 4.2 (column 5) and Figure 4.6. All the values of H_{ex} are below the maximum permissible value of 1.0 [52]. Therefore it can be concluded that radiation hazard is negligible in the Ohorongo Cement plant.

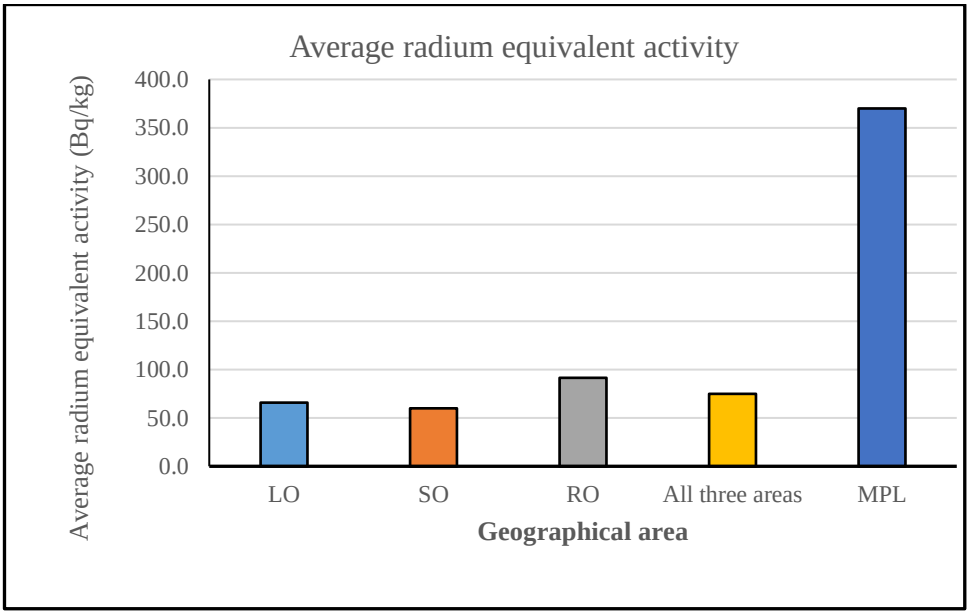

Figure 4.5: Average radium equivalent activity (Ra_{eq}) due to ^{238}U, ^{232}Th and ^{40}K in the soil samples collected from the Cement plant. The average radium equivalent activity over the three areas and the corresponding maximum permissible limit (MPL) are shown in the last two columns, respectively.

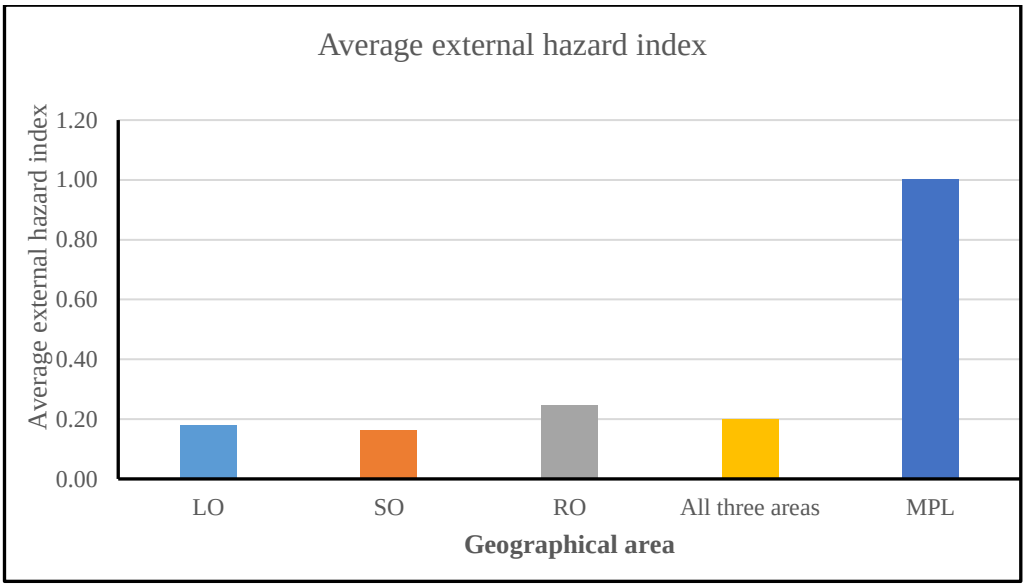

Figure 4.6: Average external hazard index (H_{ex}) due to ^{238}U, ^{232}Th and ^{40}K in the soil samples collected from the Cement plant. The average H_{ex} over the three areas and the corresponding MPL are shown in the last two columns, respectively.

4.1.3. Statistical analysis of the results obtained in the measurements of radioactivity in the soils of the Ohorongo Cement plant

Statistical parameters such as mean, standard deviation, skewness and kurtosis in the results obtained for the activity concentrations of primordial radionuclides and radiation hazard parameters in the soil of the Ohorongo Cement plant are presented in Table 4.3. Skewness is the degree of asymmetry, or more precisely a lack of symmetry, of a distribution in a set of data [69]. With the help of skewness, one can identify the shape of a distribution. Skewness can be negative, positive, or zero. The distribution with zero skewness, is said to be a normal distribution. However, in reality, data points may not be perfect symmetry. Skewness is positive if the tail of the distribution is longer on the right side than on the left side. On the contrary, skewness is said to be negative if the tail of the distribution is longer on the left side than on the right side. Kurtosis is the measure that describes the shape (tall and sharp or short and flat) of the

distribution's tail when compared with the normal distribution. It can be negative or positive. Positive kurtosis shows that the distribution is tall and sharp (peaked) and negative kurtosis shows that the distribution is short and flat (flattened).

Table 4.3: Statistical analysis of the results obtained in the measurements of natural radioactivity in the soils of the Ohorongo Cement plant

Descriptive statistics	**^{238}U conc (Bq/kg)**	**^{232}Th conc (Bq/kg)**	**^{40}K conc (Bq/kg)**	**Absorbed dose rate (nGy/h)**	**Effective dose rate (μSv/y)**	**Radium equivalent activity (Ra_{eq}) (Bq/kg)**	**External hazard index (H_{ex})**
Mean	15.0	25.1	310.7	35.1	43.0	74.9	0.20
Standard dev	4.7	9.9	97.2	11.8	14.5	25.6	0.07
Standard error	0.7	1.4	13.7	1.7	2.1	3.6	0.01
Median	14.9	21.4	286.0	31.3	38.4	66.5	0.18
Max	25.6	43.1	507.8	58.0	71.2	124.2	0.34
Min	7.3	12.7	132.2	18.1	22.2	38.7	0.10
Range	7.3-25.6	12.7-43.1	132.2-507.8	18.1-58.0	22.2-71.2	38.7-124.2	0.10-0.34
Kurtosis	-0.7	-1.1	-0.9	-1.2	-1.2	-1.2	-1.2
Skewness	0.3	0.5	0.2	0.3	0.3	0.4	0.4

The frequency distributions of all the radionuclide activity concentrations and the radiological risk parameters were analysed and summarized in Table 4.3. As observed in the Table, ^{238}U, ^{232}Th, ^{40}K, absorbed dose rate, effective dose rate, radium equivalent activity and external hazard index all have positive skewness (bottom row in the Table) and negative kurtosis (2nd to last row in the table). The negative kurtosis shows that they all have the flat frequency distribution. Figure 4.7(a) shows that the concentration of ^{238}U in most of the soil samples is between 9.0 Bq/kg and 21.0 Bq/kg, while the concentration of ^{232}Th is mostly occurring between 15.0 Bq/kg and 20.0 Bq/kg (Figure 4.7(b)). Also, the concentration of ^{40}K in most of the soil samples is between 150 Bq/kg and 500 Bq/kg, with the most frequently occurring range between 250.0 Bq/kg and 300.0 Bq/kg as could be seen in Figure 4.7(c). In fact, only two samples out of fifty

have an activity concentration less than 150 Bq/kg while only one sample has an activity greater than 500 Bq/kg. On the contrary, 9 out of 50 soil samples have the activity concentrations of ^{40}K higher than that of the corresponding worldwide average, as could be observed in figure 4.7 (c).

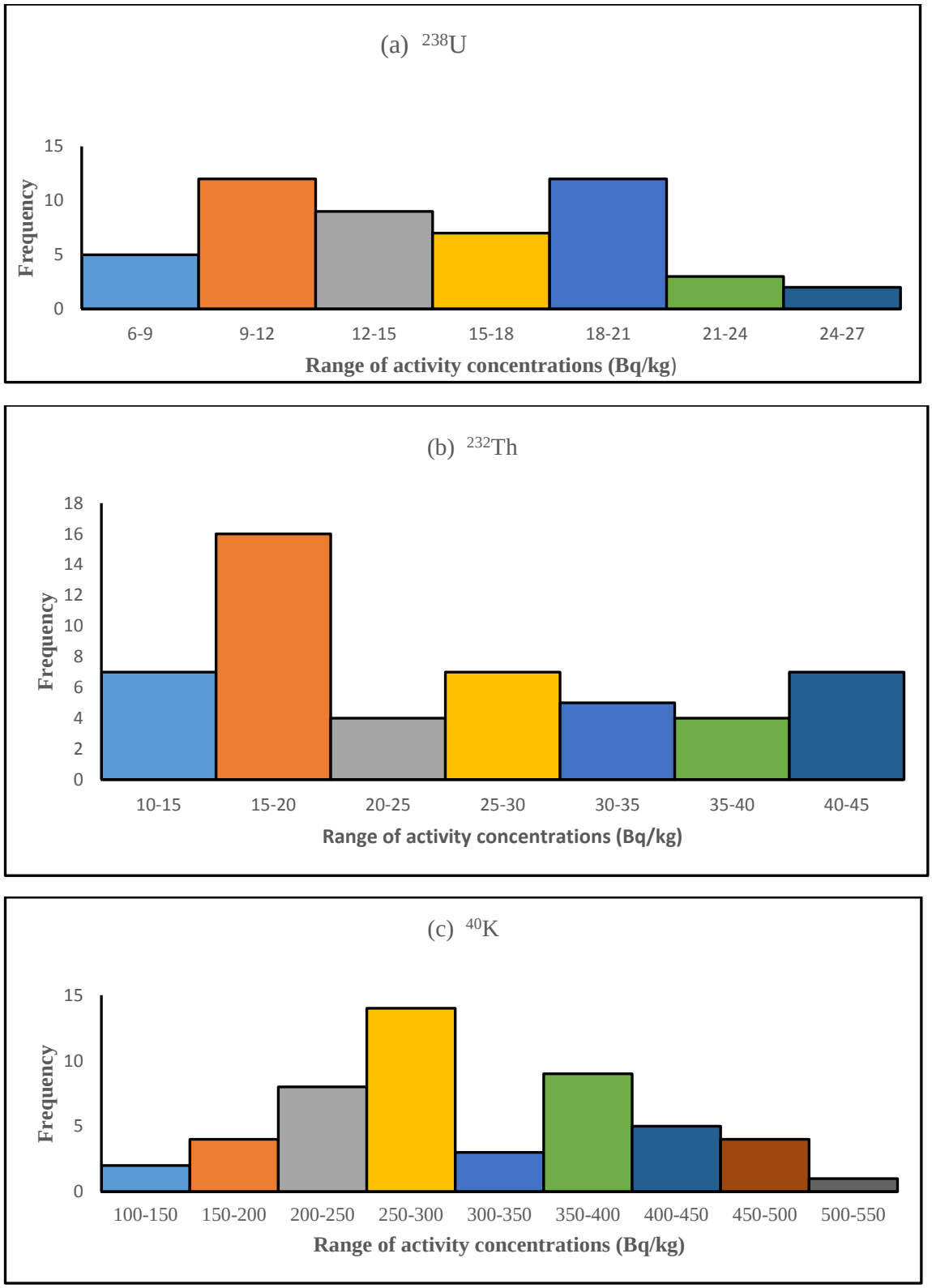

Figure 4. 7: Frequency distributions of activity concentrations of (a) ^{238}U, (b) ^{232}Th, and (c) ^{40}K in the soil samples collected from the Ohorongo Cement plant

Figure 4.8 shows the frequency distributions of (a) absorbed dose rates and (b) effective dose rates in the Ohorongo Cement plant. The absorbed dose rate due to radionuclides in most of the samples is between 20.0 nGy/h and 55.0 nGy/h as could be observed in Figure 4.8 (a). The most frequently occurring range of the absorbed dose rate is 20.0 nGy/h to 30.0 nGy/h. Also, as could be observed in Figure 4.8 (b), the effective dose rates lies most between 25.0 µSv/y and 65.0 µSv/y with the most frequently occurring range of 35.0 µSv/y to 40.0 µSv/y.

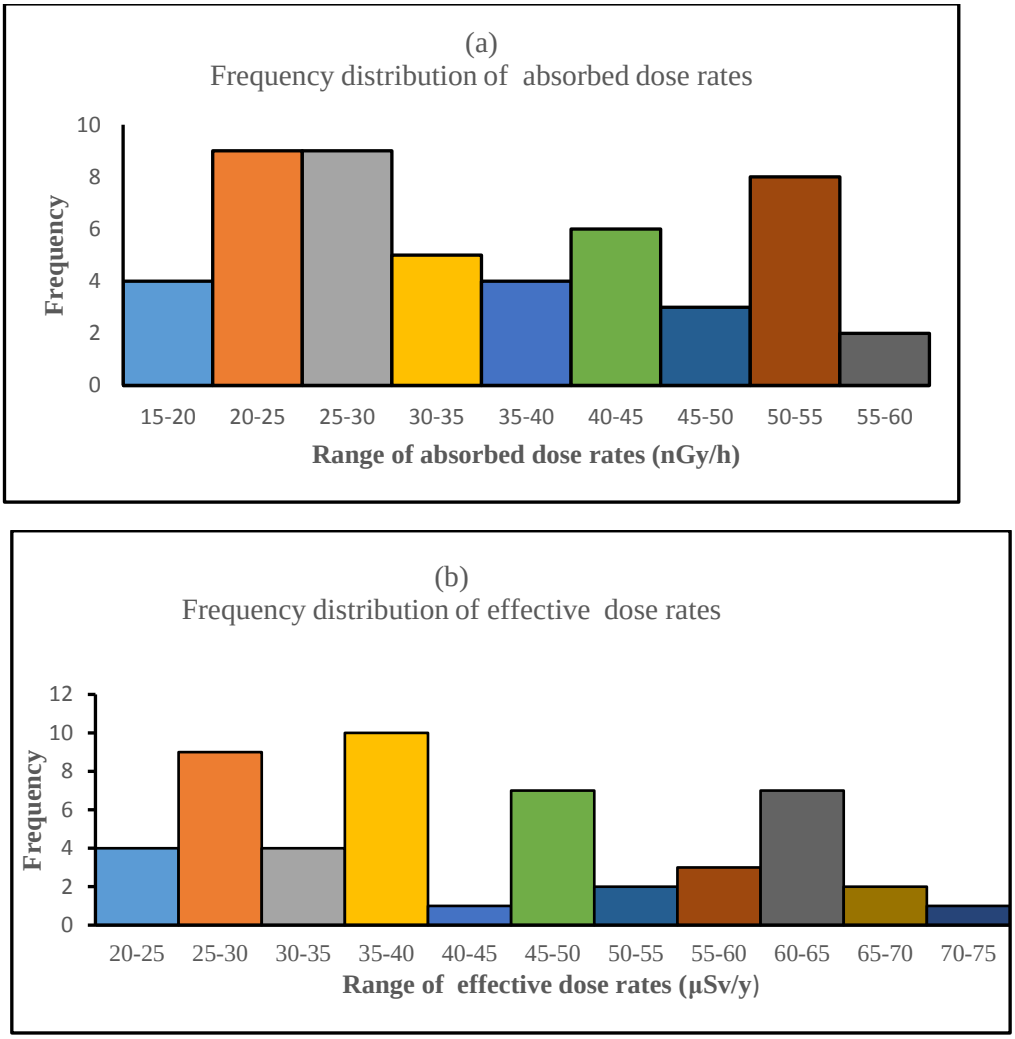

Figure 4.8: Frequency distributions of (a) absorbed dose rate and (b) effective dose rate due to primordial radionuclides in the soil samples collected from the Ohorongo Cement plant

The frequency distributions of radium equivalent activity (Ra_{eq}) and external hazard index (H_{ex}) are shown in Figure 4.9. As could be observed in Figure 4.9 (a), most of the Ra_{eq} calculated for the plant are between 40.0 Bq/kg to 120.0 Bq/kg with the most frequently occurring range between 60.0 Bq/kg and 70.0 Bq/kg. Only one sample has Ra_{eq} below 40.0 Bq/kg and only one sample has Ra_{eq} greater than 120 Bq/kg. Similarly, as observed in Figure 4.9 (b), only two samples have H_{ex} above 0.32. Most of the calculated H_{ex} are between 0.1 and 0.32.

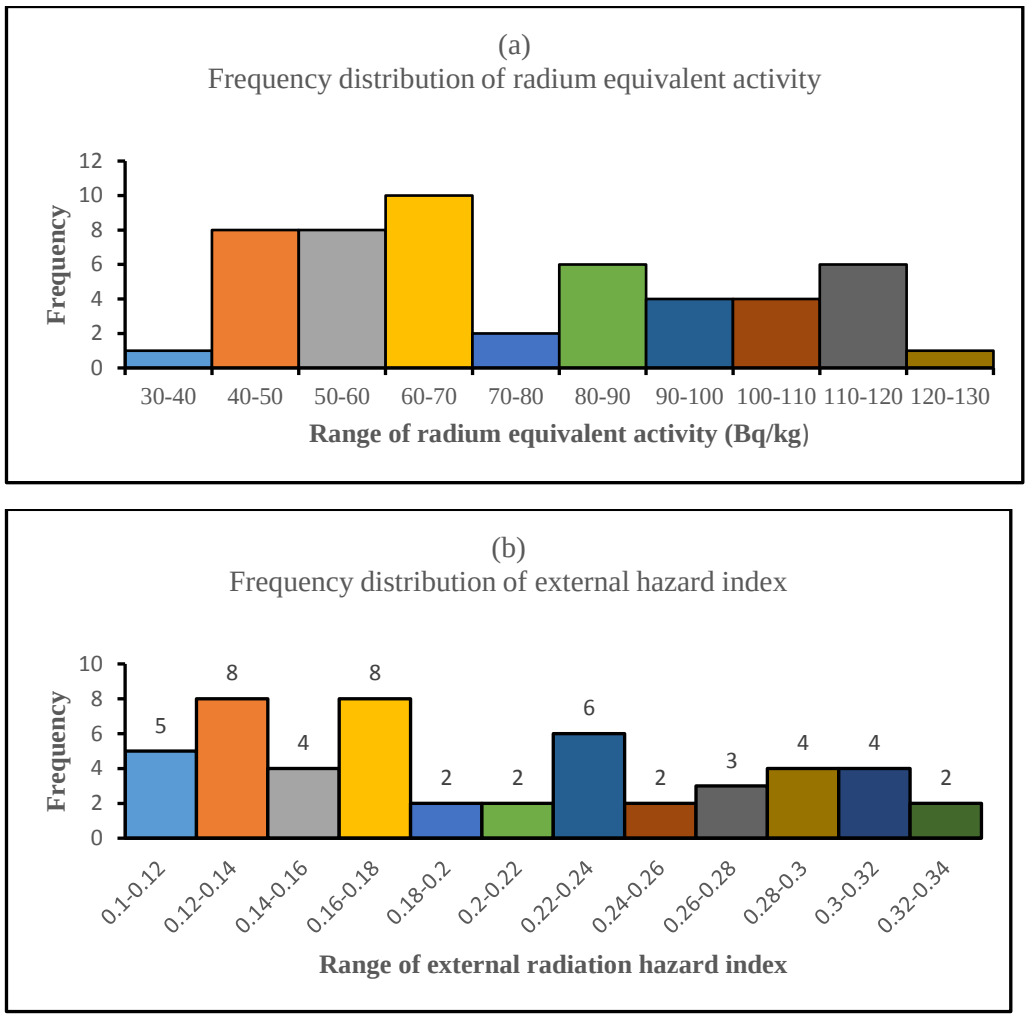

Figure 4.9: Frequency distributions of (a) Ra_{eq} and (b) H_{ex} due to primordial radionuclides in the soil samples collected from the Ohorongo Cement plant

4.2. Natural radioactivity in the soil of Otavi

4.2.1. Activity concentrations of radionuclides in the soil of Otavi

The mean and range (in brackets) of activity concentrations of ^{238}U, ^{232}Th and ^{40}K in the soil samples collected from each of the ten geographical areas in Otavi are shown in Table 4.4 and Figure 4.10. Also, the activity concentrations of the radionuclides ^{238}U, ^{232}Th, and ^{40}K measured in each of the 50 soil samples collected from Otavi are presented in Appendix 3. The activity concentrations of radionuclides in the samples vary between 6.5 ± 1.3 Bq/kg (UH area) and 39.1 ± 2.2 Bq/kg (DR area), with a mean value of 21.6 ± 7.2 Bq/kg for ^{238}U (2^{nd} column and 2^{nd} to the last row in Table 4.4), between 3.7 ± 1.5 Bq/kg (UH area) and 55.6 ± 4.4 Bq/kg (AG area), with a mean value of 20.3 ± 8.5 Bq/kg for ^{232}Th (3^{rd} column and 2^{nd} to the last row in Table 4.4) and between 76.5 ± 7.6 Bq/kg (UH area) and 645.8 ± 27.1 Bq/kg (AG area) with a mean value of 256.4 ± 113.7 Bq/kg for ^{40}K (4^{th} column and 2^{nd} to the last row in Table 4.4). As could be observed in Table 4.4 and Figure 4.10, the activity concentrations of ^{238}U, ^{232}Th and ^{40}K are lowest in the UH area while they are highest in the DR area.

Table 4.4: Average activity concentration of ^{238}U, ^{232}Th and ^{40}K in the ten geographical areas of Otavi and the corresponding worldwide average values. The range of values is given in brackets.

Area	Average activity concentration (Bq/kg)		
	^{238}U	^{232}Th	^{40}K
TH	24.4 ± 3.6 (21.0 - 30.4)	21.1 ± 2.8 (16.7 - 24.0)	227.4 ± 36.4 (167 - 261.9)
SQ	14.5 ± 1.4 (12.9 -16.2)	13.9 ± 3.3 (10.2 - 18.5)	165.8 ± 29.8 (135.9 - 206.1
KE	25.1 ± 4.3 (18.8 - 29.9)	23.3 ± 4.5 (16.1 - 27.4)	261.5 ± 44.5 (201 - 308.9)
TC	23.5 ± 4.2 (19.5 - 29.5)	23.5 ± 5.2 (18.9 - 31.8)	351.8 ± 68.7 (242.3 - 418.5)
AG	26.3 ± 3.9 (22.5 - 32.3)	28.5 ± 15.2 (19.5 - 55.6)	336.1 ±1 74.7 (220.6 - 645.8)
NM	19.5 ± 4.8 (13.9 - 24-6)	17.1 ± 3.7 (12.9 - 22.7)	182.7 ± 32.9 (136.9 - 215.4)
KS	21.1 ± 1.8 (18.5 - 23.0)	20.5 ± 2.4 (16.4 - 22.5)	278.2 ± 46.1 (217.5 - 327.0)
KH	20.8 ± 5.4 (16.6 - 28.3)	18.4 ± 6.4 (11.3 - 25.8)	224.7 ± 86.5 (148.8 - 349.7)
UH	9.2 ± 2.7 (6.5 - 13.4)	7.5 ± 2.3 (3.7 - 9.8)	113.1 ± 40.6 (76.5 - 182.4)
DR	31.8 ± 7.1 (20.2 - 39.1)	28.9 ± 6.1 (18.9 - 35.2)	422.3 ± 85.0 (218.0 - 503.7)
All ten areas	**21.6 ± 7.2 (6.5 - 39.1)**	**20.3 ± 8.5 (3.7 - 55.6)**	**256.4 ± 113.7 (76.5 - 645.8)**
Worldwide	35.0	30.0	400.0

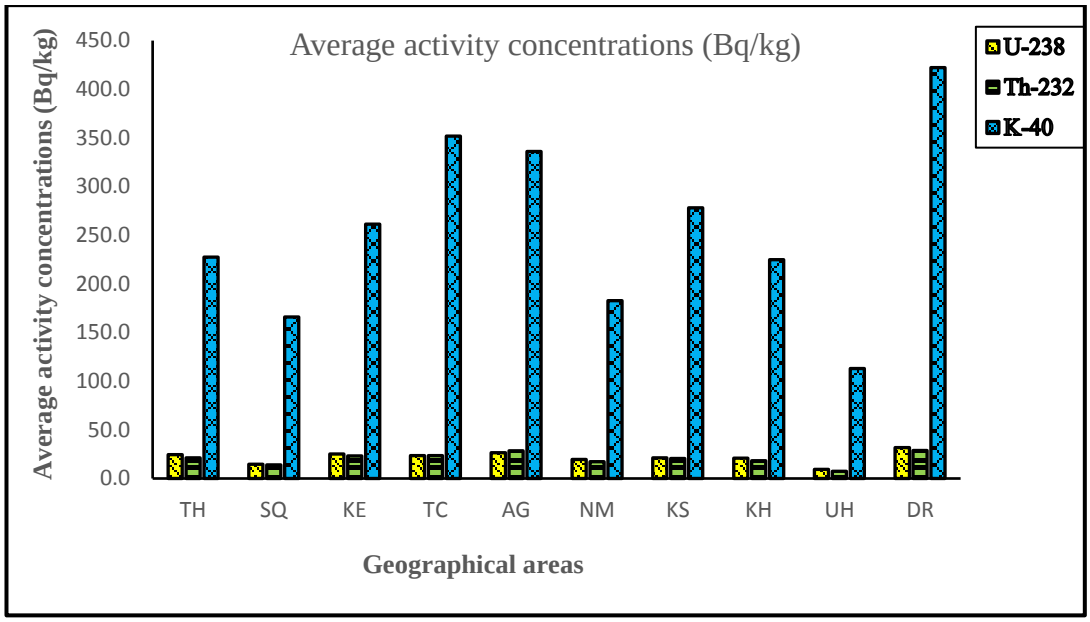

Figure 4.10: The average activity concentrations of ^{238}U, ^{232}Th and ^{40}K in the ten geographical areas of Otavi.

The highest average activity concentrations of ^{238}U, ^{232}Th and ^{40}K are 31.8 ± 7.1 Bg/kg, 28.9 ± 6.1 Bq/kg and 422.3 ± 85.0 Bq/kg, respectively in the DR area (Table 4.4, third row from the bottom). Conversely, the lowest average activity concentrations of ^{238}U, ^{232}Th and ^{40}K are 9.2 ± 2.7 Bq/kg, 7.5 ± 2.3 Bq/kg and 113.1 ± 40.6 Bq/kg respectively in the UH area (Table 4.4, fourth row from the bottom). It therefore follows that the DR area has the highest activity concentration, while the UH area has the lowest activity concentration, as could be observed in Figure 4.10.

A comparison of the average concentrations of ^{238}U, ^{232}Th and ^{40}K in the soil samples collected from Otavi (Table 4.4, second row from bottom) with the corresponding worldwide average values is shown in Table 4.4 and Figure 4.11.

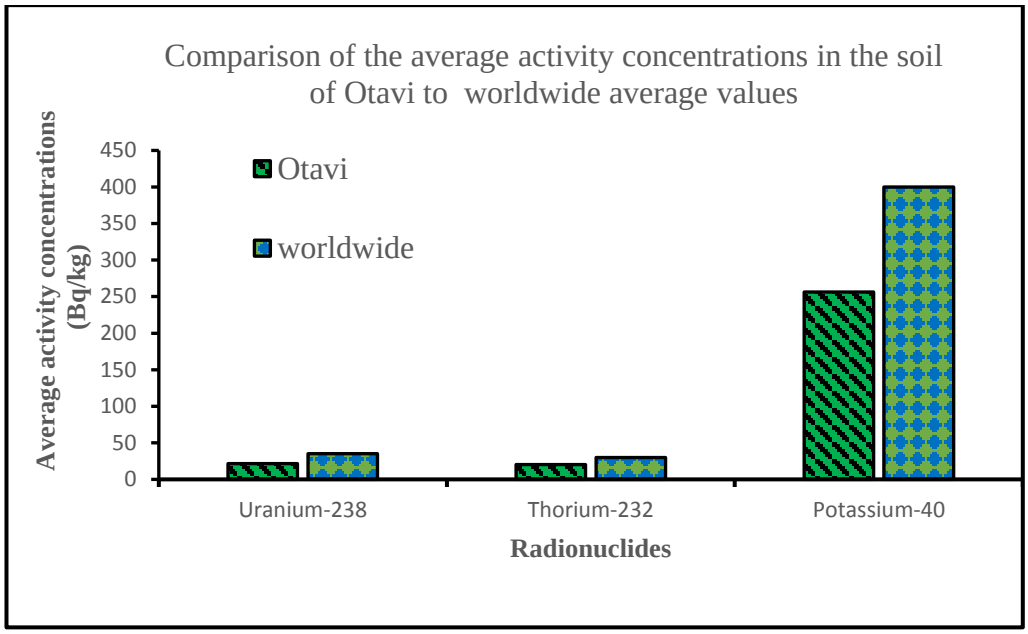

Figure 4.11: Comparison of the average activity concentrations of ^{238}U, ^{232}Th and ^{40}K in the soil of Otavi with the corresponding worldwide average values.

The mean activity concentration of ^{40}K in the DR area is slightly higher than the worldwide average value of 400 Bq/kg as could be observed in Table 4.4 (3rd row from bottom). However, the overall mean activity concentration of ^{40}K from all the samples are below the worldwide average value as could be seen in Figure 4.11. Also, the mean activity concentrations of ^{238}U and ^{232}Th from all the samples are below the worldwide average values as could be observed in Table 4.4 (last two rows) and Figure 4.11.

4.2.2. Assessment of radiation hazards in the soil of Otavi

The calculated absorbed dose rates, effective dose rates, radium equivalent activity (Ra_{eq}) and external hazard index (H_{ex}) in all the soil samples are shown in Appendix 3 (columns 8-15). Also, the results obtained for absorbed dose rates, effective dose rates, radium equivalent activity (Ra_{eq}) and external hazard index (H_{ex}) in the different geographical areas of Otavi are summarized in Table 4.5.

Table 4.5: The mean absorbed dose rate, effective dose rate, radium equivalent activity (Ra_{eq}) and external hazard index (H_{ex}) in the ten geographical areas of Otavi. The range of values is given in brackets.

Area	Absorbed dose rate (nGy/h)	Effective dose rate (μSv/y)	Radium equivalent activity (Ra_{eq}) (Bq/kg)	External hazard index (H_{ex})
TH	33.5 ± 4.1 (27.6 - 38.7)	41.0 ± 5.1 (33.9 - 47.4)	72.0 ± 8.8 (59.6 - 83.0)	0.19 ± 0.02 (0.16 - 0.22)
SQ	22.0 ± 3.2 (18.6 – 25.7)	27.0 ± 4.0 (22.9 -31.6)	47.2 ± 7.0 (39.8 - 55.2)	0.13 ± 0.02 (0.11 - 0.15)
KE	36.3 ± 5.9 (26.8 – 42.2)	44.9 ± 7.3 (32.9 - 51.7)	78.6 ± 12.8 (57.3 -90.6)	0.21 ± 0.03 (0.15 - 0.24)
TC	39.7 ± 7.2 (30.6 – 50.3)	48.7 ± 8.8 (37.6 -61.7)	84.2 ± 15.3 (65.4 - 107.1)	0.23 ± 0.04 (0.18 - 0.29)
AG	43.4 ± 18.0 (32.5 – 75.5)	53.2 ± 22.1 (39.8 - 92.5)	93.0 ± 38.6 (70.0 - 161.6)	0.25 ± 0.10 (0.19 - 0.44)
NM	27.0 ± 5.2 (19.9 – 34.1)	33.1 ± 6.3 (24.4 - 41.8)	58.0 ± 11.2 (42.9 - 73.6)	0.16 ± 0.03 (0.12 - 0.20)
KS	33.7 ± 3.2 (29.1 – 37.5)	41.4 ± 3.9 (35.7 - 46.0)	71.9 ± 6.8 (61.7 - 79.6)	0.19 ± 0.02 (0.17 - 0.21)
KH	30.1 ± 9.9 (20.7 – 43.2)	36.9 ± 12.1 (25.4 - 53.0)	64.3 ± 21.0 (44.2 - 92.1)	0.17 ± 0.06 (0.12 - 0.25)
UH	13.5 ± 3.6 (8.9 – 18.4)	16.6 ± 4.4 (10.9 - 22.6)	28.7 ± 7.5 (18.6 -38.3)	0.08 ± 0.02 (0.05 - 0.10)
DR	49.8 ± 9.8 (32.5 – 57.1)	61.0 ± 12.0 (39.9 -70.0)	105.7 ± 20.9 (68.9 -121.6)	0.29 ± 0.06 (0.19 - 0.33)
Average of all ten areas	**32.9 ± 12.5 (8.9 – 75.5)**	**40.4 ± 15.4 (10.9 -92.5)**	**70.4 ± 26.7 (18.6 – 161.6)**	**0.19 ± 0.07 (0.05 – 0.44)**

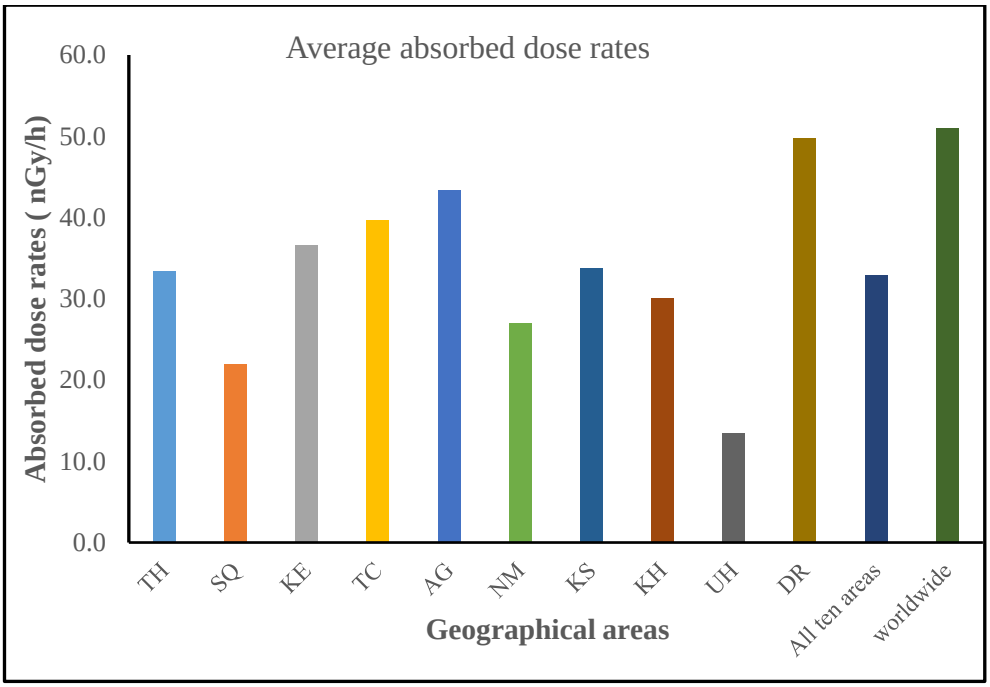

Figure 4.12: The average absorbed dose rates in the ten geographical areas of Otavi. The average absorbed dose rate over all the ten areas and the corresponding worldwide average value are shown in the last two columns.

The absorbed dose rates due to the soil samples vary between 8.9 ± 1.1 nGy/h (UH area) to 75.5 ± 3.0 nGy/h (AG area), with an overall average of 32.9 ± 12.5 nGy/h as shown in Table 4.5 (column 2, last row) . The mean absorbed dose rate is highest in the DR area with a value of 49.8 ± 9.8 nGy/h while it is lowest in the UH area, with a value of 13.5 ± 3.6 nGy/h as shown in Table 4.5 (column 2) and Figure 4.12. The DR area has relatively high concentrations of ^{40}K, as discussed earlier in this section. Therefore, it is not surprising that the highest average absorbed dose rate is observed in this area. It may be useful to mention again that ^{40}K is one of the main contributors to radiation dose. The calculated average absorbed dose rate in the soil samples collected from Otavi (32.9 ± 12.5 nGy/h) is much below the worldwide average value of 51.0 nGy/h.

As could be observed in Table 4.5 (column 3), the effective dose rates due to the soil samples range between 10.9 ± 1.3 μSv/y (UH area) and 92.5 ± 3.7 μSv/y (AG area). The overall average of 40.4 ± 15.4 μSv/y (Table 4.5, column 3, bottom row), is much below the MPL of 1.0 mSv/y recommended by ICRP for public exposure as could be seen in Figure 4.13. Therefore, it could be concluded that the town has a normal background radiation.

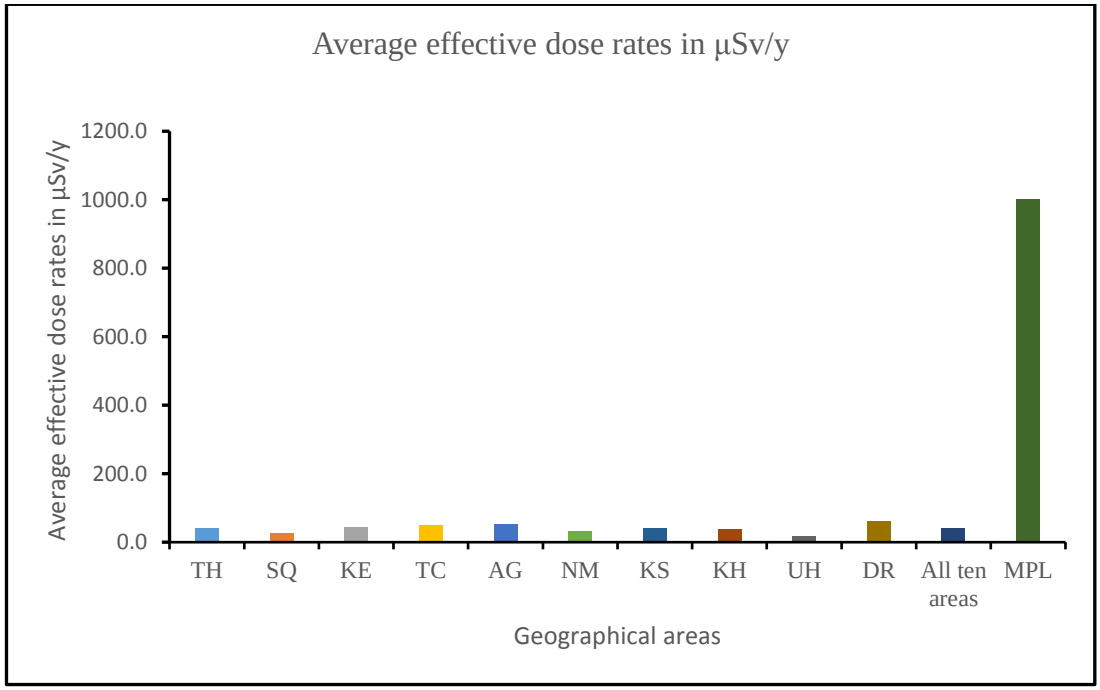

Figure 4.13: The average effective dose rates in the ten geographical areas of Otavi. The average effective dose rate over all the ten areas and the corresponding MPL are shown in the last two columns

The average radium equivalent activity (Ra_{eq}) and average external hazard index (H_{ex}) in the ten geographical areas of Otavi are shown in Table 4.5 (columns 4 and 5), respectively. The values of Ra_{eq} vary from a minimum of 18.6 ± 2.4 Bq/kg to a maximum of 161.6 ± 6.9 Bq/kg with an average of 70.4 ± 26.7 Bq/kg as shown in Table 4.5 (column 4, bottom row). Also, the values of H_{ex} vary from 0.05 ± 0.01 to

0.44 ± 0.02 with an average of 0.19 ± 0.07 as shown in Table 4.5 (column 5, bottom row). The calculated average values of Ra_{eq} and H_{ex} , are below their corresponding maximum permissible limits of 370 Bq/kg and 1.0 [52] as could be observed in Figure 4.14 and 4.15 respectively .The relatively low average values of Ra_{eq} and H_{ex} confirm that radiation hazard is negligible in the town.

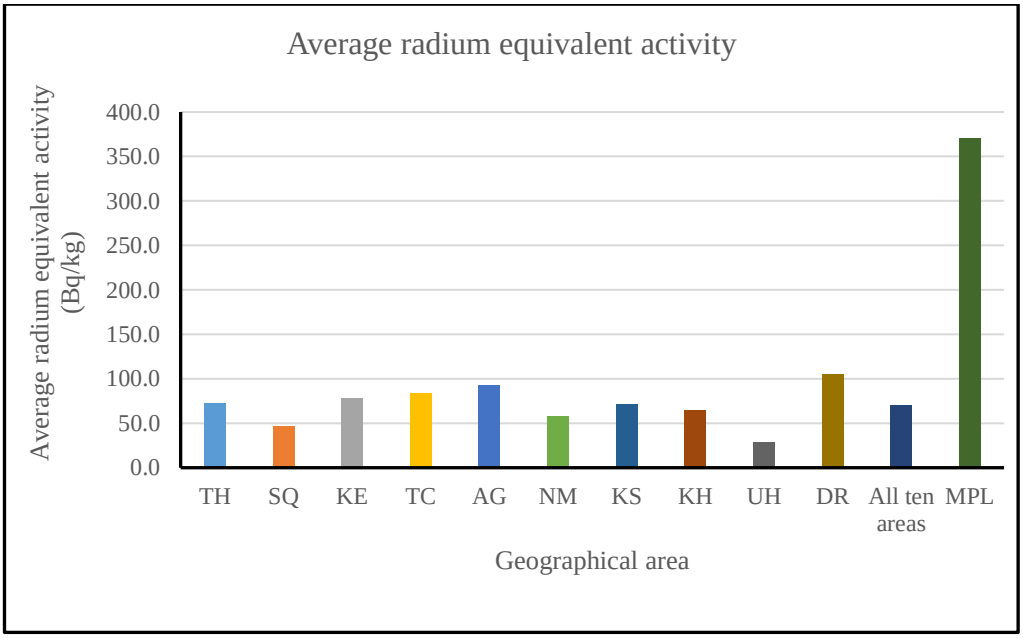

Figure 4.14: The average radium equivalent activity due to ^{238}U, ^{232}Th and ^{40}K in the ten geographical areas of Otavi. The average Ra_{eq} over all the ten areas and the corresponding MPL are also shown in the last two columns.

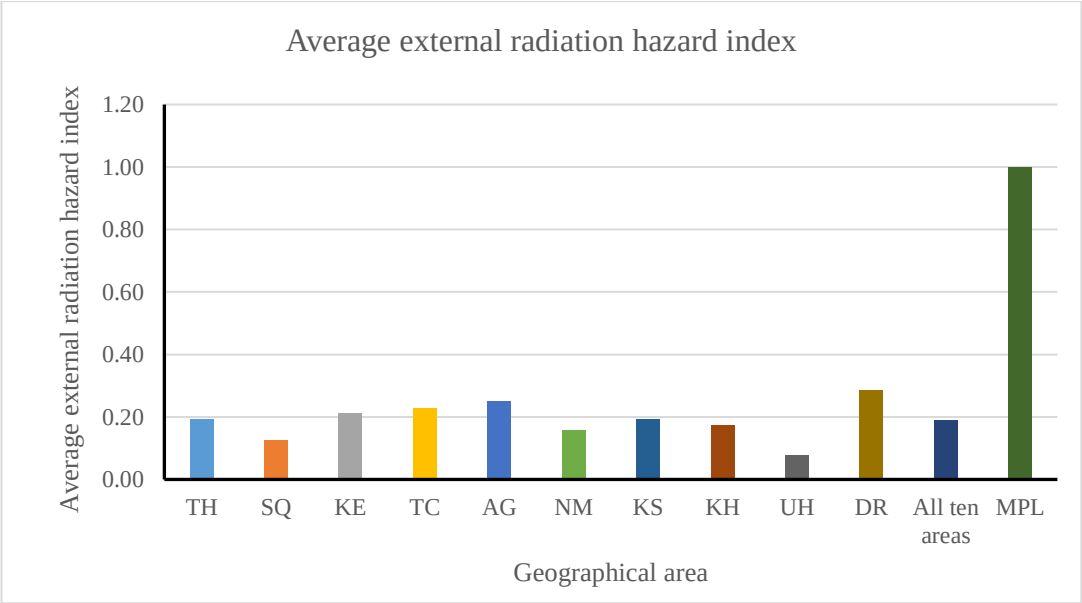

Figure 4.15: Average external radiation hazard index (H_{ex}) due to primordial radionuclides in the ten geographical areas of Otavi. The average H_{ex} over all the ten areas and the corresponding MPL are also shown in the last two columns.

4.2.3. Statistical analysis of the results obtained in the measurements of radioactivity in the soils of Otavi

The frequency distributions of all the radionuclide activity concentrations and the radiological risk parameters are shown in Table 4.6 and Figures 4.16 and 4.17.

Table 4.6: Statistical analysis of the results obtained for natural radioactivity in the soils of the town of Otavi

Descriptive statistics	^{238}U conc (Bq/kg)	^{232}Th conc (Bq/kg)	^{40}K conc (Bq/kg)	Absorbed dose rate (nGy/h)	Effective dose rate (μSv/y)	Radium equivalent activity (Ra_{eq}) (Bq/kg)	External hazard index (H_{ex})
Mean	21.6	20.3	256.4	32.9	40.4	70.4	0.19
Standard dev	7.2	8.5	113.7	12.5	15.4	26.7	0.07
Standard error	1.0	1.2	16.1	1.8	2.2	3.8	0.01
Median	22.4	20.6	242.3	32.6	40.0	70.3	0.19
Max	39.1	55.6	645.8	75.5	92.5	161.6	0.44
Min	6.5	3.7	76.5	8.9	10.9	18.6	0.05
Range	6.5-39.1	3.7-55.6	76.5-645.8	8.9-75.5	10.9-92.5	18.6-161.6	0.05-0.44
Kurtosis	-0.1	5.2	1.8	1.7	1.7	1.8	1.8
Skewness	0.0	1.3	1.1	0.8	0.8	0.8	0.8

As could be observed in Table 4.6 (column 1, bottom row) and Figure 4.16(a), the concentrations of ^{238}U has normal distribution, with the skewness being zero and the kurtosis is -0.1, which is not far from zero. Also, the concentration of ^{238}U in most of the samples is between 12.0 Bq/kg and 36.0 Bq/kg with the most frequently occurring range between 20.0Bq/kg and 24.0 Bq/kg. In fact, only four samples have concentrations below 12.0 Bq/kg and only one sample has a concentration above 36.0 Bq/kg. Similarly, as observed in Figure 4.16 (b), the concentrations of ^{232}Th in most of the samples range from 5.0 Bq/kg to 35.0 Bq/kg with the most frequently occurring range between 20.0 Bq/kg and 25.0 Bq/kg. In addition, the frequency distribution of ^{40}K is shown in Figure 4.16 (c). As could be observed from the figure, only eight samples have a concentration above 360.0 Bq/kg. Most of the samples have concentrations between 60.0 Bq/kg and 360.0 Bq/kg.

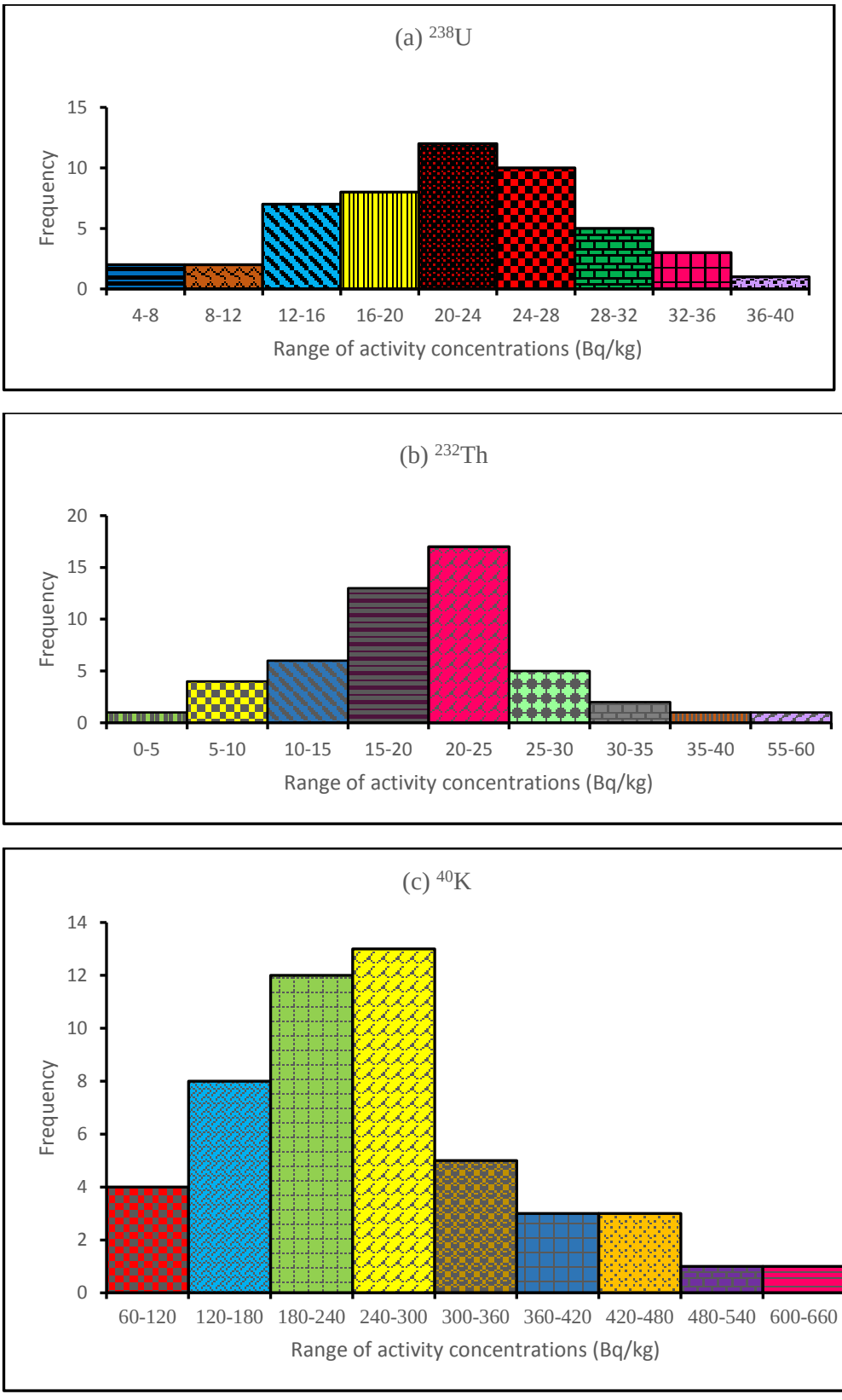

Figure 4.16: Frequency distributions of the activity concentrations of (a) ^{238}U, (b) ^{232}Th, and (c) ^{40}K in the soil samples collected from Otavi

Figure 4.17 shows the frequency distributions of (a) absorbed dose rates and (b) effective dose rates in Otavi. The absorbed dose rates due to radionuclides in the samples are mostly between 16.0 nGy/h and 56.0 nGy/h as could be observed in Figure 4.17 (a). The most frequently occurring range of the absorbed dose rate is 32.0 nGy/h to 40.0 nGy/h .Only two samples have the absorbed dose rate greater than 56.0 nGy/h and only four have absorbed dose rate below 16.0 nGy/h. Also, as could be observed in Figure 4.17 (b), the effective dose rates are mostly between 20.0 µSv/y and 65.0 µSv/y with the most frequently occurring range of 45.0 µSv/y to 50.0 µSv/y.

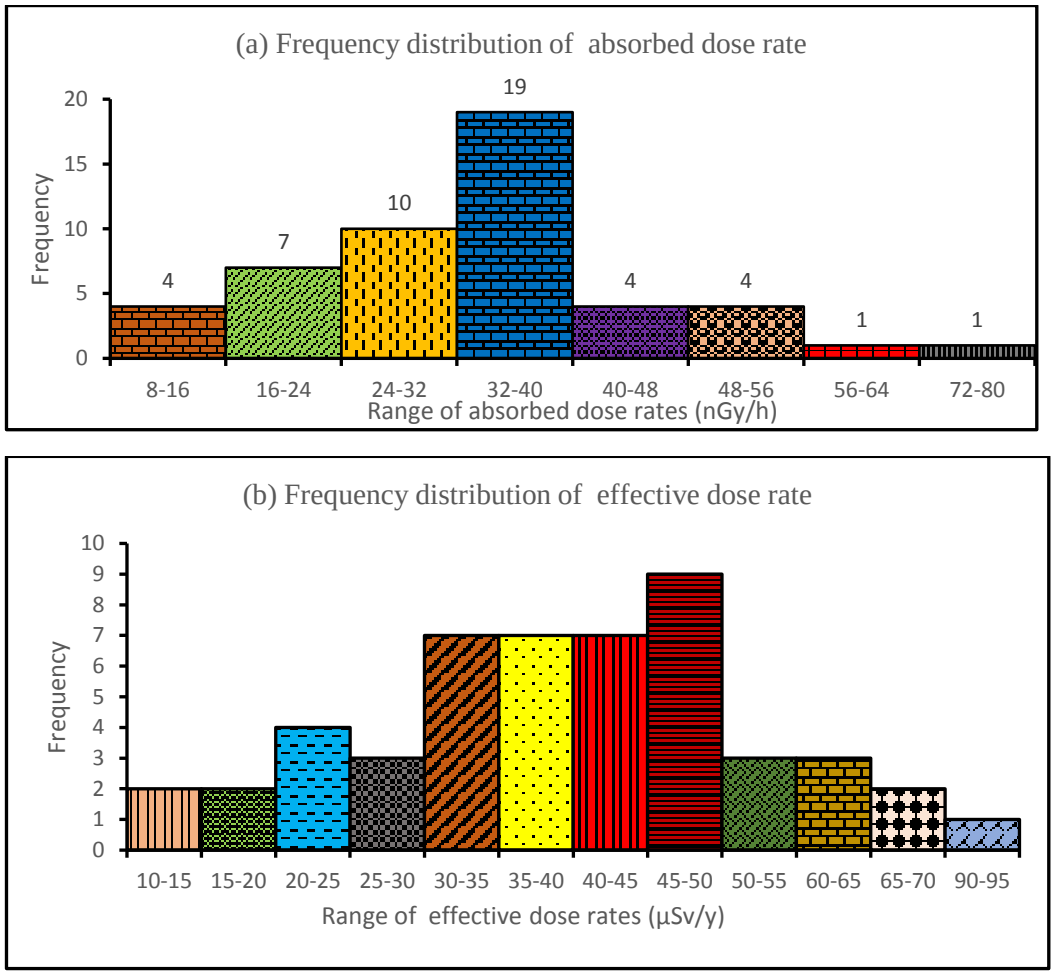

Figure 4.17: Frequency distributions of (a) absorbed dose rates and (b) effective dose rates due to radionuclides in the soil samples collected from Otavi

The frequency distributions of radium equivalent activity (Ra_{eq}) and external hazard index (H_{ex}) are shown in Figure 4.18. As could be observed in Figure 4.18 (a), most of the Ra_{eq} calculated for the town are between 30.0 Bq/kg and 120.0 Bq/kg with the most frequently occurring range between 60.0 Bq/kg and 90.0 Bq/kg. Only three samples have Ra_{eq} below 30.0 Bq/kg and only two samples have Ra_{eq} greater than 120 Bq/kg. Similarly, as could be observed from figure 4.18 (b), only one sample has H_{ex} above 0.35 and only four samples have H_{ex} below 0.10. Most of the calculated H_{ex} are between 0.10 and 0.35, with the most frequently occurring range between 0.20 and 0.25.

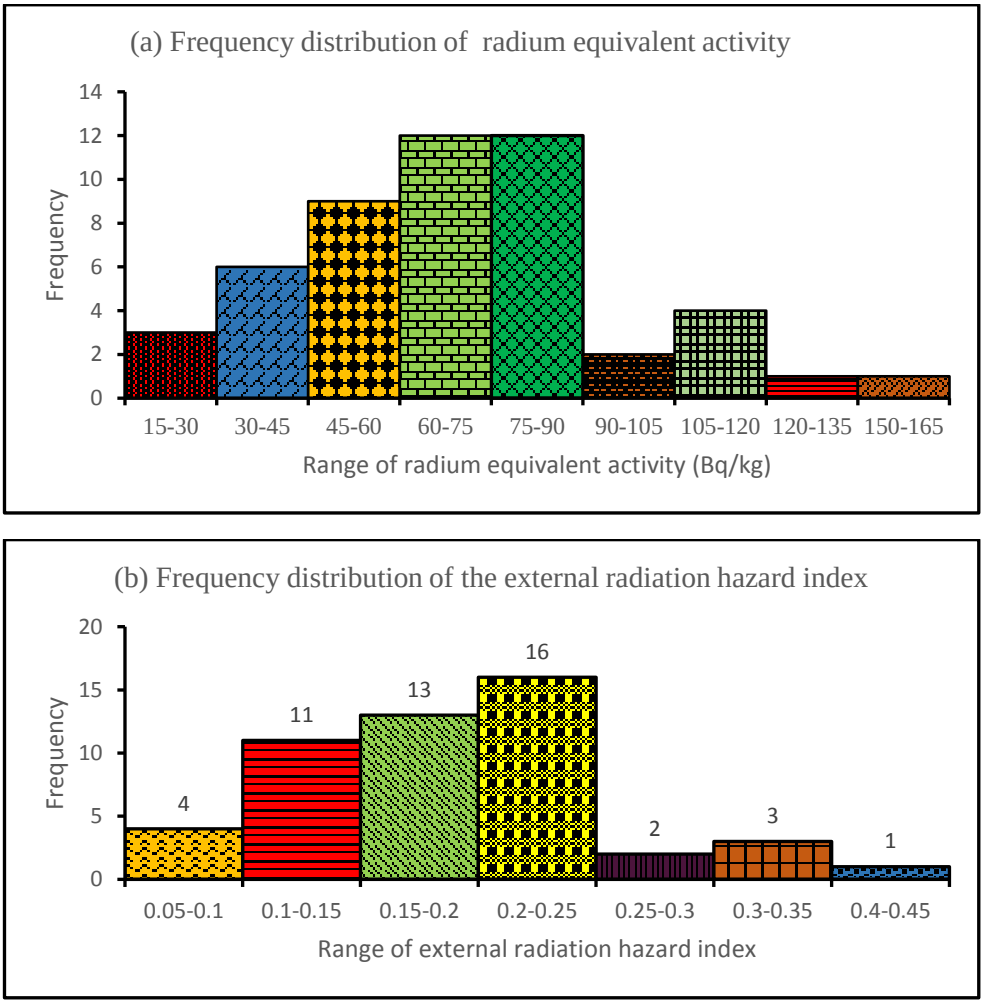

Figure 4.18: Frequency distributions of (a) Ra_{eq} and (b) H_{ex} due to primordial radionuclides in the soil samples collected from Otavi.

4.3. Comparison of the natural radioactivity in the soils of the Ohorongo Cement plant and Otavi

4.3.1. Activity concentrations of radionuclides

The average activity concentrations of ^{238}U, ^{232}Th and ^{40}K in all the soil samples collected from the Ohorongo Cement plant and the town of Otavi are shown in Table 4.7 and Figure 4.19.

Table 4.7: Average activity concentrations of radionuclides in the soil samples collected from the Ohorongo Cement plant and the town of Otavi. The range of values is given in parentheses.

Location	**Average activity concentration (Bq/kg)**		
	^{238}U	^{232}Th	^{40}K
Ohorongo Cement plant	15.0 ± 4.7 (7.3 - 25.6)	24.1 ± 9.9 (12.7 - 43.1)	310.7 ± 97.2 (132.2 – 507.8)
Otavi	21.6 ± 7.2 (6.5 – 39.1)	20.3 ± 8.5 (3.7 – 55.6)	256.4 ± 113.7 (76.5 – 645.8)

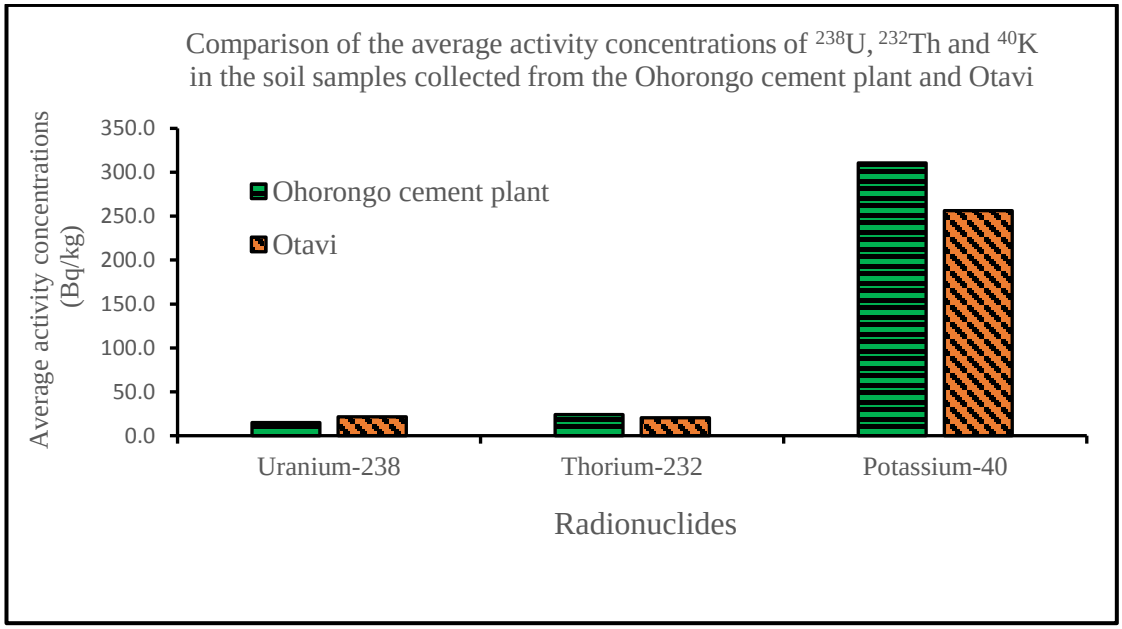

Figure 4.19: Comparison of the average activity concentration of ^{238}U, ^{232}Th and ^{40}K in the soil samples collected from the Ohorongo Cement plant and the town of Otavi

As could be seen in Table 4.7 and Figure 4.19, the average activity concentration of ^{238}U is higher in the town of Otavi (with a value of 21.6 ± 7.2 Bq/kg) than in the Ohorongo Cement plant (with a value of 15.0 ± 4.7 Bq/kg). However, the average activity concentrations of ^{232}Th and ^{40}K are higher in the Ohorongo Cement plant than in the town of Otavi. The average activity concentration of ^{40}K is much higher than those of ^{238}U and ^{232}Th in all the areas (of the Ohorongo Cement plant and Otavi), while ^{238}U has the lowest average activity concentration among all the three primordial radionuclides.

4.3.2. Radiation hazard parameters

The average absorbed dose rate, effective dose rate, radium equivalent activity (Ra_{eq}) and external hazard index (H_{ex}) in the Ohorongo Cement plant and in the town of Otavi are shown in Table 4.8 and Figures 4.20 and 4.21. As could be seen in Table 4.8 and in Figures 4.20 and 4.21, the average values of the absorbed dose rate, effective dose rate, radium equivalent activity (Ra_{eq}) and external hazard index (H_{ex}) are all only slightly higher in the Ohorongo Cement plant than in the town of Otavi. The difference in the H_{ex} in the plant and town is only 0.01. These results confirm that there is no significant difference in the natural radioactivity in the soil of the Ohorongo Cement plant and the town of Otavi.

Table 4.8: The mean absorbed dose rate, effective dose rate, radium equivalent activity (Ra_{eq}) and external hazard index (H_{ex}) in the soil samples collected from the Ohorongo Cement plant and Otavi. The range of values is given in parentheses

Location	Absorbed dose rate (nGy/h)	Effective dose rate (µSv/y)	Radium equivalent activity (Ra_{eq}) (Bq/kg)	External hazard index (H_{ex})
Ohorongo Cement plant	35.1 ± 11.8 (18.1 - 58.0)	43.0 ± 14.5 (22.2 - 71.2)	74.9 ± 25.6 (38.7 - 124.2)	0.20 ± 0.07 (0.10 - 0.34)
Otavi	32.9 ± 12.5 (8.9 - 75.5)	40.4 ± 15.4 (10.9 - 92.5)	70.4 ± 26.7 (18.6 - 161.6)	0.19 ± 0.07 (0.05 - 0.44)

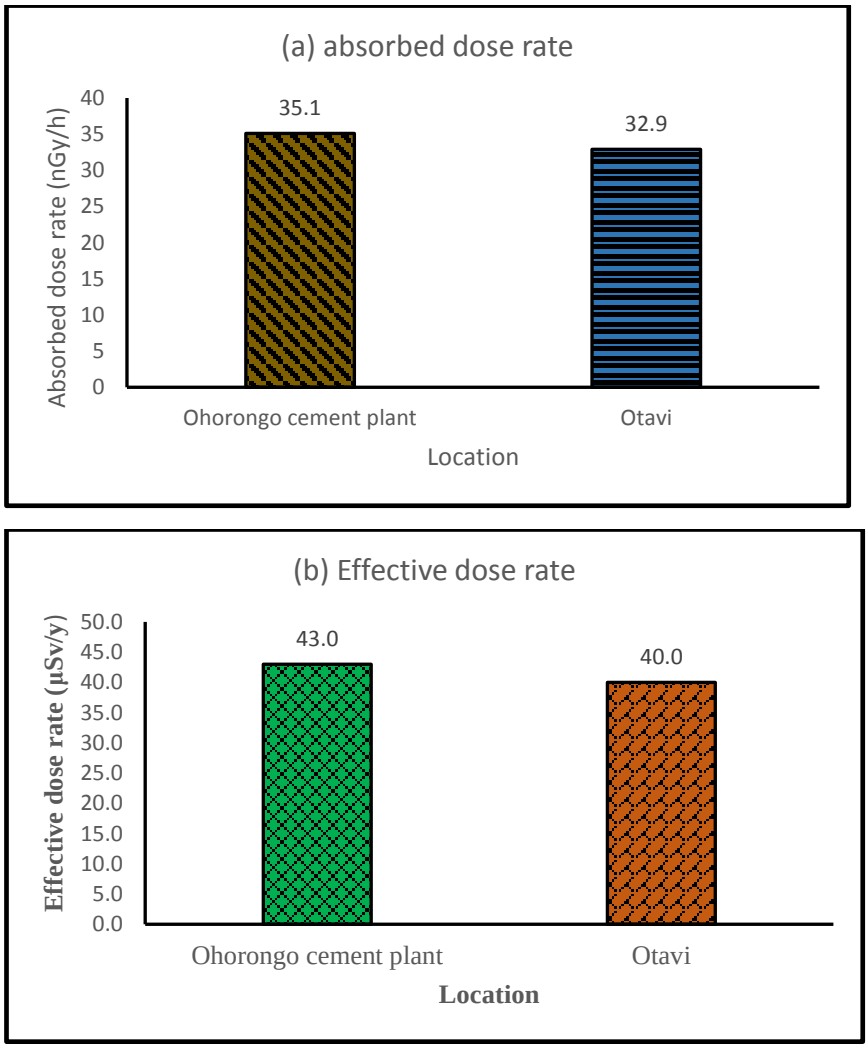

Figure 4.20: Comparison of (a) average absorbed dose rate and (b) effective dose rate due to radionuclides in the soil samples collected from the Ohorongo Cement plant and the town of Otavi.

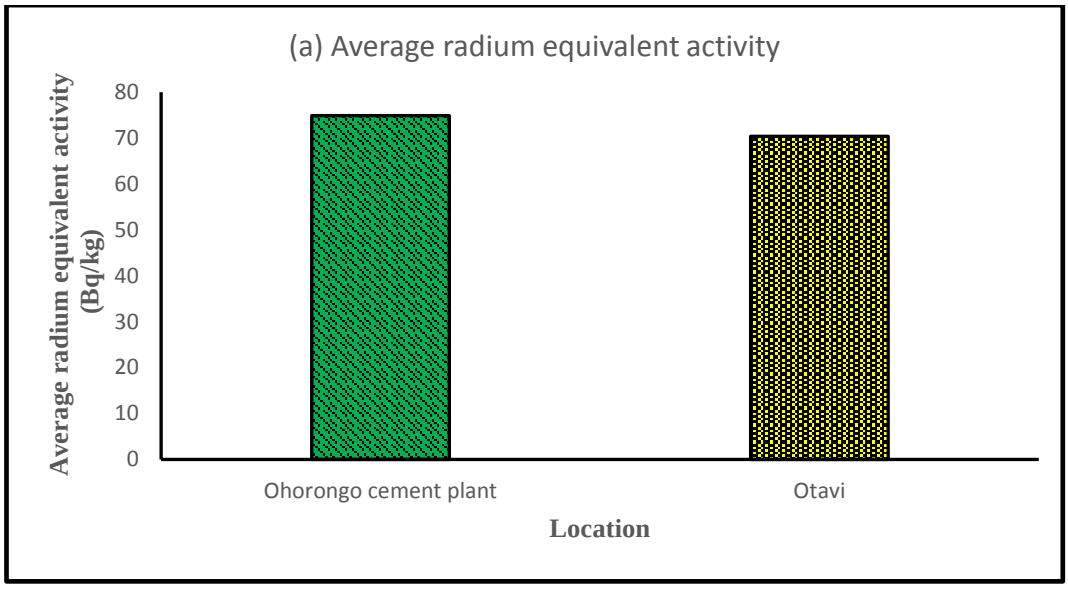

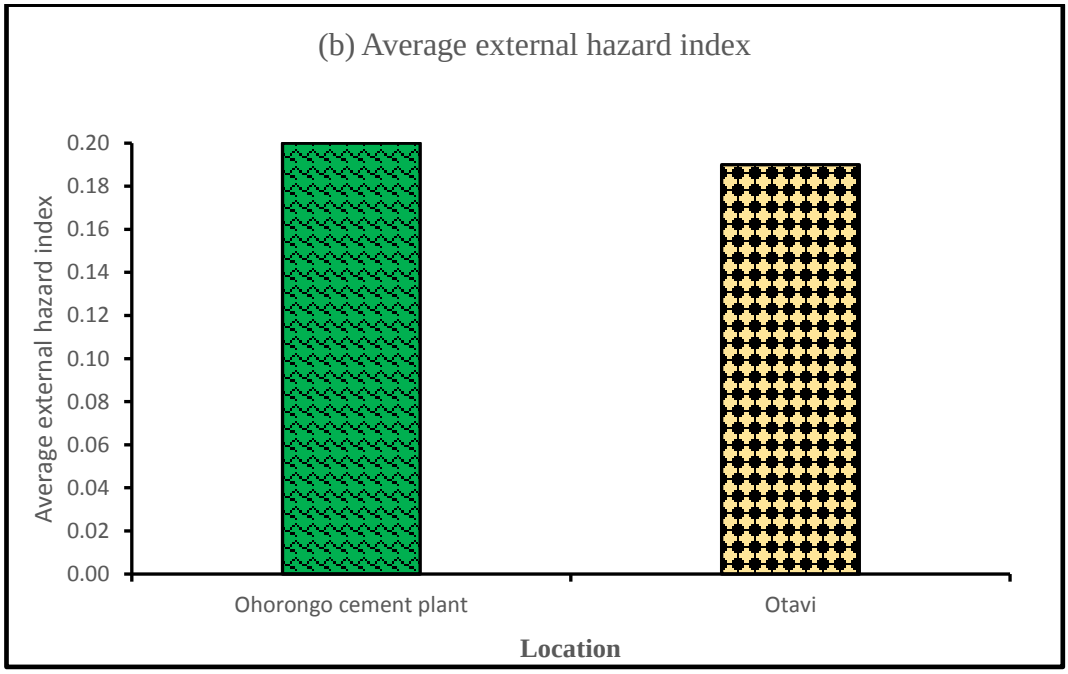

Figure 4.21: Comparison of (a) radium equivalent activity and (b) average H_{ex} due to radionuclides in the soil samples collected from the Ohorongo Cement plant and the town of Otavi.

4.4. Correlation analysis between the town of Otavi and the Ohorongo Cement plant

Correlation analysis has been carried out to determine the mutual relationship and strength of association between the radionuclides concentrations in the soils and the estimated radiological parameters. The results of the correlation coefficients are shown in Table 4.9. As could be observed from Table 4.9, a slightly lower correlation is noticed between ^{238}U and ^{232}Th ($r = 0.858$ and $r = 0.832$) and between ^{238}U and ^{40}K ($r = 0.886$ and $r = 0.814$) in both areas (Ohorongo cement plant and the town of Otavi). A strong positive correlation was observed between the activity concentrations of the three radionuclides and radiological parameters in all areas with the correlation coefficient more than the 0.9. This indicates that all the radiological parameters are strongly associated with the concentrations of the three radionuclides in the soils and these radionuclides contribute to the emission of gamma radiation in the study areas.

Table 4.9: Correlation coefficients between radionuclides and associated radiological hazards in the soil samples collected from the Ohorongo Cement plant and the town of Otavi

	Ohorongo Cement plant							Town of Otavi						
Variables	**^{238}U**	**^{232}Th**	**^{40}K**	**D_R**	**H_R**	**Ra_{eq}**	**H_{ex}**	**^{238}U**	**^{232}Th**	**^{40}K**	**D_R**	**H_R**	**Ra_{eq}**	**H_{ex}**
^{238}U	1							1						
^{232}Th	0.858	1						0.832	1					
^{40}K	0.886	0.938	1					0.814	0.909	1				
D_R	0.920	0.983	0.978	1				0.911	0.971	0.963	1			
H_R	0.920	0.983	0.978	1.000	1			0.911	0.971	0.963	1.000	1		
Ra_{eq}	0.918	0.986	0.975	1.000	1.000	1		0.912	0.974	0.958	1.000	1.000	1	
H_{ex}	0.918	0.986	0.975	1.000	1.000	1.000	1	0.912	0.974	0.958	1.000	1.000	1.000	1

Ra_{eq}: Radium equivalent activity; D_R: Absorbed dose rate; H_R: Annual effective dose rate; H_{ex}:

External hazard index

CHAPTER 5: CONCLUSIONS AND RECOMMENDATIONS

5.1. Conclusions

The activity concentrations of ^{238}U, ^{232}Th and ^{40}K in one hundred soil samples collected from the Ohorongo Cement plant and the town of Otavi have been determined using a gamma spectrometry having an HPGe detector. The results obtained show that the concentration of radionuclides in the soil is not homogeneous. The average activity concentration of ^{238}U, ^{232}Th and ^{40}K are 15.0 ± 4.7 Bq/kg, 25.1 ± 9.9 Bq/kg and 310.7 ± 97.2 Bq/kg, respectively in the Ohorongo Cement plant. Similarly in Otavi, the average activity concentration of ^{238}U, ^{232}Th and ^{40}K are 21.6 ± 7.2 Bq/kg, 20.3 ± 8.5 Bq/kg and 256.4 ± 113.7 Bq/kg, respectively. In both the Ohorongo Cement plant and the town of Otavi, ^{238}U has the lowest average activity concentration in the soils while ^{40}K has the highest activity concentration in the soils. However, the average activity concentrations of all the radionuclides in this study are lower than the corresponding worldwide average values.

The absorbed dose rates calculated for the Ohorongo Cement plant range from 18.1 ± 1.4 nGy/h to 58.0 ± 2.5 nGy/h with a mean value of 35.1 ± 11.8 nGy/h while the absorbed dose rates calculated for the town of Otavi range from 8.9 ± 1.1 nGy/h to 75.5 ± 3.0 nGy/h with a mean value of 32.9 ± 12.5 nGy/h. The corresponding average effective dose rates for the Ohorongo Cement plant is 43.0 ± 14.5 μSv/y while it is 40.4 ± 15.4 μSv/y for the town of Otavi. All the average effective dose rates in the plant and the town are lower than the maximum permissible limit of 1.0 mSv/y recommended by the ICRP. These results imply that the Ohorongo Cement plant and the town of Otavi have normal background radiation.

The radium equivalent activity varies from 38.7 ± 3.2 Bq/kg to 124.2 ± 5.6 Bq/kg with a mean of 74.9 ± 25.6 Bq/kg in the plant while it varies from 18.6 ± 2.3 Bq/kg to 161.6 ± 6.9 Bq/kg with a mean of 70.4 ± 26.7 Bq/kg in the town of Otavi. These values are below the maximum permissible limit of 370 Bq/kg. Furthermore, the calculated average external hazard index (H_{ex}) for the Ohorongo Cement plant and the town of Otavi were 0.20 ± 0.07 and 0.19 ± 0.07 respectively. These results are again below the maximum permissible value of 1.0 and thus confirm that radiological hazard is negligible at the Ohorongo Cement plant and in the town of Otavi. The results obtained in this study will contribute to the baseline data on natural radioactivity levels in Namibia.

The results obtained for Ohorongo cement plant and the town of Otavi are all below the permissible limit of 1.0 mSv/y, therefore there is no effect to the inhabitants of these areas.

5.2. Recommendations

The researcher recommends that this study be extended to determine the radiation level or radioactivity in drinking water and foodstuff such as rice and maize.

In addition, the researcher recommends that this study be extended to other important factories and town such as Tsitsabis, Okongo, Eenhana, B2-gold mine, etc, in order to assess the level of natural radioactivity in these areas and thereby confirm whether or not these areas have high or normal background radiation level.

Further study may be necessary to estimate internal doses and external doses from other sources like Radon-222 gas from dwellings for the population of Otavi and the Ohorongo Cement plant.

The equipment (gamma-ray spectrometer) used for this is rather old and consumes a lot of expensive liquid nitrogen. For this reason the time spent on measurement on each sample has to be minimized. It is therefore recommended that the University should buy a new gamma spectrometer that consumes little or no liquid nitrogen.

There are no nuclear technicians in this department of Physics (or University). As a result there are no technician to help set up nuclear experiments in the nuclear laboratory at UNAM and to provide the needed technical support for these types of a project. This makes it longer for a postgraduate student to complete the research project. It is therefore recommended that a dedicated nuclear technician be employed in the nuclear laboratory.

REFERENCES

[1] Pillai G S, Chandrasekaran S, Sivasubramanian K, Baskaran R and Venkatraman B 2017 A review on variation of natural radioactivity along the southeast coast of Tamil Nadu for the past 4 decades *Radiation Protection Dosimetry, vol 179 pp 125-135*

[2] Oyedele J A 2005 Measurements of Natural radioactivity in the soil samples of the University of Namibia, Windhoek Namibia in *Proceedings of the East and Southern Africa Environmental Chemistry Workshop (ESAECW) and the 6th Theoretical Chemistry Workshop in Africa (TCWA), Windhoek*

[3] Shimboyo S A, Oyedele J A and Sitoka S S 2016 Soil radioactivity levels and associated hazards in selected towns in Uranium-rich western Namibia *Int.Sci.technology.J.Namibia, vol. 7, pp. 73-84*

[4] Hassan N N and Khoo K S 2014 Measurement of natural radioactivity and assessment of radiation indices in the soil samples at Pengeran, Kota, tinggi ,Johor *American Institute of Physics,* vol. 1584, *no. 1, pp. 190-195*

[5] Duggal V, Rani A, Mehra R and Ramola R 2014 Assessment of natural radioactivity levels and associated dose rates in soil samples from Northern Rajasthan,India," *Radiation Protection Dosimetry vol 158 , pp. 235-240*

[6] Lilley L 2001 Nuclear Physics:Principles and Applications N*ew york: John Wiley & Son Ltd*

[7] Santawamaitre T, Malain D, Al-Sulaiti HA, Bradley DA, Matthews MC and Regan P.H 2014 Evaluation of the Level of Naturally Occuring Radioactive Materials in the soil samples along the Chao River Basin in Thailand *Journal of Environmental Radioactivity Vol 138 pp 80-86*

[8] Dizman S, Gorur F K and Keser R 2016 Determination of Radioactivity levels of soil samples and the excess of lifetime cancer risk in Rize province, turkey *International Journal of Radiation Research,* v*ol. 14, no. 3, pp. 237-244*

[9] United Nations Scientific Committee on the Effects of Atomic Radiation (UNSCEAR) 2000 Sources of ionizing radiation (Annex B) *Report to the General Assembly New York*

[10] Wrixon A D 2008 New ICRP recommendations *J. Radiol. Prot*, no. 28, pp. 161-168

[11] DEG's Bridging the skills gaps in Namibia: Ohorongo Cement (Pty) Ltd 2016 –-A Cement producer succesfully addresses skills greenfield investment DEG -*case study of Deutsche Investitions - und Entwicklungsgesellschaft mbH Kämmergasse 22, 50676 Cologne https://www.deginvest.de/DEG-Documents-in-English/About-us/What-is-our-impact/Case-Study_Ohorongo-Cement-(Pty)-Ltd._EN_2016-02.pdf [accessed 20 July 2018]*

[12] Namibia Statistics Agency Namibia 2011 Population & Housing Census Main Report, *Namibia Statistic Agency*, Windhoek,

[13] Discovery of Radioactivity- Chemistry LibreTexts 12 February 2015 *https://chem.libretexts.org/Bookshelves/Physical_and_Theoretical_Chemistry_Textbook_Maps/Supplemental_Modules_(Physical_and_Theoretical_Chemistry)/Nuclear_Chemistry/Radioactivity/Discovery_of_Radioactivity*. [Accessed 12 August 2018].

[14] Turner J E 2012 Atoms, Radiation and Radiation Protection (3rd ed). *British: Wiley*

[15] Shoqwara F, Dwaikat N and Saffarini G 2013 Measurement of Radon Exhalation from Building Materials *Journal of Physics Vol 2, Issue 1*

[16] The Nobel prize in Physics 1903 NobelPrize.org Nobel media 2019 *https://www.nobelprize.org/prizes/physics/1903/marie-curie/facts/* [Accessed 14 August 2018].

[17] The Discovery of Radioactivity 2018 webmaster. URL *https://www2.lbl.gov/abc/wallchart/chapters/03/4.html* [Accessed 16 August 2018].

[18] Young H D and Freedman R A 2008 University Physics with modern Physics *San Francisco: Pearson Addison Wesley*

[19] Glossary radioactive chain series 2018 *http://www.sukjaro.eu/cikkek/decay_chain/glossary/index.htm* [Accessed 02 September 2018].

[20] L'Annunziata M F 2012 Handbook of radioactivity analysis (3rd ed) *Netherlands: Elsevier Inc : Academic press*

[21] Bryan J C 2013 Introduction to Nuclear Science *United States Of America: CRC Press*

[22] Oyedele J A 2012 Nuclear Physics *Centre for External Studies ,University of Namibia, Windhoek*

[23] Al-Sulaiti A H 2011 Determination of Natural Radioactivity Levels in the State of Qatar using High-Resolution Gamma-ray Spectrometry *PhD dissertation University of Surrey*

[24] Krane K 1988 Introductory Nuclear Physics *Chichester: John Wiley and Sons, Inc*

[25] Image of secular equilibrium 2018 https://images.slideplayer.com/15/4577861/slides/slide_9.jpg [Accessed 20 July 2018]

[26] Radioactive Decay 2018 *https://moreira.tamu.edu/BAEN625/TOC_files/radioacDecay.pdf.*

[27] Knoll G F 2010 Radiation Detection and Measurement (4th ed) *USA: John Wiley and Sons ISBN 978-0-470-13148-0*

[28] Image of alpha decay 2018 *http://www.atnf.csiro.au/outreach//education/senior/cosmicengine/images/sun/alphadecay.gif* [Accessed 25 July 2018].

[29] Tsoulfanidis N and Landsberger S 2015 Mesurement and Detection of Radiation (4th ed) *US: Tylor & Fransis Group, LLC*

[30] Glossary term- Beta decay 2018 *https://education.jlab.org/glossary/betadecay.html* [Accessed 25 July 2018]

[31] Tahir S N, Jamil K, Zaidi J H, Arif M, Ahmed N, Ahmad S A 2005 Measurement of activity concentration of Naturally occuring radionuclides from Punjab provience of Pakistan and assesment of radiological hazards *Radiation Protection Dosimetry, Volume 113, Issue 4*

[32] L'Annunziata M F 2007 Radioactivity: Introduction and History (1st ed) *Netherland : Elsevier B V*

[33] Image of gamma-decay 2018 *https://www.liberaldictionary.com/wp-content/uploads/2019/02/gamma-decay-3579.jpg* [Accessed 25 July 2018].

[34] Eisenbud M and Gesell T 1997 Environmental radioactivity from natural, Industrial and Military sources (4th ed) *London: Academic press*

[35] Giancolli C G 2005 Physics: Principles with Apllications (6th ed) *United State of America: Pearson Education, Inc*

[36] Das A and Ferbel T 2003 Introduction to Nuclear and Particle physics (2nd ed) *London: World Scientific Pub.Co*

[37] Bailey D L, Humn J L, Todd-Pokropek A and Van Aswegen 2014 A Nuclear Medicine Physics : A handbook for Teachers and Sttudents *Vienna : International Atomic Energy Agency*

[38] The Nucleus: A chemist's view *https://slideplayer.com/slide/4919934/* [Accessed 05 October 2018]

[39] NCRP 1975 Background Radiation in the USA Recommendation of the National Council of Radiation and Measurements. *Report No.45.*

[40] Thorne M C 2003 Background radiation : natural and man- made *Journal of Radiological Protection Vol 23*

[41] National Council on Radiation Protection and Measurements (NCRP) 1987 Ionizing radiation Exposure of the population of the United States *Report No:93*

[42] Maphoto K P 2004 Determination of Natural radioactivity concentration in soil: a comparative study of Windows and Full Spectrum Analysis *Master thesis University of the Western Cape*

[43] Image of Compton scattering 2018 *http://www.mysearch.org.uk/website1/images/pictures/523.1.jpg* [Accessed 28 September 2018].

[44] File:Pairproduction.png 2018 *https://commons.wikimedia.org/wiki/File:Pairproduction.png* [Accessed 28 September 2018]

[45] Pereira W R , Carlos D U, Antonio da Silva Braga M and Galbiatti H F 2016 Evaluation of gamma-gamma well logging data applied to iron ore exploration – vale geophysical well logging test facility *Revista Brasileira de Geof´ısica, vol. 34, no. 2, pp. 207-215*

[46] Soha G B 2013 Physics and Radiobiology of Nuclear medicine (4th ed) *New york: Springer*

[47] Simon R C, James A S and Michael E P 2012 Physics in Nuclear Medicine (4th ed) *https://books.google.com/books/about/Physics_in_Nuclear_Medicine_E_Book.html?id=UnDrbqfM2HUC* [accessed 15 October 2018]

[48] Introduction to Radiation Detectors 2018 EQUIPCO *https://www.equipcoservices.com/support/tutorials/introduction-to-radiation-monitors/* [accessed 15 October 2018]

[49] Ouseph P 1975 Introduction to Nuclear Radiation Detectors [ebook] New York & London : Plenum Press. ISBN : 978-1-4160-5198-5Available from *https://books.google.com/books/about/Introduction_to_Nuclear_Radiation_Detect.html?id=nl4FCAAAQBAJ* [accessed 18 October 2018]

[50] Image result for gas-filled detector 2018 *https://www.equipcoservices.com/images/tutorials/introrad2.png* [accessed 18 october 2018]

[51] Dendooven P 2010 Basic Detection Techniques 2009-2010 *Kernfysisch Verneller Instituut* available from *http://www.astro.rug.nl/~peletier/Bas%20Det%20Tech%202009%20semiconductors.pdf* [accessed 18 october 2018]

[52] ICRP 2007 The 2007 recommendations of the International Commission on Radiological Protection (report 103) *Journal of the International Commission on Radiological Protection*

[53] Introduction to radiation safety 2018 Biological effects Nonstochastic Effects NDT, resource center *https://www.nde-ed.org/EducationResources/CommunityCollege/RadiationSafety/biological/nonstochastic/nonstochastic.php* [Accessed 20 October 2018]

[54] Deterministic effect and stochastic effects of radiation 2018 *https://www.researchgate.net/profile/Hosam_El-Din_Saleh/publication/329238059/figure/fig7/AS:703310680043522@1544693741428/Deterministic-effect-and-stochastic-effects-of-radiation.png*

[55] Chowdhurry M I , Alam M N and Hazari S K S 1999 Distribution of Radionuclides in the river sediments and Coastal Soils of Chittagong, Bangladesh and Evaluation of the radiation hazard *Applied Radiation and Isotopes, vol. 51, pp. 747-755*

[56] Tzotzis M, Svoukis E and Tsetos H 2004 A Comprehensive study of Natural Gamma radioactivitylevels and Associated Dose rates from surface soils in Cyprus *Radiation Protection Dosimetry, vol. 109, no. 3, pp. 217-224*

[57] Hasan I D 2011 Measurement of Radioactivity for Radium-226 isotopes in some Soil Samples from Defferent regions in Karbala Governorate using Gamma Ray Spectromtry *Journal of Babylon University/Pure and Applied Sciences,* vol. 1

[58] Valan I I, Mathiyarasu R , Sridhar S G D, Narayanan V and Stephen A 2015 Investigation of background radiation level in Krusadai Island Mangrove, Gulf of Mannar, India *Journal of Radioanalytical and Nuclear Chemistry Vol 304 pp 735-744*

[59] Faanu A, Darko E O and Ephraim J 2011 Determination of Natural radioactivity and Hazard in Soil and Rock samples in Mining area in Ghana *Applied Ecology, Vol. 19, pp. 77-92.*

[60] Reda Elsaman, Mohammed Ahmed Ali Omer, El-Montaser Mahmoud Seleem and Atef El-Taher 2018 Natural Radioactivity Levels and Radiological Hazards in Soil Samples Around Abu Karqas Sugar Factory *Journal of Environmental Science and Technology, 11: 28-38*

[61] Lawluvi H, Darko E O, Schandorf C, Faanu A, Awudu R and Kpeglo D O 2011 Natural radioactivity concentrations in Beach sands from some tourists resorts *Journal of environmental and earth sciences Vol 3 pp 729-736*

[62] Njinga L R and Tshivhase M V Lifetime cancer risk due to gamma radioactivity in soils from Tudor Shaft mine environs, South Africa *Journal of Radiation Research and Applied SciencesVol 9 pp 310-315*

[63] Shimboyo S A and Oyedele J A 2015 Determination of natural radioactivity in soils of Henties Bay, Namibia *Int. Sci. Technol. J. Namibia, Vol. 5, pp. 104-110*

[64] Oyedele J A , Sitoka S S and Davids I 2008 Radionuclide Concentration in soils of Northern Namibia,Southern Africa *Radiation Protection Dosimetry, Vol. 131, pp. 482-486*

[65] Oyedele J A 2006 Measurement of the natural radioactivity at the *International High Energy Stereoscopic System (HESS) project in Southern Africa Applications Radiation and Isotopes, Vol. 64, pp. 686-688*

[66] Oyedele J A 2006 Assessment of the natural radioactivity in the soils of Windhoek city, Namibia, Southern Africa *Radiation Protection Dosimetry, Vol. 121, no. 3, pp. 337-340*

[67] Mendelsohn J, Jarvis A, Roberts C and Robertson T 2002 Atlas of Namibia: a portrait of the lands and its people

[68] Avwiri G O, Osimobi J C and Agbalagba E O 2012 Evaluation of Radiation Hazard indices and Excess lifetime Cancer isk due to natural radioactivity in soil of Udi and Ezeagu local government areas of Enugustate, Nigeria *Comprehensive journal of Environmental and Earth Sciences Vol. 1 no. 1 pp. 1-10*

[69] Chen J 2018 Skewness 2018 *https://www.investopedia.com/terms/s/skewness.asp*. [Accessed 20 September 2018].

APPENDICES

Appendix 1

The matlab manuscript used to calculate the radionuclides activity concentrations, the absorbed dose and the effective dose

```
%calculates the concentration (Bq/kg) of the nuclides 238-U, 232-Th,
40-K in a given sample with net peak area Unpa for 238-U, Thnpa for
232-Th and
%Knpa for 40-K.
% It also calculates the Dose rate in nGy/h and the Effective dose
rate in mSv/y
function
[Uc,Thc,Kc,Dt,Effective_Dose_Rate]=Ohorongo_Soil_Sample(npU, npTh,
npK);
g=xlsread('C:\Users\User\Documents\2017\RESEARCH\Data
analysis\Ohorongo Cement Samples_Net peak areas.xls');
%To read the data from the excel spreadsheet
npU  =g(:,3);delta_npU=g(:,4);
npTh  =g(:,6);delta_npTh=g(:,7);
npK  = g(:,9);delta_npK=g(:,10);
data = xlsread('C:\Users\User\Documents\2017\RESEARCH\Data
analysis\Ohorongo Cement Standard_Net peak areas-editha.xls');
%To read the standard peak area and error standard peak from the
excel
RGU_nPa=data(:,2); delta_RGU_nPa=data(:,3);
RGTh_nPa=data(:,5); delta_RGTh_nPa=data(:,6);
RGK_nPa=data(:,8); delta_RGK_nPa=data(:,9);
%Standard values of the Concentrations and the error standard
%concentrations
StdC=[4940.00; 3250.00;
14000.00];Error_of_StdC=[30.00;90.00;400.00];
nPA=[RGU_nPa;RGTh_nPa;RGK_nPa];Error_of_nPA=[delta_RGU_nPa;delta_RGT
h_nPa;delta_RGK_nPa];
x1=StdC(1);x2=StdC(2);x3=StdC(3);%Assigned value for the standard
concentration 238-U,232-Th and 40-K
y1=nPA(1);y2=nPA(2);y3=nPA(3);%Assigned value for the standard net
peak area of 238-U,232-Th and 40-K
%K Standard
kU =y1/x1;
kTh =y2/x2;
kK =y3/x3;
%Calculating the concentration of radionuclides
Uc=npU/kU; Thc=npTh/kTh; Kc=npK/kK;
% K Standard error
delta_nPA_RGU  =  Error_of_nPA(1);delta_StdC_U=Error_of_StdC(1);
delta_nPA_RGTh=Error_of_nPA(2);delta_StdC_Th=Error_of_StdC(2);
delta_nPA_RGK=Error_of_nPA(3);delta_StdC_K=Error_of_StdC(3);

delta_kU  =
abs(kU)*sqrt((delta_nPA_RGU(1)/y1)^2+(delta_StdC_U/x1)^2);
```

```
delta_kTh  =
abs(kTh)*sqrt((delta_nPA_RGTh(1)/y2)^2+(delta_StdC_Th/x2)^2);
delta_kK= abs(kK)*sqrt((delta_nPA_RGK(1)/y3)^2+(delta_StdC_K/x3)^2);

delta_Uc= abs(Uc).*sqrt((delta_npU./npU).^2+(delta_kU./kU).^2);
delta_Thc=
abs(Thc).*sqrt((delta_npTh./npTh).^2+(delta_kTh./kTh).^2);
delta_Kc= abs(Kc).*sqrt((delta_npK./npK).^2+(delta_kK./kK).^2);
  %Calculation of  the Dose rates in Grays per hour(Gy/h),Dt and
also it's error we call delta_Dt.
Dt= 0.0417.*Kc+0.462.*Uc+0.604.*Thc;
delta_Dt=
sqrt((0.0417.*delta_Kc).^2+(0.462.*delta_Uc).^2+(0.604.*delta_Thc).^
2);
% calculation of the Effective_Dose_Rates in milli Sievert per
year(mSv/y)
Effective_Dose_Rate=Dt.*8760*0.7*0.2*10^-3;
delta_Effective_Dose_Rate=delta_Dt.*8760*0.7*0.2*10^-3;
%To create an excel file
fid  = fopen('C:\Users\User\Documents\2017\RESEARCH\Data
analysis\Ohorongo Cement_Samples_results_17-10-18.xls','wt');
fprintf(fid,'Ohorongo Cement plant _sample Results\n')
fprintf(fid,'\n')
fprintf(fid,    'Sample  \t     Uc(Bq/kg)  \t  delta_Uc(Bq/kg)  \t
Thc(Bq/kg)  \t  delta_Thc(Bq/kg)  \t   Kc(Bq/kg)   \t
delta_Kc(Bq/kg)  \t    Dose(Gy/h)  \t    delta_Dt(Gy/h)   \t
EffectiveDoseRate(mSv/y)   \t
delta_EffectiveDoseRate(mSv/y)\n');
for i     =   1:50
fprintf(fid, '%1.0f       \t        %3.2f   \t      %2.2f     \t
%2.2f     \t        %2.2f       \t    %2.2f       \t         %2.2f
\t    %2.2f         \t          %2.2f      \t              %2.5f
\t       %2.5f\t\n',...
[(i),  Uc(i),  delta_Uc(i) ,  Thc(i)  ,  delta_Thc(i)   ,  Kc(i)  ,
delta_Kc(i)  , Dt(i)  , delta_Dt(i) ,  Effective_Dose_Rate(i)  ,
delta_Effective_Dose_Rate(i)]);
end
fprintf(fid,'\n')
fclose(fid);
```

Appendix 2

Natural radioactivity in the soil samples of the Ohorongo Cement plant

S/N	U_C (Bq/kg)	δU_C (Bq/kg)	Thc (Bq/kg)	δThc (Bq/kg)	Kc (Bq/kg)	δK_C (Bq/kg)	Dose (nGy/h)	δDt (nGy/h)	Effective Dose rate (µSv/y)	δEffective DoseRate (µSv/y)	Ra_{eq} (Bq/kg)	δRa_{eq} (Bq/kg)	H_{ex}	δH_{ex}
1	17.2	1.5	19.4	2.5	277.4	15.3	31.2	1.8	38.3	2.2	66.2	4.1	0.18	0.01
2	13.5	1.5	15.7	2.3	243.4	13.6	25.9	1.7	31.7	2.0	54.7	3.8	0.15	0.01
3	16.1	1.5	21.9	2.5	281.0	15.2	32.3	1.8	39.7	2.2	68.9	4.1	0.19	0.01
4	14.3	1.4	19.2	2.6	250.2	14.2	28.6	1.8	35.1	2.2	61.0	4.1	0.16	0.01
5	10.9	1.4	23.5	2.5	269.0	14.8	30.4	1.8	37.3	2.2	65.2	4.0	0.18	0.01
6	14.3	1.5	28.1	2.9	291.5	15.8	35.7	2.0	43.8	2.5	76.9	4.6	0.21	0.01
7	14.8	1.4	18.5	2.4	264.3	14.8	29.0	1.7	35.6	2.1	61.6	3.9	0.17	0.01
8	10.4	1.5	14.6	2.3	238.7	14.0	23.6	1.7	28.9	2.0	49.6	3.8	0.13	0.01
9	17.8	1.6	27.2	2.6	354.7	17.9	39.4	1.9	48.3	2.3	83.9	4.2	0.23	0.01
10	11.9	1.4	19.9	2.4	275.3	15.2	29.0	1.7	35.6	2.1	61.6	3.8	0.17	0.01
11	9.3	1.4	17.0	2.2	214.7	13.0	23.5	1.6	28.8	2.0	50.1	3.6	0.14	0.01
12	7.7	1.3	12.7	2.2	261.2	14.4	22.1	1.6	27.2	1.9	46.0	3.5	0.12	0.01
13	8.9	1.4	19.1	2.5	276.9	15.0	27.1	1.7	33.3	2.1	57.4	3.9	0.16	0.01
14	12.9	1.4	18.6	2.3	289.4	15.5	29.3	1.7	35.9	2.0	61.8	3.8	0.17	0.01
15	18.4	1.7	27.5	2.9	358.4	17.7	40.0	2.1	49.1	2.6	85.3	4.7	0.23	0.01
16	20.1	1.8	33.1	3.0	381.9	18.5	45.2	2.1	55.5	2.6	96.9	4.8	0.26	0.01
17	15.9	1.7	26.4	2.7	335.9	17.0	37.3	1.9	45.8	2.4	79.5	4.4	0.21	0.01
18	10.6	1.3	16.3	2.4	249.2	14.1	25.1	1.7	30.8	2.0	53.1	3.8	0.14	0.01
19	9.6	1.4	13.1	2.1	204.8	12.7	20.9	1.5	25.6	1.9	44.1	3.5	0.12	0.01
20	18.0	1.5	31.9	3.3	379.3	18.5	43.4	2.2	53.3	2.7	92.9	5.1	0.25	0.01
21	9.0	1.3	16.1	2.5	204.8	12.7	22.4	1.7	27.5	2.1	47.8	4.0	0.13	0.01
22	8.4	1.2	12.7	2.0	157.2	11.0	18.1	1.4	22.2	1.7	38.7	3.2	0.10	0.01
23	10.5	1.4	15.1	1.9	132.2	9.7	19.5	1.4	23.9	1.7	42.2	3.2	0.11	0.01
24	11.2	1.2	16.1	2.3	228.3	13.3	24.4	1.6	29.9	1.9	51.8	3.6	0.14	0.01
25	9.4	1.3	17.0	2.2	221.5	13.0	23.8	1.5	29.2	1.9	50.7	3.5	0.14	0.01
26	10.0	1.5	17.6	2.3	199.6	12.6	23.6	1.7	28.9	2.0	50.5	3.8	0.14	0.01
27	18.6	1.9	35.6	3.1	390.2	18.8	46.4	2.2	56.8	2.7	99.5	5.0	0.27	0.01
28	14.9	1.5	21.0	2.6	285.2	15.5	31.4	1.8	38.5	2.2	66.8	4.1	0.18	0.01
29	14.9	1.6	20.1	2.7	286.8	15.7	31.0	1.9	38.0	2.4	65.7	4.4	0.18	0.01
30	15.1	1.6	28.7	3.0	383.4	18.5	40.3	2.1	49.4	2.5	85.6	4.7	0.23	0.01
31	7.3	1.2	14.2	2.0	165.1	11.1	18.8	1.4	23.1	1.7	40.3	3.2	0.11	0.01
32	10.6	1.4	13.8	2.1	137.9	10.2	19.0	1.5	23.3	1.8	40.9	3.3	0.11	0.01
33	15.9	1.6	18.0	2.5	274.8	15.2	29.7	1.8	36.4	2.2	62.8	4.0	0.17	0.01
34	12.7	1.4	15.2	2.4	266.4	14.5	26.2	1.7	32.1	2.1	55.0	3.9	0.15	0.01
35	11.4	1.5	14.4	2.1	179.7	11.5	21.5	1.5	26.4	1.9	45.9	3.5	0.12	0.01
36	15.8	1.6	29.3	2.9	376.6	18.5	40.7	2.1	49.9	2.6	86.6	4.7	0.23	0.01
37	13.9	1.4	32.1	3.0	354.7	17.6	40.6	2.1	49.7	2.5	87.0	4.7	0.24	0.01
38	18.3	1.6	32.5	2.9	344.8	17.6	42.5	2.0	52.1	2.5	91.3	4.6	0.25	0.01
39	21.3	1.7	34.6	3.3	467.5	21.5	50.2	2.3	61.6	2.9	106.7	5.3	0.29	0.01
40	25.6	1.8	35.2	3.0	432.5	20.4	51.1	2.2	62.7	2.7	109.1	4.9	0.29	0.01
41	18.8	1.8	42.1	3.6	438.3	20.5	52.4	2.5	64.3	3.0	112.8	5.6	0.30	0.02
42	23.4	2.0	43.0	3.8	452.9	21.0	55.7	2.6	68.3	3.2	119.7	6.0	0.32	0.02
43	19.9	1.8	40.9	3.5	442.5	20.8	52.4	2.4	64.2	3.0	112.5	5.5	0.30	0.01
44	18.6	1.5	41.2	3.3	431.0	20.1	51.5	2.3	63.1	2.8	110.7	5.2	0.30	0.01
45	23.4	1.9	43.1	3.5	507.8	22.5	58.0	2.5	71.2	3.0	124.2	5.6	0.34	0.02
46	18.8	1.6	28.2	2.8	336.9	17.3	39.8	2.0	48.8	2.4	85.1	4.4	0.23	0.01
47	19.9	1.7	42.4	3.4	409.6	19.5	51.9	2.3	63.6	2.9	112.0	5.3	0.30	0.01
48	18.1	2.0	36.2	3.0	394.9	19.0	46.7	2.2	57.3	2.7	100.3	5.0	0.27	0.01
49	19.4	1.8	42.0	3.5	483.7	21.8	54.5	2.5	66.8	3.0	116.7	5.6	0.32	0.02
50	24.7	1.9	35.3	3.4	450.8	20.8	51.5	2.4	63.2	2.9	109.9	5.5	0.30	0.01

Appendix 3

Natural radioactivity in the soil samples of the town of Otavi

S/N	Uc (Bq/kg)	δUc (Bq/kg)	Thc (Bq/kg)	δThc (Bq/kg)	Kc (Bq/kg)	δKc(Bq/kg)	Dose (nGy/h)	δDt (nGy/h)	EffectiveDoseRate(μ	δEffective DoseRate (μSv/y)	Ra_{eq} (Bq/kg)	$δRa_{eq}$ (Bq/kg)	H_{ex}	$δH_{ex}$
1	30.4	2.0	22.7	2.8	261.9	15.1	38.7	2.0	47.4	2.5	83.0	4.6	0.22	0.01
2	21.0	1.6	20.7	2.8	244.9	14.1	32.4	2.0	39.7	2.4	69.4	4.5	0.19	0.01
3	24.3	1.8	24.0	2.8	242.3	13.8	35.8	1.9	43.9	2.4	77.3	4.4	0.21	0.01
4	23.4	1.4	21.2	3.0	220.1	13.1	32.8	2.0	40.2	2.4	70.6	4.6	0.19	0.01
5	22.8	1.7	16.7	2.3	167.9	11.4	27.6	1.7	33.9	2.1	59.6	3.8	0.16	0.01
6	15.5	1.4	14.1	2.1	159.6	11.0	22.3	1.5	27.4	1.8	47.9	3.4	0.13	0.01
7	12.9	1.5	18.5	2.5	206.1	12.6	25.7	1.7	31.6	2.1	55.2	3.9	0.15	0.01
8	16.2	1.7	15.5	2.1	186.0	11.8	24.6	1.6	30.2	1.9	52.7	3.6	0.14	0.01
9	14.8	1.4	10.2	2.1	135.9	9.8	18.6	1.5	22.9	1.8	39.8	3.4	0.11	0.01
10	13.3	1.4	11.3	2.3	141.6	10.3	18.8	1.6	23.1	1.9	40.3	3.6	0.11	0.01
11	18.8	1.6	16.1	2.5	201.0	12.4	26.8	1.8	32.9	2.2	57.3	4.0	0.15	0.01
12	27.6	1.9	27.4	2.9	308.9	16.1	42.2	2.1	51.7	2.5	90.6	4.7	0.24	0.01
13	29.9	1.8	23.4	2.6	229.9	13.4	37.6	1.9	46.1	2.3	81.1	4.3	0.22	0.01
14	22.9	1.9	23.1	2.9	285.7	15.7	36.5	2.1	44.7	2.5	77.9	4.7	0.21	0.01
15	26.4	1.9	26.5	2.8	282.1	15.6	40.0	2.0	49.1	2.5	86.1	4.5	0.23	0.01
16	19.5	1.7	23.9	2.7	334.2	17.1	37.3	1.9	45.8	2.4	79.3	4.4	0.21	0.01
17	29.5	2.0	31.8	3.1	418.5	19.8	50.3	2.3	61.7	2.8	107.1	5.1	0.29	0.01
18	24.5	1.7	23.9	2.7	394.2	18.9	42.2	2.0	51.7	2.4	89.0	4.5	0.24	0.01
19	19.5	1.7	19.1	2.6	242.3	14.0	30.6	1.9	37.6	2.3	65.4	4.2	0.18	0.01
20	24.6	1.9	18.9	2.8	369.9	18.3	38.2	2.1	46.9	2.5	80.1	4.7	0.22	0.01
21	22.5	1.6	21.3	2.5	220.6	13.3	32.5	1.7	39.8	2.1	70.0	4.0	0.19	0.01
22	32.3	2.0	55.6	4.4	645.8	27.1	75.5	3.0	92.5	3.7	161.6	6.9	0.44	0.02
23	24.4	1.9	19.5	2.4	262.4	14.6	34.0	1.8	41.7	2.2	72.5	4.0	0.20	0.01
24	24.6	1.9	24.0	2.8	286.7	15.5	37.8	2.0	46.4	2.5	81.0	4.5	0.22	0.01
25	27.9	2.0	22.2	2.7	265.0	14.7	37.4	2.0	45.8	2.4	80.1	4.4	0.22	0.01
26	24.6	1.7	22.7	2.6	215.4	13.6	34.1	1.9	41.8	2.3	73.6	4.2	0.20	0.01
27	22.8	1.8	15.8	2.6	210.8	12.5	28.9	1.9	35.4	2.3	61.7	4.2	0.17	0.01
28	21.2	1.6	15.5	2.3	186.5	12.0	26.9	1.6	33.0	2.0	57.7	3.7	0.16	0.01
29	13.9	1.4	12.9	2.0	136.9	10.1	19.9	1.4	24.4	1.8	42.9	3.3	0.12	0.01
30	15.0	1.5	18.6	2.3	163.8	11.0	25.0	1.6	30.7	2.0	54.3	3.7	0.15	0.01
31	18.5	1.7	16.4	2.3	255.7	14.3	29.1	1.7	35.7	2.1	61.7	3.8	0.17	0.01
32	22.2	1.8	22.5	2.6	327.0	16.9	37.5	1.9	46.0	2.3	79.6	4.3	0.21	0.01
33	23.0	1.6	21.5	2.6	269.7	14.9	34.9	1.8	42.7	2.3	74.5	4.2	0.20	0.01
34	20.2	1.6	20.6	2.8	321.3	16.5	35.2	2.0	43.1	2.4	74.4	4.5	0.20	0.01
35	21.7	1.7	21.5	2.5	217.5	13.1	32.1	1.8	39.3	2.2	69.1	4.1	0.19	0.01
36	16.6	1.5	16.4	2.4	187.0	11.8	25.4	1.7	31.1	2.0	54.5	3.8	0.15	0.01
37	16.7	1.6	11.3	2.2	148.8	10.4	20.7	1.6	25.4	1.9	44.2	3.6	0.12	0.01
38	17.5	1.4	14.0	2.2	159.6	10.7	23.2	1.5	28.5	1.9	49.9	3.5	0.13	0.01
39	24.7	1.7	24.5	2.7	278.5	15.0	37.8	1.9	46.4	2.3	81.1	4.3	0.22	0.01
40	28.3	2.0	25.8	3.0	349.7	17.7	43.2	2.2	53.0	2.7	92.1	4.9	0.25	0.01
41	6.5	1.3	7.9	1.6	94.5	9.0	11.7	1.2	14.3	1.5	25.0	2.7	0.07	0.01
42	13.4	1.3	7.6	1.8	182.4	11.5	18.4	1.4	22.6	1.7	38.3	3.1	0.10	0.01
43	7.4	1.2	3.7	1.5	76.5	7.6	8.9	1.1	10.9	1.3	18.6	2.4	0.05	0.01
44	8.7	1.3	8.5	2.2	103.8	9.1	13.5	1.5	16.5	1.8	28.8	3.5	0.08	0.01
45	10.1	1.4	9.8	2.0	108.5	8.7	15.1	1.4	18.6	1.7	32.5	3.2	0.09	0.01
46	35.1	2.0	35.2	3.3	469.6	21.3	57.1	2.4	70.0	2.9	121.6	5.4	0.33	0.01
47	30.9	2.1	28.8	2.9	503.7	22.4	52.6	2.2	64.6	2.7	110.8	5.0	0.30	0.01
48	20.2	1.6	18.9	2.6	281.0	15.5	32.5	1.8	39.9	2.3	68.9	4.2	0.19	0.01
49	33.9	2.3	32.1	3.0	424.7	20.2	52.7	2.2	64.7	2.7	112.4	5.0	0.30	0.01
50	39.1	2.2	29.5	3.2	432.4	20.1	53.9	2.3	66.1	2.8	114.6	5.3	0.31	0.01

Permission letter to collect soil samples from Otavi

University of Namibia, Private Bag 13301, Windhoek, Namibia
340 Mandume Ndemufayo Avenue, Pioneerspark
☎ +264 61 206 3111, URL: http://www.unam.edu.na

UNAM
UNIVERSITY OF NAMIBIA

August 22, 2017.

Mr Moses Matyayi
The Chief Executive Officer
Otavi Town Council
Otavi

Dear Sir,

REQUEST FOR PERMISSION TO TAKE SOIL SAMPLES IN OTAVI

I wish to apply for your permission to take some small soil samples from different parts of Otavi for research studies at the University of Namibia (UNAM).

A research group in the Physics Department of UNAM is interested in studying soils in different parts of the Country and will therefore like to take a small amount of soil (about one kilogram) from different sites in Otavi during the period 31 August - 1 September 2017. The activity will not affect the landscape and does not have any financial implication for the town. In fact, the results of the study should benefit Otavi.

Thank you.

OTAVI TOWN COUNCIL
2017 -09- 01
Approved.

Mr Simon A Shimbuyo
Senior Lecturer
Department of Physics
Faculty of Science
University of Namibia
E-mail: sshimbuyo@unam.na
Cell: 0816771618
Phone: (061) 206-3427
Fax: (061) 206-3791

Ethical clearance certificate

UNAM
UNIVERSITY OF NAMIBIA

ETHICAL CLEARANCE CERTIFICATE

Ethical Clearance Reference Number: FOS /302/2017 **Date: 10 October, 2017**

This Ethical Clearance Certificate is issued by the University of Namibia Research Ethics Committee (UREC) in accordance with the University of Namibia's Research Ethics Policy and Guidelines. Ethical approval is given in respect of undertakings contained in the Research Project outlined below. This Certificate is issued on the recommendations of the ethical evaluation done by the Faculty/Centre/Campus Research & Publications Committee sitting with the Postgraduate Studies Committee.

Title of Project: Assessment Of Natural Radioactivity In The Soils Of The Ohorongo Cement Plant And The Neighbouring Town Of Otavi, Namibia

Researcher: Monica Mwadinomo Nambinga

Student Number: 200970941

Faculty: Faculty of Science

Supervisor: Prof James A. Oyedele

Take note of the following:

(a) Any significant changes in the conditions or undertakings outlined in the approved Proposal must be communicated to the UREC. An application to make amendments may be necessary.

(b) Any breaches of ethical undertakings or practices that have an impact on ethical conduct of the research must be reported to the UREC.

(c) The Principal Researcher must report issues of ethical compliance to the UREC (through the Chairperson of the Faculty/Centre/Campus Research & Publications Committee) at the end of the Project or as may be requested by UREC.

(d) The UREC retains the right to:

(i) Withdraw or amend this Ethical Clearance if any unethical practices (as outlined in the Research Ethics Policy) have been detected or suspected,

(ii) Request for an ethical compliance report at any point during the course of the research.

UREC wishes you the best in your research.

Prof. P. Odonkor: UREC Chairperson

Ms. P. Claassen: UREC Secretary